Ultrafast Excited-State Dynamics in Nucleic Acids

Carlos E. Crespo-Hernández, Boiko Cohen, Patrick M. Hare, and Bern Kohler*

Department of Chemistry, The Ohio State University, 100 West 18th Avenue, Columbus, Ohio 43214

Received June 16, 2003

Contents

* To whom correspondence should be addressed. E-mail: kohler@chemistry.ohio-state.edu. Phone: (614) 688-3944. Fax: (614) 292-1685.

1. Introduction

The scope of this review is the nature and dynamics of the singlet excited electronic states created in nucleic acids and their constituents by UV light. Interest in the UV photochemistry of nucleic acids has long been the motivation for photophysical studies of the excited states, because these states are at the beginning of the complex chain of events that culminates in photodamage. UV-induced damage to DNA has profound biological consequences, including photocarcinogenesis, a growing human health problem.[1−3]

Sunlight, which is essential for life on earth, contains significant amounts of harmful UV ($\lambda < 400$ nm) radiation. These solar UV photons constitute one of the most ubiquitous and potent environmental carcinogens. This extraterrestrial threat is impressive for its long history; photodamage is as old as life itself. The genomic information encoded by these biopolymers has been under photochemical attack for billions of years. It is not surprising then that the excited states of the nucleic acid bases (see Chart 1), the most important UV chromophores of nucleic acids, are highly stable to photochemical decay, perhaps as a result of selection pressure during a long period of molecular evolution. This photostability is due to remarkably rapid decay pathways for electronic energy, which are only now coming into focus through femtosecond laser spectroscopy.

The recently completed map of the human genome and the ever-expanding crystallographic database of nucleic acid structures are two examples that illustrate the richly detailed information currently available about the *static* properties of nucleic acids. In contrast, much less is known about the *dynamics* of these macromolecules. This is particularly true of the dynamics of the excited states that play a critical role in DNA photodamage.

Efforts to study nucleic acids by time-resolved spectroscopy have been stymied by the apparent lack of suitable fluorophores. In contrast, dynamical spectroscopy of proteins has flourished thanks to intrinsically fluorescent amino acids such as tryptophan, tyrosine, and phenylalanine.[4] The primary UV-absorbing constituents of nucleic acids, the nucleic acid bases, have vanishingly small fluorescence quantum yields under physiological conditions of temperature and pH.[5] In fact, the bases were frequently described as "nonfluorescent" in the early literature.

10.1021/cr0206770 CCC: $48.50
Published on Web 04/14/2004

Carlos E. Crespo-Hernández was born in Lares, Puerto Rico, in 1971. He received his Ph.D. degree in chemistry with high honors in 2002 from the University of Puerto Rico, Río Piedras Campus, under the supervision of Professor Rafael Arce. His dissertation work concerned the steady-state photochemistry and nanosecond laser flash photolysis of DNA and RNA model compounds. He augmented his experimental work with ab initio calculations on these compounds in the gas and aqueous phases. In November 2002 he joined the group of Professor Bern Kohler with support from an NIH postdoctoral fellowship. His present research is devoted to understanding the ultrafast photophysics of DNA and RNA base multimers.

Boiko Cohen was born in Sofia, Bulgaria, in 1973. He received his B.Sc. and M.Sc. degrees from the University of Sofia, where he worked with Prof. Boryan Radoev. In 2003 he received his Ph.D. in physical chemistry under the supervision of Prof. Dan Huppert at Tel Aviv University and Prof. Noam Agmon at the Hebrew University of Jerusalem. He is currently carrying out postdoctoral research in the ultrafast spectroscopy group of Prof. Bern Kohler. His research interests include ultrafast proton-transfer reactions, ultrafast processes in confined volumes, and DNA and RNA photophysics. He is married and has one daughter.

Patrick M. Hare was born in 1979 in Canton, OH. He received his bachelor's degree in chemistry with a minor in computer science in 2001 from Case Western Reserve University in Cleveland, OH. While a student there, he did undergraduate research in the laboratory of Cather Simpson on the vibrational structure of styrene. Since then he has been a graduate student at The Ohio State University, where he studies the excited-state dynamics of nucleic acids.

Bern Kohler was born in Chicago, IL, in 1964 and is currently Associate Professor of Chemistry at The Ohio State University. He received his B.S. degree from Stanford in 1985 and his Ph.D. from the Massachusetts Institute of Technology in 1990 under the mentorship of Keith A. Nelson. After postdoctoral work at ETH Zürich with Urs P. Wild, and at the University of California, San Diego, with the late Kent R. Wilson, he joined the Ohio State faculty in 1995. He first began working in femtosecond laser spectroscopy as a graduate student in the mid-1980s. His research group studies condensed-phase biomolecular photoprocesses and ultrafast charge-transfer dynamics. He is currently an Associate Editor for *Photochemistry and Photobiology*.

The low fluorescence quantum yields are a consequence of the very short lifetimes of the excited singlet states produced by UV light absorption, and femtosecond time resolution is required to study their dynamics. Although much has been learned through the introduction of exogenous photophysical probe molecules into DNA,[6,7] time-resolved experiments using the intrinsic fluorophores offer the possibility of studying nucleic acids in the absence of unwanted structural and dynamical modifications.

A goal of photophysical investigations is to understand how excited electronic states produce photochemical outcomes. Photochemistry and photophysics of nucleic acids are so intertwined that they often have been reviewed together.[8,9] Here, our review is restricted to those works that provide insight into the excited singlet states. This choice reflects our own research interests, as well as our admittedly limited perspective on the vast area of DNA photochemistry, an area which has been reviewed more frequently.[10−15] Although triplet states are important precursors of many photoproducts,[8] the intersystem crossing yields are very low as a result of the rapid singlet-state dynamics that are the focus of this review. A few new photophysical results have been obtained about base triplet states in recent years,[16−18] but since light absorption initially produces states of singlet multiplicity, intersystem crossing yields can only be rationalized when the decay pathways of the excited singlet states are understood.

A review of DNA photophysics is timely in light of three new developments since the last comprehensive reviews,[8,9] which have led to a renaissance in experimental and theoretical studies. First, rapid advances

Chart 1

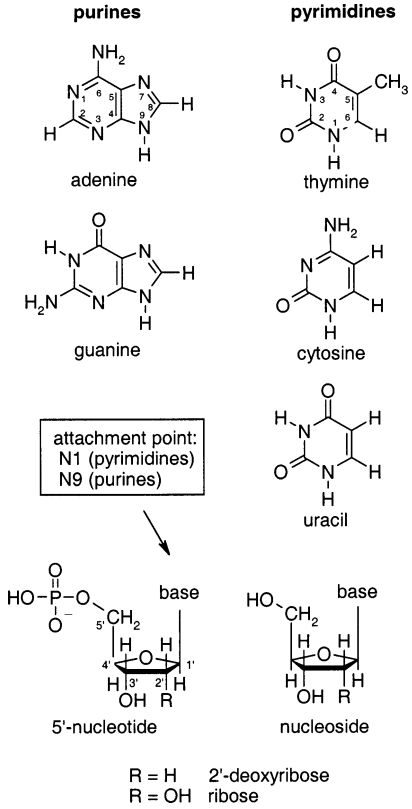

in quantum chemistry have made it possible to model excited states of DNA and RNA bases with increasing accuracy. Second, improved molecular beam techniques now permit increasingly sophisticated studies of isolated bases and base pairs, despite their low vapor pressure and propensity for thermal decomposition.[19] This has spawned a vigorous and exciting new research area that uses high-resolution spectroscopy to understand base properties, including photophysical ones, in the absence of a solvent.[20] The third development is the revolutionary impact femtosecond laser techniques are having on the study of electronic energy relaxation in nucleic acids and their constituents. The successful measurement of the fluorescence lifetimes of various nucleosides in 2000 is a representative milestone.[21] We will review progress in all three areas and critically discuss the extent to which the seemingly disparate results can be integrated into a comprehensive model for explaining the remarkable photophysical properties of nucleic acids.

The last substantive review of DNA photophysics appeared in 1995 and covered photophysical results through 1991.[9] Here, we have attempted to review the literature from 1992 through 2003. Most activity has taken place in the past five years since the introduction of femtosecond laser and molecular beam techniques. For completeness, we mention several earlier reviews[22−28] that provide an excellent summary of the many steady-state experiments performed in the period from the early 1960s through the early 1980s—the first Golden Age of DNA photophysics.

This review is organized as follows: Excited singlet states of single-chromophore constituents of nucleic acids are discussed in section 2. Excitations in di-, oligo-, and polynucleotides are presented in section 3. Both sections are organized similarly: Experimental work, primarily of a time-resolved nature, is discussed first, followed by a review of computational studies of the excited singlet states. Each section ends with an attempt to reconcile the diverse experimental and theoretical findings to the extent possible. Although comprehensive understanding is not yet at hand, particularly for excitations in systems containing two or more linked bases, it is hoped that this review will communicate the current excitement in the field and the enticing opportunities for future experimental and theoretical work. In section 4, conclusions and an outlook for future progress are presented.

2. Singlet-Excited-State Dynamics of Individual Bases, Nucleosides, and Nucleotides

Ozone and other atmospheric gases absorb high-energy solar photons, drastically attenuating the UV irradiance at the earth's surface. As a result, there is very little flux at wavelengths shorter than 290 nm and electronic excitation is restricted to the nucleic acid bases. To understand the photophysics of DNA and RNA polymers, it is therefore essential to first consider excited-state dynamics in single bases. The structures and standard ring numbering for the five nucleic acid bases are shown in Chart 1. The purines, adenine and guanine, and the pyrimidines thymine and cytosine are found in DNA. In RNA, the pyrimidine base uracil takes the place of thymine (5-methyluracil). Ribonucleosides and 2′-deoxyribonucleosides are formed by attaching ribose or deoxyribose to the N1 position of the pyrimidine bases, or to the N9 position of the purines. Attaching a phosphate group to the 5′-position of (deoxy)ribose, as illustrated in Chart 1, forms mononucleotides, the monomeric units of polynucleotides. Nomenclature and standard abbreviations for nucleic acids and their constituents are discussed in ref 29. These abbreviations are used throughout this review and are collected at the end for convenience. Hereafter, we will use the terms *base monomers* or simply *monomers* to refer generically to free bases, nucleosides, and nucleotides.

Each base has a number of structural isomers, formed by permuting hydrogen atoms among the set of heteroatoms. The possible structural isomers are known as tautomers, and tautomers of Ade (as a representative purine base) and Cyt (as a representative pyrimidine base) are shown in Charts 2 and 3, respectively. Each of the imino tautomers in Charts 2 and 3 can exist further as *E* and *Z* stereoisomers. The specific tautomers depicted in Chart 1 are called canonical because they have the requisite structures for Watson−Crick base pairing.[30] Tautomerism complicates the interpretation of photophysical experiments because electronic structure can differ dramatically for individual tautomers. It is thus essential to determine what tautomers are actually present in a given experiment. The canonical tautomers are believed to be the lowest energy forms in aqueous solution, but they are not always lowest in

Chart 2. Adenine Tautomers

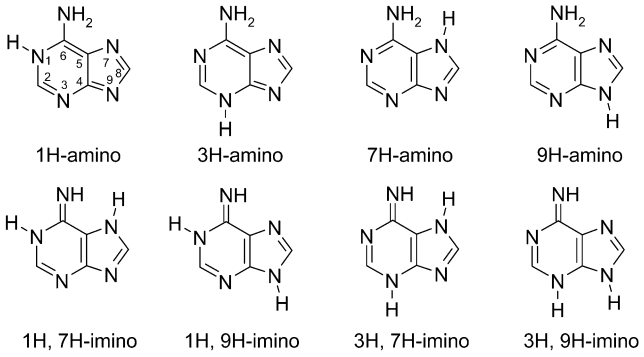

Chart 3. Cytosine Tautomers

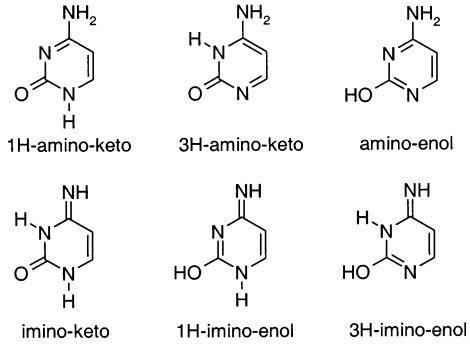

the gas phase. Awareness that minor tautomers occasionally dominate base luminescence[31,32] was a major milestone in the history of DNA photophysics. Fortunately, most tautomers have energies sufficiently greater than that of the minimum-energy tautomer that they do not occur to any significant extent. In addition, (deoxy)ribose substitution removes a heteroatom from the set that can accept hydrogen, decreasing the number of possible tautomers in the nucleosides and nucleotides. Occasionally, two or more tautomers are close enough in energy to coexist in significant amounts, as will be discussed later for Ade.

The bases have strong $^1\pi \rightarrow \pi^*$ transitions, which are responsible for the bands seen in their UV absorption spectra.[33] The lone electron pairs of the various heteroatoms are responsible for additional $^1n \rightarrow \pi^*$ excitations, but these are poorly characterized due to their forbidden character. Although the sunlight that reaches the earth's surface excites only the longest wavelength absorption band of each base, laboratory investigations that aim to understand photophysics frequently use higher energy UV photons. This is commonly a choice of convenience: absorption cross sections are larger at shorter wavelengths, and many UV laser sources operate only at particular fixed wavelengths. The precise excitation wavelength will determine the excited singlet state (S_1, S_2, S_3, ..., S_N) that is initially populated and its initial excess vibrational energy. Electronic and vibrational energy relaxation is ultrafast in solution for upper singlet states with the result that the observable properties are those of the vibrationless level of the lowest singlet excited state (S_1). Thus, properties such as fluorescence quantum yields and fluorescence lifetimes are frequently (but not always) independent of excitation wavelength.

The most distinctive photophysical attribute of each nucleobase is the very low yield of fluorescence produced by UV excitation. In 1971, Daniels and Hauswirth reported the first measurements of the fluorescence quantum yields of nucleic acid bases in aqueous solution at room temperature.[5] Later measurements, reviewed by Callis[27] and by Vigny and Cadet,[8] confirmed the low yields, which vary between 3×10^{-5} for Ura and Urd and 2.6×10^{-4} for Ade.

The fluorescence lifetime, τ_f, of any molecule is proportional to its fluorescence quantum yield, ϕ_f,

$$\tau_f = \phi_f \tau_0 \qquad (1)$$

where τ_0 is the radiative lifetime. The latter quantity is not directly measurable but can be estimated from the steady-state absorption and emission spectra using the Strickler−Berg equation.[34] The radiative lifetime depends inversely on the oscillator strength of the lowest energy absorption band. For chromophores with highly allowed transitions such as the DNA and RNA bases, a typical value for τ_0 is several nanoseconds. Equation 1 indicates that low fluorescence quantum yields correspond to short excited-state lifetimes. Daniels and Hauswirth combined their ϕ_f values with Strickler−Berg estimates of the radiative lifetimes and first predicted τ_f to be ≤ 1 ps.

Kasha's rule[35] ("emission is always from the lowest excited electronic state of a given multiplicity regardless of excitation energy") is obeyed so frequently in molecular photophysics that "S_1 lifetime" is often used as a synonym for τ_f. This usage is widespread in the literature on DNA photophysics, and we will adopt the same convention for consistency. However, it is important to keep in mind that the emitting state may not actually be the lowest singlet excited state. In fact, there is good theoretical and experimental evidence that the excited state responsible for the bulk of the fluorescence of some bases is actually S_2. Of course, the excited-state order also changes with nuclear coordinates, making labels such as S_1, S_2, S_3, ... of limited usefulness unless geometries are stated. In nonadiabatic dynamics, changes in electronic structure with nuclear coordinates are particularly important.

Further indirect evidence for ultrashort lifetimes was provided by room temperature fluorescence measurements, which showed a high degree of polarization in aqueous solution, indicating that emission must take place prior to reorientation of the transition dipole.[36] From the measured polarization ratios and rotational relaxation times estimated by hydrodynamic modeling with stick boundary conditions, Callis reported upper limits for the S_1 lifetimes of ~1 ps for Cyt and Thy and ~10 ps for Ade and Gua.[36] Triplet quantum yields (ϕ_T) are low at room temperature (≤ 0.01),[8] suggesting that relaxation from S_1 to the electronic ground state, S_0, i.e., internal conversion, is responsible for the low ϕ_f values.

The excited singlet states of the DNA and RNA bases differ dramatically from those of aromatic hydrocarbons. The latter compounds generally obey the relation $\phi_f + \phi_T \approx 1$, but the nucleic acid bases do not.[37] The next section briefly reviews efforts to

Table 1. Lifetimes (ps) of DNA and RNA Monomers in Neutral pH Aqueous Solution from Early Time-Resolved Measurements at Room Temperature

Ade	Gua	Cyt	Thy	Ura	time resolution, technique[a]	ref
<4		<4	4 ± 2	4 ± 2 4 ± 2[b]	~4 ps, TA	43
1.0 ± 0.5	3.2 ± 1.6	5.2 ± 2.6	3.5 ± 1.7	5.2 ± 2.6	30 ps, TA/UV photolysis	54
<100[b]	<100[b]	<100[b]	<100[c]		1.76 ns, single-photon counting	44
6					24 ps, streak camera	45
				≥6.6[d]	23 ps, TA	55
5[f]					20 ps, streak camera	56
1.6 ± 0.3 1.9 ± 0.3[c] 2.1 ± 0.3[d]					1.5 ps, TA	46
			1.2 ± 0.2		180 fs, TA	47
8.5 ± 0.5 3.3 ± 0.5[b] 1.6 ± 0.5[d]	5.7 ± 0.5	2.2 ± 0.5	1.5 ± 0.5 1.8 ± 0.5[c] 1.5 ± 0.5[e]	1.3 ± 0.5	4 ps, streak camera	49
	5 ± 2 (85%),[g] 81 ± 11 (15%) 4 ± 1[b,d]				7−18 ps, streak camera	50
			720		<10 ps, single-photon counting	57
1.1 ± 0.2		1.1 ± 0.2	1.2 ± 0.2	0.9 ± 0.2	180 fs, TA	48

[a] TA = transient absorption. See original publication for further details. [b] Ribonucleoside. [c] 2′-Deoxyribonucleoside. [d] 5′-Ribonucleotide. [e] TMP. [f] m^9Ade. [g] Relative amplitudes of each lifetime component.

directly measure the S_1 lifetimes, a goal that was not achieved until recently.[21,38−41]

2.1. Time-Resolved Absorption and Fluorescence

2.1.1. Early Experiments

Nikogosyan pioneered the time-resolved study of excited electronic states in base monomers using high-intensity picosecond laser pulses in the early 1980s. This early work was reviewed in 1983.[42] He and co-workers performed the first transient absorption measurements in 1981 with picosecond UV pulses at $\lambda = 264$ nm obtained from the fourth-harmonic output of a mode-locked Nd/glass laser.[43] In this study, a high-intensity UV laser pulse excited an aqueous solution of the base under study, and a second, variably delayed probe pulse at the same wavelength recorded a transient bleaching signal. S_1 lifetimes estimated from these measurements are listed in the first row of Table 1. The values are equal to or somewhat shorter than the instrumental time resolution. An undesirable aspect of probing in the UV is the superposition of signals from S_1 decay and from the relaxation of vibrationally highly excited molecules in S_0 (i.e., vibrational cooling). This issue has been clarified by recent femtosecond experiments,[38] and will be discussed in the next section.

The first time-resolved emission experiments were also reported in the 1980s. Ballini et al.[44] used streak camera detection and ~1.8 ns pulses from a synchrotron source to study time-resolved emission from Ade, Gua, Cyt, and Thy. They were unable to distinguish emission decays from their instrumental response function, and were only able to establish an upper limit of 100 ps for the monomer fluorescence lifetimes.[44] Kobayashi et al.[45] used a streak camera synchronized to a mode-locked CW dye laser to study fluorescence from Ade and the homopolymer poly(A) in room temperature aqueous solution. Lifetimes from these and other studies discussed in this section can be found in Table 1.

These two approaches of transient absorption and time-resolved emission measurements by a streak camera continued into the 1990s. Nikogosyan extended his earlier experiments to the femtosecond time scale with the groups of Lindqvist[46] and Laubereau.[47] The use of femtosecond instead of picosecond excitation pulses significantly improved the instrumental response time, but the high pump intensities (20−200 GW cm^{-2}) used in these experiments led to substantial multiphoton absorption and ionization. The resulting complex mixture of excited states, neutrals, and ions produced complex dynamical signals due to the overlapping absorption bands of these species. Reuther et al.[48] used the same technique with probing at visible wavelengths, where the S_1 states have now been shown to absorb,[21,38] but strong absorption by other species masked the S_1 dynamics. Lifetimes were estimated through indirect calculations using a complex, seven-level kinetic scheme, resulting in equal lifetimes of ~1 ps (see Table 1) for Ade, Cyt, Thy, and Ura.[48]

Streak camera fluorescence measurements were also carried out with femtosecond excitation pulses in the 1990s.[49,50] In contrast to the pump−probe experiments, the use of femtosecond laser pulses did not significantly improve the time resolution, which was still limited by the streak camera to between 4 and 10 ps. In a widely cited study, Häupl et al.[49] used 200 fs, UV excitation pulses to study the lifetimes of purine and pyrimidine bases in aqueous solution. The measured lifetimes (see Table 1) are of the same order as or even shorter than the instrumental response function, which was estimated to be ~4 ps. Their finding that the lifetime of Ado is longer than that of Thd has been contradicted by more recent ultrafast measurements described in the next section. These studies have shown that 1 ps is not a lower limit for internal conversion, as claimed by Häupl et al.[49]

Fujiwara et al.[50] studied fluorescence by Gua, Guo, and GMP in neutral and acidic aqueous solutions at room temperature. Using UV femtosecond laser pulses and a sensitive streak camera, they observed mono- and biexponential emission decays for Guo and Gua at pH 7, respectively. The shorter decay time

Scheme 1

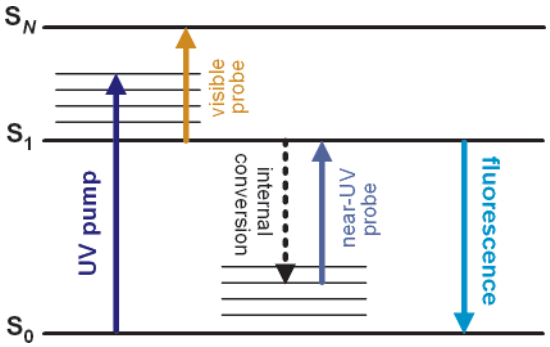

for Guo and the fast component observed for Gua are slightly below their instrumental response time (see Table 1). At low pH values, they measured significantly longer decay times for Gua, Guo, and GMP.[50] These decay times are slower than the instrumental response time, and they arise from the considerably more fluorescent cations (see section 2.1.3). The lifetime of the Guo cation, which has been confirmed by recent experiments with much higher time resolution,[38,39] is listed in Table 3. As will be discussed later in more detail, protonation and deprotonation can dramatically affect nucleobase fluorescence, a point established much earlier in steady-state experiments.[51,52]

Table 1 illustrates the lack of consensus among experimentalists before the year 2000. Many of the lifetimes in Table 1 are shorter than the experimental time resolution. The next section will show that the S_1 lifetimes of the DNA bases are actually $\leq$1 ps, and it is obvious in hindsight that these early studies lacked the necessary time resolution to follow the singlet dynamics. Table 1 also shows that Ade was one of the most frequently studied DNA bases. This choice was unfortunate because Ade is present in room temperature aqueous solution in two tautomeric forms, one of which, the 7H-amino tautomer, has a lifetime of ~8 ps.[53] The presence of this long-lived tautomer masks the subpicosecond character of the biologically important 9H-amino form, as will be discussed in section 2.1.3.

2.1.2. Femtosecond Transient Absorption and Fluorescence Upconversion in Aqueous Solution

In 2000, Pecourt et al.[21] reported dramatically shorter singlet lifetimes for a series of nucleosides. This study, which provided the first direct evidence for subpicosecond S_1 lifetimes, used 150 fs, UV pump pulses and continuum-derived visible probe pulses to measure transient absorption signals from aqueous solutions of nucleosides at room temperature. In their experiments, a UV pump pulse populates S_1, generally with some amount of vibrational excess energy, while a visible probe pulse detects excited-state absorption (ESA) due to transitions from S_1 to a higher lying singlet state, S_N. This is depicted by the two leftmost arrows in Scheme 1. Depopulation of the S_1 state (e.g., by internal conversion or fluorescence, as shown in Scheme 1) can be monitored either by measuring the decay of the ESA signal or by time-resolving the fluorescence, as will be discussed below.

The transient decays observed by Pecourt et al.[21] at a probe wavelength of 570 nm are shown in Figure

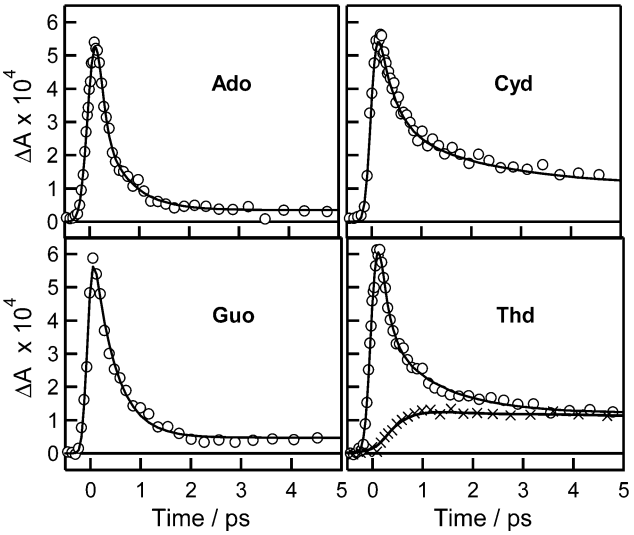

Figure 1. Transient absorption signals (263 nm pump, 570 nm probe) of the indicated nucleosides in room temperature aqueous solutions. The transient absorption signal of the solvent blank (×), scaled to the Thd signal at long times, is shown at lower right. The pump intensity was kept as low as possible to minimize two-photon ionization of the solvent. The pump intensity was 8.3 GW cm^{-2} for the pyrimidine bases and 3.5 GW cm^{-2} for the purine bases. Adapted with permission from ref 38. Copyright 2001 American Chemical Society.

1. The decays are independent of probe wavelength between 450 and 750 nm. Absorption in this spectral region is assigned to ESA, and the decay of the ESA band thus provides a measure of the S_1 lifetime. Lifetimes were estimated by global fitting[58] to transients at 3−6 different wavelengths.[21,38] The values are summarized in Table 2 along with others from this section.

The ESA spectrum of Cyd recorded 500 fs after the UV excitation pulse is shown in Figure 2 by the dashed curve labeled $S_1 \rightarrow S_N$. Similar, equally broad spectra with λ_{max} between 550 and 600 nm have been observed for the other bases[38] and for 2-aminopurine,[59] a highly fluorescent isomer of Ade. Since the adiabatic transition energies (see Table 7 and Table 1.2 in ref 8) to the S_1 state are between 4.0 and 4.5 eV, the final state of the $S_1 \rightarrow S_N$ transition is more than 6 eV above the electronic ground state. All of the bases have strong ground-state absorption near 200 nm (6.2 eV),[33] and this could explain why the ESA spectra of the bases studied to date are similar. ESA by the bases is, however, characterized by very small cross sections. This suggests some degree of forbidden character or poor Franck−Condon factors between the S_1 and S_N states, but this is poorly understood at present.

An important consequence of the small cross sections is the generation of solvated or hydrated electrons by two-photon ionization. These species are clearly identifiable by the well-known absorption spectrum[60] shown in Figure 2 by the hollow circles and dashed curve labeled e_{aq}^-. These strongly absorbing species are responsible for the long-time signal offsets seen in Figure 1. They do not contribute significantly to the short-time signal as can be seen from the solvent blank signal shown with the Thd data in Figure 1.

Table 2. Lifetimes (ps) of DNA and RNA Monomers in Neutral pH Aqueous Solution at Room Temperature from Recent Femtosecond Experiments

Ade	Gua	Cyt	Thy	Urd	time resolution, technique[a]	ref
0.29 ± 0.04[b]	0.46 ± 0.04[b]	0.72 ± 0.04[b]	0.54 ± 0.04[c]		200 fs, TA	21, 38
0.53 ± 0.12[b]	0.69 ± 0.10[b]	0.76 ± 0.12[b]	0.70 ± 0.12[c]		300 fs, FU	39
0.52 ± 0.16[d]	0.86 ± 0.10[d]	0.95 ± 0.12[d]	0.98 ± 0.12[e]			
			<0.15 (66%), 0.58 ± 0.05 (34%)		500 fs, FU	40
			<0.15 (72%), 0.69 ± 0.05 (28%)[c]			
			0.20 ± 0.05 (68%), 1.10 ± 0.10 (32%)[e]			
0.23 ± 0.05 (65%), 8.0 ± 0.3 (35%)					450 fs, FU	41
<0.1 (94%), 0.5 ± 0.1 (6%)[c,e]						
		1.0 ± 0.2			200 fs, TA	72
		1.0 ± 0.1[b]				
0.18 ± 0.03[f]					200 fs, TA	53
8.8 ± 1.2[g]						
				0.21 ± 0.03	200 fs, TA	62

[a] TA = transient absorption. FU = fluorescence upconversion. [b] Ribonucleoside. [c] 2′-Deoxyribonucleoside. [d] Nucleotide. [e] 2′-Deoxynucleotide. [f] 9H tautomer of Ade. [g] 7H tautomer of Ade.

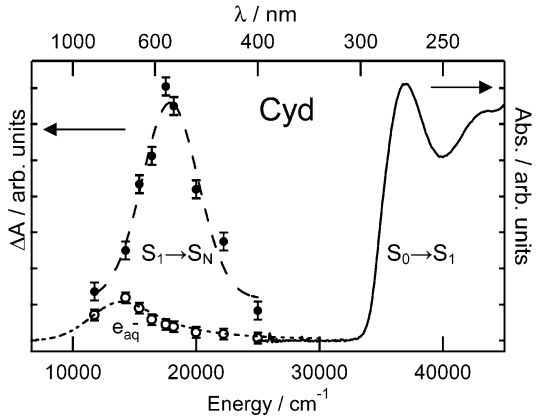

Figure 2. Transient spectra from a 4.3 mM aqueous solution of Cyd recorded 500 fs (solid circles) and 15 ps (hollow circles) after excitation with a 150 fs, 263 nm pump pulse. The short-dashed curve is the absorption spectrum of the solvated electron from ref 60. The long-dashed curve was obtained by fitting a Gaussian to the short-time spectrum as a function of frequency. The solid curve is the steady-state UV/vis spectrum of Cyd.

As shown elsewhere,[53,61] the water ionization signals can be easily removed to yield "water-subtracted" transients (symbol ΔA^s; see later figures). Weaker ESA by the pyrimidine bases is the reason that the water ionization signal visible at long times in Figure 1 is larger for these bases than for the purine ones. Although two-photon ionization of the bases is energetically allowed, the solvated electrons are formed overwhelmingly from two-photon ionization of the far more abundant solvent molecules.[38] In fact, the weak ESA signals are completely overwhelmed by the solvent ionization signal at higher laser intensities. Pecourt et al.[21,38] successfully located the weak ESA signals because they were able to work at much lower laser intensities than in previous femtosecond pump−probe experiments.[47,48]

Recently, the ribonucleoside Urd was studied by femtosecond transient absorption.[62] The S_1 lifetime determined by globally fitting a single exponential to water-subtracted decays at three probe wavelengths is 210 ± 30 fs. This lifetime is essentially the same as the instrumental response function, and may be more uncertain than indicated by the fit. According to Table 2, Urd has the shortest S_1 lifetime of any of the pyrimidine nucleosides. The lifetime is comparable to or even somewhat shorter than that observed for Ado.

Soon after publication of the femtosecond transient absorption results by Kohler and co-workers,[21,38] two groups independently reported femtosecond fluorescence upconversion measurements of the S_1 lifetimes of nucleic acid bases.[39,40] In these experiments, a femtosecond UV pump pulse induces fluorescence, which is upconverted by a second, femtosecond gate pulse in a nonlinear optical crystal. This technique allows fluorescence decays to be measured down to the femtosecond time scale by varying the delay between pump and gate pulses. Results from the study by Peon and Zewail[39] are shown in Figure 3. The time resolution is somewhat poorer than in the transient absorption studies (~450 vs ~200 fs), but the lifetimes (see Table 2) are in good agreement with the results of Pecourt et al.[21,38] This agreement indicates unambiguously that the transient absorption experiments monitor the decay of the fluorescent state.

Gustavsson et al.[40] studied Thy, Thd, and TMP in aqueous solution using the fluorescence upconversion technique. The authors found that the fluorescence decays between 310 and 380 nm could not be fitted satisfactorily to single exponentials, but were best described by biexponential functions. Biexponential fits for Thy and Thd yielded one component with a lifetime of 150 fs (25% contribution), and a longer one on the order of several hundred femtoseconds. Addition of a sugar or sugar−phosphate moiety increased the lifetime, in agreement with the findings of Peon and Zewail.[39] For TMP, the biexponential fits gave time constants of 200 ± 50 fs and 1.1 ± 0.1 ps. The lifetime of the fast component is faster than the experimental time resolution (~450 fs), and may be

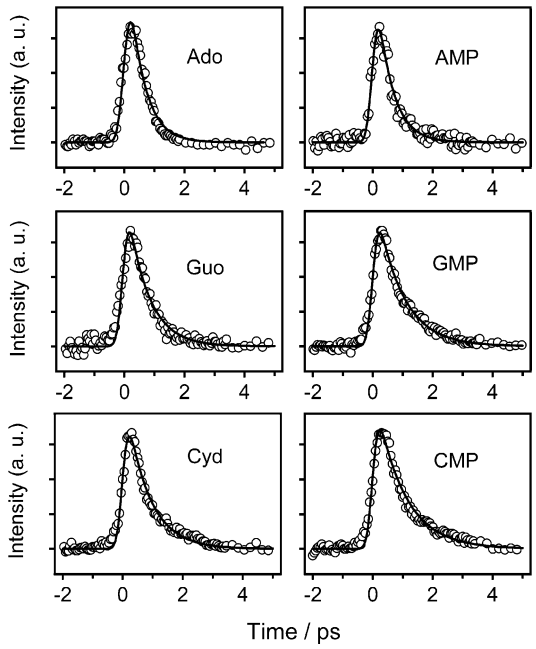

Figure 3. Femtosecond fluorescence upconversion transients from aqueous solutions of nucleosides (left panels) and 5′-nucleotides (right panels) of adenine, guanine, and cytosine in a 50 mM, pH 7 phosphate buffer. Reprinted with permission from ref 39. Copyright 2001 Elsevier Science.

subject to considerable uncertainty. The average lifetimes obtained from their fits are in good agreement with the transient absorption measurements of Pecourt et al.[21,38] In agreement with Peon and Zewail,[39] Gustavsson et al.[40] found no dependence of the kinetics on emission wavelength for any of the compounds studied.

Gustavsson and co-workers later studied Ade, dAdo, and dAMP by the same technique.[41] Here again, the fluorescence decays were better described by biexponential functions, according to the authors. The fast component was much faster than their time resolution, while the slow component for dAdo and dAMP was 500 ± 100 fs. They found a lifetime of 160 fs when they fitted a monoexponential function to their transients for dAdo and dAMP,[41] in rough agreement with the lifetime of 290 fs measured for Ado by transient absorption.[21] For Ade, Gustavsson et al. reported a slow component of 8.0 ± 0.3 ps and a fast one of 230 ± 50 fs. Although the meaning of the biexponential decays is unclear for the other bases, biexponentiality has a straightforward interpretation in the case of Ade: the two decay components reflect the presence of two tautomers in solution, 7H-Ade and 9H-Ade, as will be discussed in the next section.[41,53]

Gustavsson and co-workers calculated fluorescence anisotropy decays in the standard way from upconversion signals recorded for parallel and perpendicular polarizations. The time-zero fluorescence anisotropy was found to be 0.30 ± 0.03 for Ade and 0.25 ± 0.05 for dAdo and dAMP.[41] A slightly higher initial anisotropy of 0.35 ± 0.03 was observed for all thymine compounds studied,[40] while a value of 0.40 ± 0.05 was measured for Cyt.[63] These last two values are close to the maximum possible value of 0.4, suggesting that the emitting transition dipole is the same as the absorbing one, indicating no significant change in electronic structure at early times.

Onidas et al.[64] studied a series of DNA nucleosides and nucleotides using steady-state and time-resolved fluorescence and rotational anisotropy measurements. In steady-state experiments, they found ϕ_f values that are 20−50% higher than literature values. They attributed the increase to their detection of the entire fluorescence spectrum, including the long-wavelength tail. In fluorescence upconversion experiments, biexponential signals were again observed, which the authors suggested may be due to relaxation in two or more electronic states, or an excited-state proton-transfer reaction.[64] Zero-time anisotropies recorded at 330 nm are larger for the pyrimidine than for the purine bases, suggesting that the latter compounds undergo a change in electronic structure faster than the experimental time resolution. The authors compared results from 2′-deoxynucleosides and 2′-deoxynucleotides to study the effect of the phosphate group on photophysical properties. In the case of the purine bases, identical fluorescence lifetimes and quantum yields were observed. In contrast, the fluorescence quantum yields of pyrimidine nucleotides were higher and the fluorescence decays were somewhat slower compared to those of the corresponding nucleosides, showing that the phosphate moiety affects excited-state relaxation.[64]

The lack of a long-lived signal in the transient absorption experiments that can be assigned to a triplet state or photoproduct is consistent with fluorescence quenching by internal conversion. Strong evidence for this conclusion was provided by transient absorption experiments conducted by Kohler and co-workers at wavelengths on the red edge of the ground-state absorption band of the DNA bases.[38] Nonradiative decay produces vibrationally highly excited molecules in S_0. Intramolecular vibrational energy redistribution (IVR) quickly redistributes this energy among the available vibrational modes, and an initial vibrational temperature of 1200−1300 K was estimated for the DNA bases.[38] Intermolecular vibrational energy transfer returns these hot molecules to thermal equilibrium with the surrounding solvent molecules. This vibrational cooling process can be followed using a UV pump pulse and a near-UV probe pulse to detect the significantly red-shifted absorption by the vibrationally hot population in S_0. The middle arrow in Scheme 1 illustrates this detection step.

Pecourt et al.[21,38] detected hot ground-state absorption at probe wavelengths between 270 and 400 nm for several nucleosides. Results for Ado are shown in Figure 4b. These transients were much stronger than the ones due to ESA at visible probe wavelengths (Figure 4a) because of the highly allowed nature of the $^1\pi \rightarrow \pi^*$ transition that characterizes absorption by the ground-state chromophores. The UV probe signals decayed on a time scale characteristic of the vibrational cooling process. The decay times in the near UV decreased from 2.0 to 0.4 ps as the probe wavelength increased.

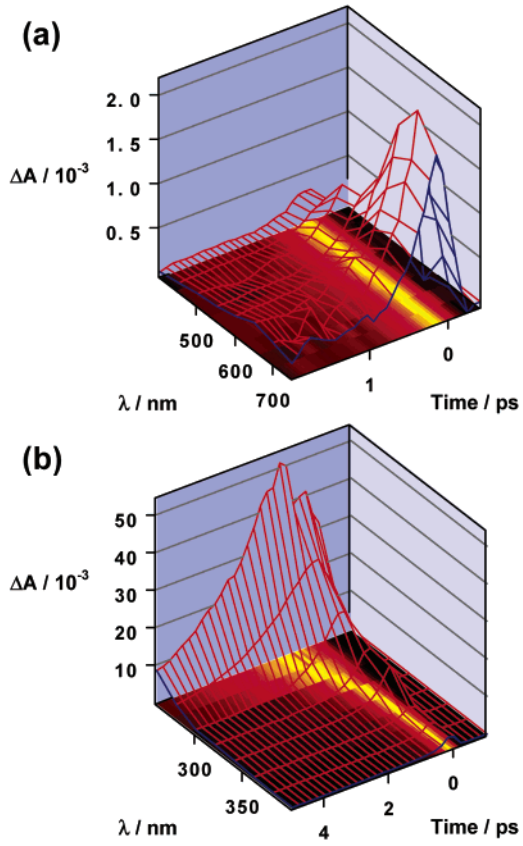

Figure 4. Transient absorbance induced by a 150 fs, 263 nm pump pulse for a 4.0 mM solution of Ado in water. Transient signals recorded as a function of the delay time between pump and probe pulses at 16 separate probe wavelengths are combined in the red wireframe plots for the (a) visible and (b) near-UV spectral regions. The image beneath each wireframe displays the same data after the transient signal at each probe wavelength was divided by its maximum value. The colormap used in these images displays regions of low and high amplitude by dark red and bright yellow, respectively. Reprinted with permission from ref 21. Copyright 2000 American Chemical Society.

The observation of shorter decay times at longer probe wavelengths is a hallmark of vibrational cooling dynamics.[65] The decay times measured by Pecourt et al.[38] for Ado and Cyd are several times shorter than typical vibrational cooling time constants of ~10 ps seen for other vibrationally highly excited chromophores in organic solvents.[66] The difference was attributed to fast intermolecular vibrational energy transfer via hydrogen bonds between the hot chromophore and the surrounding solvent molecules.[38,67] Finally, transient bleach signals corresponding to depletion of the ground-state population were looked for in this spectral region without success. The interfering spike at time zero due to two-photon absorption by the solvent, as well as the lower time resolution (~300 fs) in these UV pump−UV probe experiments may have masked any such bleach signal.[38] It is also possible that the S_1 states may absorb at near-UV wavelengths.

Internal conversion from S_1 to S_0 initially deposits over 4 eV of vibrational energy in the latter state. It is important to consider whether this energy can induce chemical reactions in the electronic ground state. This will depend in turn on the time scale for intermolecular vibrational energy transfer to the solvent. The pump−probe experiments demonstrate that this relaxation occurs in a few picoseconds. Nielsen and co-workers showed that statistical fragmentation of isolated AMP anion (the same form found in aqueous solution) occurs with a lifetime of 16 μs.[68,69] Vibrational energy relaxation in solution is thus rapid enough to prevent unimolecular fragmentation of a UV-excited base.

As already mentioned, the Strickler−Berg equation[34] has been used for many years to estimate τ_0 of a given base, allowing τ_f to be estimated using eq 1. For example, Nishimura et al. estimated τ_f of m^7GMP to be 250 ps in this manner.[70] This value agrees well with $\tau_f \approx 200$ ps later measured directly by Georghiou et al.[71] Interestingly, the good agreement between experimentally measured lifetimes and Strickler−Berg predictions holds also for most of the natural bases despite their femtosecond lifetimes.[38,62,64,72]

Strickler−Berg analysis significantly overestimates τ_f for the purine bases when only the lowest electronic transition is considered. Better agreement is obtained when both of the lowest energy $^1\pi \rightarrow \pi^*$ transitions are used in the estimate of τ_0 for purine bases.[62] For the remaining bases, the good agreement indicates that the $^1\pi\pi^*$ state responsible for the lowest energy absorption band is also the emitting state. The high initial anisotropy measured in the femtosecond upconversion experiments provides further evidence that emission is from a $^1\pi\pi^*$ excited state, and not from a $^1n\pi^*$ state because the latter is expected to have a different transition dipole moment direction.[40]

2.1.3. Lifetimes of Modified Bases

Several naturally occurring minor RNA bases are significantly fluorescent,[73] as are a number of synthetic bases.[74] 2-Aminopurine (2AP), a highly fluorescent isomer of Ade, is frequently incorporated into oligo- and polynucleotides as a photophysical probe.[75−80] The femtosecond experiments of the past few years have shown that covalent modification profoundly affects the S_1 dynamics of the less fluorescent, natural bases.[53,72,81] Here we review the experimental findings, but postpone a discussion of the implications for the nonradiative decay mechanism until section 2.4.

Simultaneous substitution at the N7 and N9 positions of purine bases significantly increases their fluorescence. Georghiou et al.[71] determined τ_f values of 180−210 ps for m^7GMP, depending on the emission wavelength, using a streak camera−optical multichannel analyzer system and 25 ps, 266 nm laser excitation pulses. Similar S_1 lifetimes were found for protonated Guo in streak camera,[50] femtosecond transient absorption,[38] and femtosecond fluorescence upconversion experiments.[39] Results from the latter two techniques are compared in Figure 5, illustrating the excellent agreement between these complementary methods.

Because protonation of Gua occurs at N7, as illustrated by the structure in Figure 5a, the Gua cation is a 7,9-substituted purine, and thus has excited-state dynamics similar to that of m^7GMP.

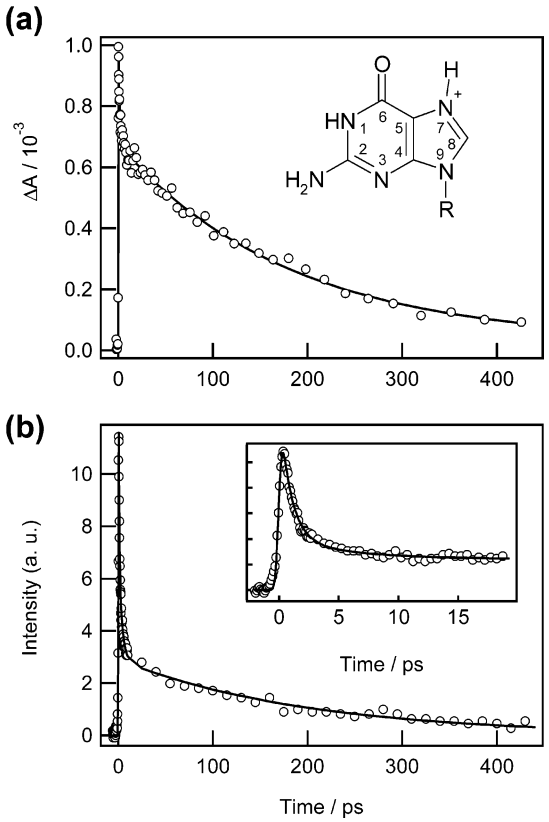

Figure 5. (a) Transient absorption (263 nm pump, 570 nm probe) of a 3 mM solution of Guo in water at pH 2. The inset shows the structure and ring numbering of protonated guanosine. R stands for ribose. Reprinted with permission from ref 38. Copyright 2001 American Chemical Society. (b) Femtosecond fluorescence upconversion transients obtained as a function of pump-gate delay time. Aqueous solutions of 3 mM Guo at pH 3 were used. The inset shows the same data at short delay. Adapted with permission from ref 39. Copyright 2001 Elsevier Science.

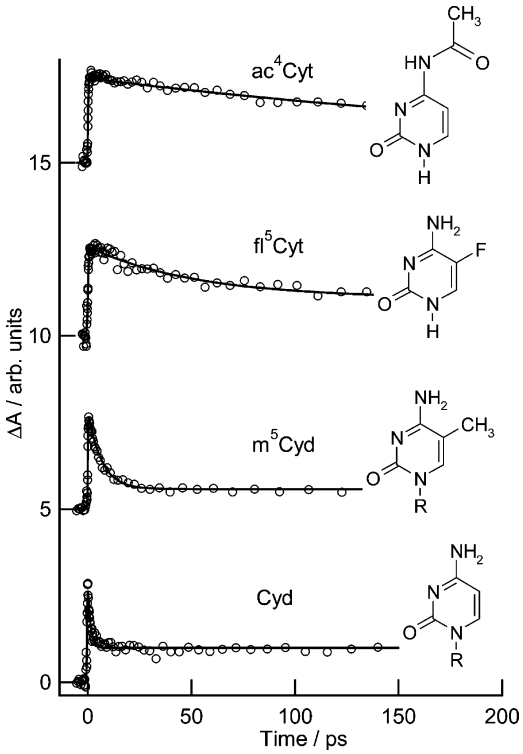

Figure 6. Transient absorption at 570 nm for the various cytosine derivatives shown in pH 7-buffered solutions after femtosecond UV photoexcitation at 265 nm. Circles: experimental data. Lines: global fits to exponential decays convoluted with a Gaussian instrument response function. Reprinted with permission from ref 72. Copyright 2003 American Society for Photobiology.

Decay times for these and other compounds discussed in this section are summarized in Table 3. The S_1 lifetimes of Guo (Table 2) and its cation (Table 3) provide a striking example of the effect of pH on base photophysics: a single proton increases the fluorescence lifetime by a factor of ~400.

Malone et al.[72] measured the S_1 lifetimes of a series of Cyt derivatives using femtosecond transient absorption. Figure 6 shows the transient absorption signals recorded at 570 nm for various Cyt derivatives after femtosecond UV photoexcitation at 265 nm. This figure shows how sensitive the S_1 lifetime is to covalent modification. Transients at several wavelengths were globally fitted to a monoexponential function since similar kinetics were observed at all visible probe wavelengths. The important minor base m^5Cyt has a lifetime of 7.2 ± 0.4 ps. The longer lifetime compared to that of natural Cyt may be associated with this minor base's role as a mutational hotspot.[14,82−85] An identical lifetime was found for m^5Cyd,[72] but excited-state absorption was significantly stronger by the ribonucleoside, as determined in back-to-back scans recorded on equal absorbance solutions (see Figure 7). This result suggests that the ribose group increases the oscillator strength of the

Table 3. Lifetimes of Modified Bases in Room Temperature Aqueous Solution[a]

nucleobase[b]	lifetime/ps	ref
Cyt, Cyt^-	1.0 ± 0.2, 13.3 ± 0.4 (pH 13)	72
Cyd, Cyd^+	1.0 ± 0.1, 0.63 ± 0.06 (pH 0.08)	72
m^5Cyt, m^5Cyt^+, m^5Cyt^-	7.2 ± 0.4, 2.57 ± 0.22 (pH 1.5), 250 ± 30 (pH 13)	72
m^5Cyd	7.2 ± 0.2	72
m^5dCyd	1.2 (310 nm), 2.8 (330 nm), 3.6 (350 nm), 3.9 (370 nm), 4.2 (380 nm), 4.0 (420 nm)[c]	81
fl^5Cyt	88 ± 5	72
ac^4Cyt	280 ± 30	72
m^1Ade	0.26 ± 0.03	53
m^3Ade	0.18 ± 0.06	53
m^7Ade	4.23 ± 0.13	53
m^9Ade	0.22 ± 0.02	53
m^7Guo	180−210	71, 95
Guo^+	196 ± 7,[50] 191 ± 4,[38] 209[39]	

[a] Measured at pH ≈ 7, unless otherwise indicated. [b] A plus (minus) sign following an abbreviation indicates the cation (anion) produced by protonation (deprotonation). [c] Average decay time, $\langle\tau\rangle = a\tau_1 + (1 - a)\tau_2$, from biexponential fits.

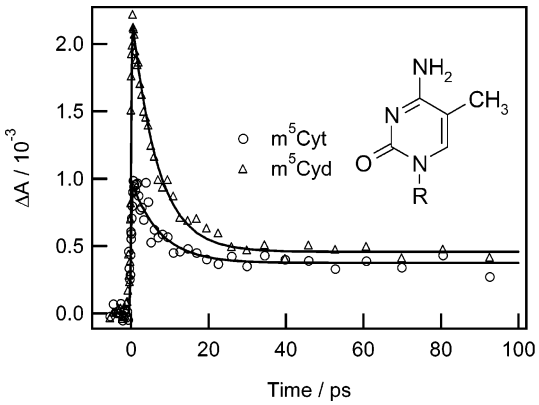

Figure 7. Transient absorption at 570 nm by m^5Cyt (circles) and m^5Cyd (triangles) recorded under identical experimental conditions. The solid curves are from global nonlinear least-squares fits. Reprinted with permission from ref 72. Copyright 2003 American Society for Photobiology.

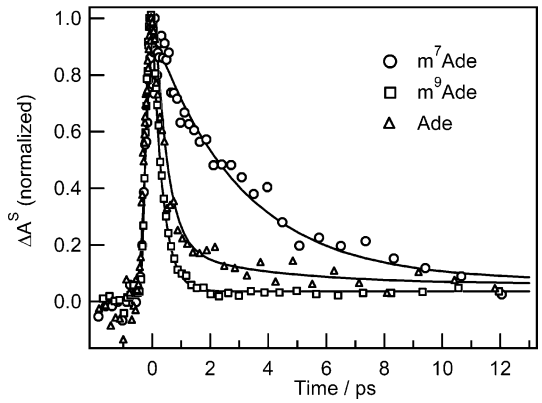

Figure 8. Normalized transient absorption signals for Ade (open triangles), m^7Ade (open circles), and m^9Ade (open squares) in water at 570 nm. Global, nonlinear least-squares fits are shown by the solid curves.

$S_1 \rightarrow S_N$ transition, but does not alter the deactivation mechanism.[72]

All of the cytosine derivatives studied by Malone et al.[72] have longer S_1 lifetimes at pH 7 than Cyt, the naturally occurring nucleobase. This observation suggests that rapid nonradiative decay may have been advantageous during molecular evolution. To understand why this might be so, it is necessary to consider the UV environment of the early earth.

During the Archean era (3.8−2.5 Ga ago) the UV flux on the earth's surface was much higher than today due to the absence of atmospheric ozone.[86−88] Sagan hypothesized that these conditions created UV selection pressure on the earliest organisms that promoted the evolution of repair enzymes and photoprotective compounds.[86] UV light at the surface of the ancient earth would have rapidly degraded many molecules, particularly aromatic ones. Only the most photostable compounds would have survived for appreciable periods of time in prebiotic environments exposed to sunlight. Hence, the primordial soup may have been enriched in compounds with high intrinsic photostability.

On account of their high absorption cross sections and ultrashort lifetimes, Pecourt et al.[38] observed that the bases have the same photophysical functionality as sunscreens that function by absorption. According to Mulkidjanian et al.,[89] the UV-protective or sunscreening properties of the bases may have been a driving force for the primordial synthesis of oligonucleotides. Since ultrafast nonradiative decay reduces the likelihood of photodegradation, we speculate that the rate of nonradiative decay by each base may be approximately maximal among a set of closely related structures. The findings of Malone et al.[72] are consistent with but do not prove this conjecture. Results on methylated adenines (described next) indicate that some modifications result in slightly higher rates of nonradiative decay. Of course, factors such as base-pairing possibilities should be considered alongside photostability when the molecular architectures of the building blocks of life are rationalized.

Cohen et al.[53] studied Ade and four monomethylated derivatives—m^1Ade, m^3Ade, m^7Ade, and m^9Ade—in aqueous solution by femtosecond transient absorption spectroscopy. Results for a few of these compounds are shown in Figure 8. In aqueous solution, each of the monomethylated adenines is present as a single amino tautomer, while Ade exists as both 7H- and 9H-amino forms (see Chart 2).[90] The transient absorption signals from Ade decay biexponentially with lifetimes of 180 ± 30 fs and 8.8 ± 1.2 ps. These values agree very well with fluorescence upconversion results from Gustavsson et al., who determined lifetimes of 230 ± 50 fs and 8.0 ± 0.3 ps.[41] This once again illustrates the excellent agreement between the transient absorption and fluorescence upconversion experiments.

In contrast to the biexponential signals seen for Ade, transient absorption signals from the monomethylated adenines decay monoexponentially, consistent with the presence of a single tautomer.[53] From this study, the S_1 lifetimes of m^1Ade, m^3Ade, and m^9Ade are the same (~200 fs) within experimental uncertainty, while m^7Ade shows a 20-fold longer lifetime (4.23 ± 0.13 ps). m^7Ade and m^9Ade are assumed to be suitable proxies for the 7H- and 9H-amino tautomers of Ade, which cannot be studied independently of one another. Justification for this assumption comes from semiempirical calculations, which show that m^7Ade and m^9Ade do not differ significantly in their electronic properties from the 7H- and 9H-amino tautomers of Ade.[91] Indeed, the fast and slow decay components seen for Ade agree reasonably well with the monoexponential lifetimes seen for m^9Ade and m^7Ade, respectively, demonstrating unambiguously that Ade is an equilibrium mixture of the 7H and 9H tautomers.

ESA by m^9Ade is 50% stronger than by m^7Ade. Cohen et al.[53] used the relative ESA cross sections and the measured amplitudes of the biexponential signal seen for Ade to estimate the fractional population of 7H-Ade in water at room temperature to be 22 ± 4%. This result is in excellent agreement with earlier estimates made by nitrogen-15 NMR[92] and temperature-jump experiments.[90]

In summary, the lifetimes of the 7H and 9H tautomers of Ade differ by a factor of about 40 in aqueous solution at room temperature.[41,53] Substitution by ribose blocks 7H,9H tautomerism, and only

a single amino tautomer is present for the Ade nucleoside and nucleotide. As discussed in section 2.1.2, these N9-substituted compounds have subpicosecond lifetimes as does 9H-Ade.

These findings contrast sharply with ones from an early report by Nikogosyan et al.,[46] who reported no significant differences in lifetimes in the series Ade, dAdo, and AMP. They are also at odds with recent results from femtosecond pump−probe ionization experiments on jet-cooled adenines by Kim and coworkers.[93] In contrast to the pronounced differences seen in solution, this group reported identical lifetimes of ~1 ps for m^7Ade and m^9Ade in molecular beam experiments.[94] This last result will be discussed more fully in section 2.3.

Sharonov et al.[81] found somewhat shorter lifetimes for m^5dCyd in their fluorescence upconversion experiments than were determined by Malone et al.[72] In the experiments of Sharonov et al.,[81] lifetimes were found to vary significantly with emission wavelength. They suggested that this might be due to a complex deactivation mechanism or solvent rearrangement. The latter suggestion appears especially probable since the longer lifetime of this base will make the emission time-dependent due to dynamic solvation. This idea will be explored more fully in the next section.

2.1.4. Solvent Effects

What is the role of the solvent in radiationless decay by the nucleobases? This question is at the heart of whether the low values of ϕ_f are intrinsic properties of the bases, or the consequence of solute−solvent quenching. For example, a protic solvent could photochemically quench S_1 states by intermolecular proton transfer, or by catalyzing intramolecular hydrogen atom shifts that convert one tautomeric form into another ("phototautomerism"). These possibilities will be critically discussed in section 2.4.1. Here, we review experimental results on base monomer photophysics as a function of the solvent. A valuable perspective on solvent effects comes from studies of isolated bases in the gas phase, and these results will be described in section 2.3.

Significant solvent effects have been observed for more fluorescent modified bases.[96,97] For example, ϕ_f of 2AP increases dramatically as the solvent polarity is increased.[98] When a more fluorescent base is inserted into single- and double-stranded DNA, the solvent environment experienced by the base changes significantly, and ϕ_f values can change considerably. For example, both m^7GMP and ac^4CMP are moderately fluorescent when free in aqueous solution, but their fluorescence is quenched in native transfer RNA structures.[73] Many of the modified bases sufficiently differ in redox properties (i.e., ionization potentials and electron affinities) from the natural bases that fluorescence quenching in DNA likely involves some degree of charge transfer, as recently established by Wan et al.[99] for 2AP-containing oligonucleotides, and by Fiebig et al.[100] for 2AP complexed with single nucleotides. Although these studies are interesting for their own sake, many have limited relevance to solvent effects on the photophysics of the naturally occurring bases.

Early workers investigated the solvent dependence of ϕ_f for the natural bases (reviewed in ref 24). These steady-state fluorescence experiments are difficult because small concentrations of highly fluorescent impurities can obscure the bases' ultraweak emission. As a result, solvent effects on the steady-state luminescence of the bases have been difficult to characterize. In addition to concerns about fluorescent impurities, the bases frequently have very poor solubility, especially in nonaqueous solvents.

Daniels reviewed solvent effects on steady-state emission properties at low and room temperature in 1976.[24] In this review, unpublished work by Daniels and Hauswirth is described, which found modest changes in ϕ_f for Thy in a series of solvents.[24] From solvent-dependent shifts of the absorption and fluorescence spectra, the change in dipole moment upon electronic excitation was estimated for Thy from a solvatochromic analysis. The resulting prediction that the excited-state dipole moment doubles from ~4 to 8 D[24] is at odds with quantum chemical calculations for the lowest $^1\pi\pi^*$ excited state in a vacuum.[101] In fact, the use of solvatochromic models to predict excited-state dipole moments for the bases is highly questionable in light of their ultrashort fluorescence lifetimes. Although dynamic Stokes shift measurements have shown that solvent reorganization is partially complete on the subpicosecond time scale,[102,103] fluorophores with sufficiently short S_1 lifetimes will not be completely solvated prior to emission, violating the assumption used in most solvatochromic analyses that the excited fluorophore is in equilibrium with the solvent. Solvation in water is particularly rapid, with 50% of the solvation energy achieved in ~50 fs,[103] but solvent reorganization occurs significantly more slowly in most nonaqueous solvents, making nonequilibrium solvation effects even more important.

Of course, it must first be demonstrated that excited-state lifetimes are indeed ultrafast in nonaqueous solvents. Georghiou and Gerke[104] observed lower values of ϕ_f for Thd in nonaqueous solvents, consistent with shorter S_1 lifetimes. Haüpl et al.[49] measured the fluorescence lifetimes of Ade and Thy in ethanol and acetonitrile using a streak camera. The lifetimes reported for Thy are instrument-limited and therefore inconclusive. However, Haüpl et al.[49] reported a large increase in lifetime from 8 to 16 ps for Ade in ethanol, which they attributed to stabilization of the excited state in the less polar solvent. In contrast, no difference has been found in recent femtosecond transient absorption experiments on Ade in ethanol.[105]

Not surprisingly, improved understanding of solvent effects is only now being obtained by means of the newly introduced femtosecond techniques. Pal et al.[106] studied the hydration dynamics of the DNA bases and 2AP. The emission transients detected in the blue region of the fluorescence spectrum for 2AP in water showed an instantaneous rise and a picosecond decay component. When detection was made in the red region, the decays slowed and an initial rise on a picosecond time scale was observed. These signals reflect a shift of the time-resolved emission

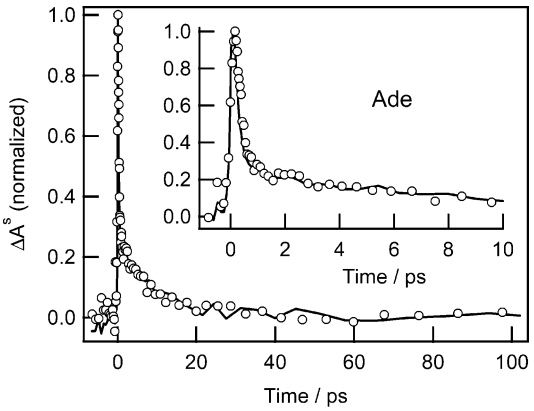

Figure 9. Normalized transient absorption signals of Ade in H_2O (solid line) and D_2O (open circles) pumped at 263 nm and probed at 570 nm. The inset shows the same data at short times. Reprinted with permission from ref 53. Copyright 2003 American Chemical Society.

spectrum to longer wavelengths as a result of solvation dynamics. Time constants of 200 fs (15%) and 870 fs (85%) characterize these dynamics.[106] Even slower dynamics were observed for 2AP in ethanol,[106] as expected from this solvent's slower solvation time. In bulk ethanol, the transients on the blue side of the emission spectrum decayed with two lifetime components of 14 ps (50%) and a nanosecond component (50%). At the red edge of the spectrum, a rise with a time constant of 28 ps was observed in addition to a nanosecond component. Sharonov et al.[81] also reported a pronounced dependence of the fluorescence decay times on the emission wavelength in their study of m^5dCyd, as seen in Table 3.

The effects seen by Pal et al.[106] and by Sharonov et al.[81] are typical solvation effects for fluorophores whose lifetimes exceed the time scale of solvent reorganization. When the same experiments are carried out on the natural nucleobases, the decay times at all emission wavelengths are the same within experimental error for the nucleosides and nucleotides.[40,41,106] It would be interesting to confirm the lack of time-dependent spectral shifts for the natural bases by performing fluorescence upconversion experiments with higher time resolution.

Cohen et al.[53] performed the first femtosecond study of the S_1 lifetimes of the natural bases in solvents other than H_2O. They described femtosecond transient absorption experiments on Ade, m^7Ade, and m^9Ade in D_2O and in acetonitrile. The S_1 lifetime of m^9Ade was 50−100% shorter in water than in acetonitrile, while the lifetime of the longer lived S_1 state of m^7Ade was approximately unchanged. Similar trends were found when the fast and slow components of the Ade decays in both solvents were compared. In addition, Cohen et al. found no solvent kinetic isotope effect for Ade. As shown in Figure 9, identical dynamics were observed in H_2O and D_2O within experimental uncertainty.

The absence of a deuterium isotope effect indicates that proton transfer to or from the solvent is not the rate-limiting step in S_1 decay (see section 2.4.1). The similar dynamics observed in water and acetonitrile support the conclusion that protic solvents are not required for ultrafast decay. While much additional work is needed, the experimental evidence indicates that solvent effects on the singlet excited states of the DNA bases studied to date are quite modest. This naturally focuses attention on intramolecular relaxation pathways. Calculations of excited singlet states are invaluable for assessing these pathways, and they are discussed next.

2.2. Excited-State Calculations

Single DNA and RNA bases in their electronic ground states have been frequently investigated by quantum chemical methods.[107,108] Our focus here is on the smaller number of studies of excited singlet states of individual bases. Early calculations of excited states in DNA constituents were reviewed by Callis in 1983.[27] Since then, computing power has improved enormously, and a variety of new methods for calculating excited states have been introduced (vide infra). Routine modeling of solvent effects is now possible, enabling more realistic comparison with the large number of experimental studies in solution.

Several theoretical approaches are used to study molecular excited states. A relatively inexpensive ab initio method for modeling excited states is configuration interaction with single excitations (CIS).[109] This level of theory significantly overestimates transition energies since dynamic electron correlation is neglected. A common approach is to scale CIS transition energies by an empirical factor before comparison with experiment. A second technique is the complete active space self-consistent-field (CASSCF) method.[110] More accurate predictions are obtained from the so-called CASPT2 method, which applies multiconfigurational, second-order perturbation theory to a CASSCF reference wave function.[110] The use of multiconfigurational perturbation theory for modeling excited states is reviewed in ref 111. A further technique for generating high-quality excited-state wave functions is the CIPSI method,[112,113] a multireference second-order perturbation configuration interaction method, which has been extended to include solvation effects.[114] The CASPT2 method can also be extended to treat solvent effects,[115] but such calculations have not yet been done for the DNA bases.

Time-dependent density functional theory (TD-DFT) is an increasingly popular technique for calculating excited-state energies. It is fast and simple to use. TD-DFT calculations have given good agreement with experimental excitation energies for many molecules, but there are some indications of the method's limitations.[116] TD-DFT results can depend sensitively on the exchange-correlation functional employed, and all methods can show some variation with basis set. For example, inclusion of diffuse basis functions reduces the energies of $^1\pi \rightarrow \pi^*$ transitions in Cyt[117] and Gua.[118] As with the previously discussed methods, solvent effects can be treated within the TD-DFT formalism.[119] Finally, the recently introduced multireference configuration interaction DFT method (MRCI/DFT)[120] shows great promise as it can obtain

Table 4. Lowest Calculated Vertical Excitation Energies (eV) for 7H and 9H Tautomers of Adenine[a]

type	7H-Ade	9H-Ade	method	ref
$\pi\pi^*$	4.61 (0.050)	5.13 (0.070)	CASPT2	123
$\pi\pi^*$	4.97 (0.187)	5.20 (0.370)		
$n\pi^*$	*b*	6.15 (0.001)		
$\pi\pi^*$	4.45 (0.160)	4.61 (0.350)	scaled CIS[c]	91
$\pi\pi^*$	4.81 (0.082)	4.67 (0.065)		
$n\pi^*$	5.01 (0.005)	5.11 (0.001)		
$\pi\pi^*$		4.58 (0.380)	scaled CIS[c]	124
$\pi\pi^*$		4.64 (0.040)		
$n\pi^*$		5.08 (0.001)		
$n\pi^*$	4.80 (0.001) [+0.32]	4.97 (0.000) [+0.14]	TD-DFT(B3LYP)	126
$\pi\pi^*$	4.97 (0.093) [+0.00]	5.08 (0.167) [−0.06]		
$\pi\pi^*$	5.36 (0.002) [−0.01]	5.35 (0.065) [−0.06]		
$n\pi^*$	4.85 (0.071)	4.96 (0.001) [+0.07]	CIPSI	126
$\pi\pi^*$	4.89 (0.076) [−0.25]	4.97 (0.010) [−0.36]		
$\pi\pi^*$	5.56 (0.037) [−0.56]	5.34 (0.359) [−0.36]		
$n\pi^*$		5.04 (0.005)	TD-DFT(B3LYP)	135
$\pi\pi^*$		5.09 (0.205)		
$\pi\sigma^*$		5.11 (0.001)		
$\pi\pi^*$	4.42 (0.02) [+0.02]	4.62 (0.38) [−0.03]	scaled CIS[d]	125
$\pi\pi^*$	4.54 (0.16) [+0.25]	4.71 (0.01) [+0.01]		
$n\pi^*$	4.75 (0.07) [+0.32]	4.72 (0.01) [+0.40]		

[a] The oscillator strength in vacuo follows each transition energy in parentheses. The energy change (eV) upon solvation is given in brackets, if available. Consult the references for details about the calculations and solvation model used. [b] $n \rightarrow \pi^*$ transitions not reported. [c] Scaled by 0.72. [d] Scaled by 0.70.

Table 5. Lowest Vertical Excitation Energies (eV) Calculated for 7H-Keto and 9H-Keto Tautomers of Guanine[a]

type	7H-Gua	9H-Gua	method	ref
$\pi\pi^*$		4.76 (0.133) [−0.03]	CASPT2	123
$\pi\pi^*$		5.09 (0.231) [+0.02]		
$n\pi^*$		5.79 (0.000)		
$\pi\pi^*$	4.32 (0.245) [+0.00]	4.44 (0.345) [+0.07]	scaled CIS[b,c]	122
$n\pi^*$	4.60 (0.001) [+0.70]	4.53 (0.002) [+0.71]		
$\pi\pi^*$	5.12 (0.098) [+0.03]	5.05 (0.104) [−0.06]		
$\pi\pi^*$	4.94 (0.155) [−0.58]	4.76 (0.135) [−0.35]	CIPSI	140
$\pi\pi^*$	5.55 (0.157) [−0.56]	5.64 (0.184) [−0.70]		
$\pi\pi^*$		4.96 (0.161)	TD-DFT(B3LYP)	136
$n\pi^*$		5.33 (0.008)		
$\pi\pi^*$		5.40 (0.173)		

[a] The oscillator strength follows each transition in parentheses. The energy change (eV) upon solvation is given in brackets, where available. Consult the references for details about the solvation model used. [b] Scaled by 0.703. [c] Excited states are calculated for unconstrained (nonplanar) geometries.

results of quality comparable to that of results obtained by TD-DFT(B3LYP) at a fraction of the computational cost.[121]

The electronic structure of the individual nucleobases is complex because of the existence of multiple $^1\pi \rightarrow \pi^*$ and $^1n \rightarrow \pi^*$ transitions in the low-energy region. For example, m^{9}Ade has five $^1\pi \rightarrow \pi^*$ transitions between 180 and 300 nm in addition to a number of poorly characterized $^1n \rightarrow \pi^*$ transitions.[91] It is generally assumed that the nucleosides and nucleotides differ insignificantly in electronic structure from the free bases, but steady-state and time-resolved fluorescence measurements have occasionally identified subtle differences.[64] Insofar as these differences do not reflect changes in tautomer populations, they could indicate subtle electronic structure effects. To date, no calculations have been reported on excited states of nucleosides or nucleotides.

After reviewing in vacuo calculations in the next section, we review solvation effects on the lowest excited singlet states in section 2.2.2, and finally discuss optimized excited-state geometries in section 2.2.3.

2.2.1. Lowest Singlet States: Vertical Transition Energies

Tables 4−6 list vertical transition energies and oscillator strengths calculated since 1995 for the lowest three or four excited singlet states of the five bases. These quantities have been computed most often, enabling broad comparisons to be made. We include details about the exchange-correlation functional used in TD-DFT studies, but the reader is referred to the original publications for basis set details. Studies have been included in Tables 4−6 generally only when both $^1\pi\pi^*$ and $^1n\pi^*$ excited states were calculated because the latter states are thought to be vitally important for ultrafast internal conversion (see section 2.4.2). Comparing results that calculate both states also highlights differences between theoretical methods. The $^1\pi \rightarrow \pi^*$ transitions are highly allowed, and most computational studies predict transition energies in reasonable agreement with the measured values. On the other hand, reliable experimental data for the $^1n \rightarrow \pi^*$ transitions is lacking because of their low oscillator strengths and the difficulties of detecting these weak transitions when they are overlapped by the much stronger

Table 6. Lowest Vertical Excitation Energies (eV) Calculated for the Pyrimidine Bases[a]

type	Cyt	Thy	Ura	method	ref
nπ^*		4.39 (0.00019)	4.54 (0.00018)	CASPT2	101
$\pi\pi^*$		4.88 (0.17)	5.00 (0.19)		
$\pi\pi^*$	4.39 (0.061)			CASPT2	132
nπ^*	5.00 (0.005)				
$\pi\pi^*$	4.50 (0.065)			CASPT2	141
nπ^*	4.88 (0.001)				
nπ^*	5.23 (0.003)				
nπ^*			4.01 (0.0008) [+0.09]	MM/INDO	142
nπ^*			4.76 (0.0000) [+0.00]		
$\pi\pi^*$			5.05 (0.39) [−0.05]		
nπ^*		4.22 (0.000)	4.20 (0.001)	scaled CIS[b]	133
$\pi\pi^*$		4.75 (0.505)	4.82 (0.502)		
$\pi\pi^*$	4.39 (0.151)			scaled CIS[b]	133
nπ^*	4.52 (0.001)				
$\pi\pi^*$	4.71 (0.036)			TD-DFT(B3LYP)	134
nπ^*	4.76 (0.002)				
nπ^*	5.15 (0.001)				
$\pi\pi^*$	4.64 (0.043) [+0.18]			TD-DFT(B3LYP)	117
nπ^*	4.77 (0.001) [+0.45]				
nπ^*	5.11 (0.001) [+0.43[c]]				
nπ^*		4.76 (0.0001)		TD-DFT(B3LYP)	136
$\pi\pi^*$		5.17 (0.124)			
nπ^*		5.89 (0.0000)			
nπ^*			4.69 (0.000) [+0.20]	scaled CIS[d]	143
$\pi\pi^*$			4.92 (0.446) [−0.07]		
nπ^*			4.61 (0.0002)	DFT/MRCI/TZVPP + Ryd	144
$\pi\pi^*$			5.44 (0.263)		
nπ^*			4.64	TD-DFT(B3LYP)	121
$\pi\pi^*$			5.11		
$\pi\pi^*$			5.85		

[a] Results are only presented for the highest level of theory used in each study. Oscillator strengths are in parentheses. The canonical tautomer was studied for each base. The energy change (eV) upon solvation is given in brackets. Consult the original literature for details of the solvation model used. [b] The scale factor is 0.697. [c] Solvation changes this state from S_3 to S_4. [d] The scale factor is 0.72.

$^1\pi \rightarrow \pi^*$ transitions. It is not surprising then that there is considerable agreement among theoretical studies about the energetics of the "bright" $^1\pi\pi^*$ states, and considerable disagreement about the locations of the "dark" ^{1}nπ^* states. The answer is of more than academic interest because of the vital role that dark states such as ^{1}nπ^* and $^1\pi\sigma^*$ have been suggested to play in radiationless decay by the bases (see sections 2.4.2 and 2.4.3).

Tautomerism must also be considered in electronic structure studies of the bases. The experimental work on 7H/9H tautomerism in Ade (section 2.1.3) is an excellent example of how individual tautomers differ in excited-state properties. Fortunately, it is rarely necessary to consider the electronic structure of more than one tautomer for condensed-phase work because the (deoxy)ribosyl-substituted bases found in DNA and RNA polymers are generally present in a single tautomeric form. Thus, calculations on 9H-Ade are the only ones relevant to the dynamics of the Ade nucleoside and nucleotide. Nonetheless, many theoretical studies have modeled both 7H and 9H tautomers of the purine bases in deference to the long-standing interest in Ade tautomerism, and we include results for both tautomers in Tables 4 and 5. It is also true that multiple tautomers are frequently detected in supersonic jet experiments (see section 2.3), making excited-state modeling of different tautomers necessary for understanding results from those experiments.

The vertical transition energy is the difference in energy between an excited state and the ground state evaluated at the optimized geometry of the ground state. It can therefore depend sensitively on the ground-state geometry used in the calculations. For example, constraining the ground state of Gua to be planar alters the lowest vertical excited states.[122] According to CIS calculations by Shukla et al.,[122] the three lowest excited singlet states, S_1, S_2, and S_3, of the 7H-keto and 9H-keto tautomers optimized in the C_s point group in the gas phase are $^1\pi\pi^*$, ^{1}nπ^*, and ^{1}nπ^*, respectively. Optimizing these tautomers without any constraints leads to nonplanar geometries in the electronic ground state, and a new order for the vertical excited-state energies: $S_1(^1\pi\pi^*)$, $S_2(^1$n$\pi^*)$, and $S_3(^1\pi\pi^*)$.[122] The results of calculations on Ade, Gua, Cyt, Thy, and Ura will be briefly reviewed next.

Adenine. As shown in Table 4, CIS, CASPT2, CIPSI, and TD-DFT calculations all predict two nearby $^1\pi\pi^*$ states.[91,123−126] Numerous experimental studies have shown that the lowest energy absorption band of Ade and its derivatives consists of two closely spaced $^1\pi \rightarrow \pi^*$ transitions.[91,127,128] For dAdo these two states are split by 0.16 eV in the molecular crystal.[128] From linear dichroism and isotropic absorption measurements in stretched poly(vinyl alcohol) films, Holmén et al. found that the two lowest energy $^1\pi \rightarrow \pi^*$ transitions of m^{9}Ade are separated by 0.26 eV.[91] Experimentally, the lowest energy transition has the smaller oscillator strength,[91,128] consistent with CASPT2[123] and CIPSI[126] results. For both 7H- and 9H-Ade, CIS and CASPT2 predict S_1 to be a $^1\pi\pi^*$ state, while TD-DFT calculations predict a lowest energy ^{1}nπ^* state. CASPT2 calculations

predict that the lowest $^1n\pi^*$ state lies ~1 eV above the $^1\pi\pi^*$ states.

Guanine. Gua has keto and enol tautomers in addition to the 7H and 9H tautomers found in Ade. All four tautomers have now been observed in supersonic jet experiments,[129−131] which are described in section 2.3. The enol forms are calculated to have significantly higher transition energies than the keto forms,[122] a prediction which agrees qualitatively with gas-phase experiments by Mons et al.[131] Most authors have calculated excited-state properties of the 7H-keto and 9H-keto tautomers because these forms are predicted to be lowest in energy in solution. All computational studies in Table 5 predict that the lowest energy transition is $^1\pi \rightarrow \pi^*$ for both tautomers. However, Langer and Doltsinis reported that addition of diffuse basis functions to TD-DFT calculations results in a lowest energy $^1n \rightarrow \pi^*$ transition for the 9H-keto tautomer.[118] In their paper, Langer and Doltsinis only list transition energies for the lowest $^1\pi \rightarrow \pi^*$ transition, and their results are therefore not included in Table 5. It does not appear that a TD-DFT study on both $^1n\pi^*$ and $^1\pi\pi^*$ excited states has been published for Gua. By comparing the CASPT2 calculations in Tables 4 and 5, it can be seen that the state order is $S_1(^1\pi\pi^*) < S_2(^1\pi\pi^*) < S_3(^1n\pi^*)$ for both purine bases at this level of theory.[123] The energy gap between the two lowest $^1\pi\pi^*$ states is, however, larger for Gua than for Ade. For the 9H tautomers of Ade and Gua CASPT2 calculations predict that the lowest $^1n \rightarrow \pi^*$ transition is ~1 eV higher than the lowest $^1\pi \rightarrow \pi^*$ transition.

Cytosine. Cyt is predicted to have a lowest energy $^1\pi \rightarrow \pi^*$ transition in recent computational studies (see Table 6).[117,132−134] There is good consensus that S_2 is a $^1n\pi^*$ state located close in energy to S_1.[117,132−134] The spacing between these states is smaller for scaled CIS than for CASPT2, and the smallest spacing is observed in the TD-DFT calculations.

Thymine and Uracil. Ab initio calculations predict a lowest energy $^1n \rightarrow \pi^*$ transition for Ura and Thy in vacuo (see Table 6), in contrast to what has been found for the other bases, with the exception of the TD-DFT calculations for Ade.[126,135] The presence of a lowest energy $^1n\pi^*$ state in vacuo may be responsible for the absence of sharp vibronic resonances in supersonic jet experiments on these bases (see section 2.3). Neiss et al.[121] calculated transition energies for Ura at CIS and TD-DFT levels of theory as a function of basis set size. They found that $^1n \rightarrow \pi^*$ excitation energies were largely invariant to the size of the basis set, while $^1\pi \rightarrow \pi^*$ transitions red-shifted by 0.2−0.3 eV as basis set size increased. The entry in Table 6 is for the largest basis set used in ref 121. Table 6 includes our unpublished results for Thy at the TD-DFT level of theory.[136] These calculations were done with the B3LYP functional and the 6-31G* basis set using the Gaussian 03 program.[137] The same basis set was used for geometry optimization with no symmetry constraints and for the calculation of vertical excitation energies. Note that Table 5 contains a similar calculation for 9H-Gua.[136] Inspection of Table 6 shows that results for Thy (m^5-Ura) and Ura are similar and that essentially all studies agree on the state order.

Results in Tables 4−6 must be compared with caution due to the very different methods used. Nevertheless, we comment briefly on one general pattern. The bright $^1\pi\pi^*$ states have relatively well characterized energies, so the most interesting comparison is to consider the $^1n\pi^*$ states, and this is where the greatest differences are found. With the exception of Thy and Ura, there is significant disagreement between CASPT2 and TD-DFT about the location of the $^1n\pi^*$ excited states relative to the $^1\pi\pi^*$ ones. Compared with CASPT2, TD-DFT predicts slightly higher and significantly lower transition energies for the $^1\pi \rightarrow \pi^*$ and $^1n \rightarrow \pi^*$ excitations, respectively.

Which method correctly describes the vertical state order? Holmén et al.[91] argue that semiempirical INDO/S calculations agree well with the experimental $^1n \rightarrow \pi^*$ and $^1\pi \rightarrow \pi^*$ transition energies of 9-methylpurine and 2-amino-9-methylpurine, especially after correcting the theoretical values upward by ~500 cm^{-1}. Applying the same theoretical method to Ade in water, they suggest that the lowest $^1n \rightarrow \pi^*$ transition for 9-substituted adenines, including 9H-Ade, should be nearly isoenergetic with the lowest $^1\pi \rightarrow \pi^*$ transition.[91] If this is true, then only the TD-DFT calculations have the correct vertical state order, while the CIS and CASPT2 methods place the $^1n\pi^*$ states too high in energy. This conclusion is also suggested by CIPSI calculations by Mennucci et al.[126] The authors state that this method provides a more balanced description of all excited states. As seen in Table 4, Mennucci et al.[126] obtained essentially the same in vacuo transition energies for Ade by the TD-DFT and CIPSI methods. In section 2.3, experimental studies will be discussed that indicate a lowest energy $^1n\pi^*$ state for Ade.[138,139] Finally, in section 2.4, the issue of whether state proximity correlates with lifetimes will be addressed.

2.2.2. Solvent Effects

Incorporating solvent effects into calculations allows comparisons to be made with the large number of solution-phase experiments. The simulated solvent is almost always water because of its obvious biological importance. The self-consistent reaction field (SCRF) method is used most often,[123,125,145] but a growing number of works have investigated specific solute−solvent effects by including a small number of discrete solvent molecules.[122,143,145] In Tables 4−6, the change in transition energy upon solvation is given in brackets. Generally, $^1n \rightarrow \pi^*$ transitions increase in energy upon solvation, while $^1\pi \rightarrow \pi^*$ transition energies are perturbed only slightly. This finding holds for CIS, CASSCF, and TD-DFT, independent of whether the solvent is modeled as a dielectric continuum, or whether explicit solvent molecules are included.

The calculations thus confirm the well-known experimental observation that increasing the solvent polarity causes blue shifting of $^1n \rightarrow \pi^*$ excitations. In essence, the ground electronic state is stabilized more effectively by water than the $^1n\pi^*$ state, on account of the reduced ability of the latter state to

form hydrogen bonds. The $^1\pi\pi^*$ states are not perturbed greatly, and similar hydrogen bonding is found in the excited state. Blue shifting of $^1n \rightarrow \pi^*$ transitions of 2AP was observed in an SCRF study by Rachofsky et al.,[146] who concluded that dipolar electrostatic interactions can account for much of this effect.

The greater solvent sensitivity of $^1n\pi^*$ states leads to changes in state order, especially when in vacuo calculations predict a $^1n\pi^*$ state to be slightly lower in energy than a $^1\pi\pi^*$ one. For example, Shukla and Leszczynski[117] observed an interchange of the S_3 and S_4 states of Cyt upon solvation. For Ura, the same authors found that the lowest transition was $^1n \rightarrow \pi^*$ in the gas phase, while hydration led to a lowest energy $^1\pi \rightarrow \pi^*$ transition.[143] In contrast, Broo et al.[142] found that solvation did not alter the in vacuo energy of the $^1n\pi^*$ state of Ura. Using the integral equation formalism polarized continuum model (IEF-PCM), Mennucci et al.[126] found that the lowest $^1n\pi^*$ state of Ade shifts to near degeneracy with the lowest $^1\pi\pi^*$ state. The only exception to the lack of a solvent effect on $^1\pi \rightarrow \pi^*$ transitions comes from CIPSI calculations by Mennucci et al.[126] These authors observed a dramatic red shift of both $^1\pi\pi^*$ excited states of Ade in their IEF-PCM solvation model. This model was stated to be particularly suitable for modeling vertical transitions, but no other studies have predicted such large shifts.

In addition to state reordering, tautomeric equilibria can be affected by solvation, and this possibility must be considered before calculations are compared to experiment. This is most evident for Ade, where the 9H tautomer is the only tautomer present in the gas phase,[147] but the higher dipole moment of the 7H tautomer allows it to be dramatically stabilized by a polar solvent such that it accounts for 20% of the total population in aqueous solution at room temperature.[53,90,148] In Cyt and Gua, the opposite effect occurs, and aqueous solvation reduces rather than increases the number of significantly populated tautomers.[140]

2.2.3. Excited-State Geometries

Determining the minimum-energy geometry in an excited electronic state is immensely challenging. Frequently, the most accurate methods for calculating excited-state wave functions cannot be used because they lack analytical gradients, and geometry optimization must be performed at a lower level of theory, making the predictions of uncertain value. It is also nearly impossible to calibrate these predictions by experiment, because so little information is available about excited-state geometries. With this warning, some general comments are made in this section about excited-state geometries found in quantum chemical studies.

Geometry optimization of the excited singlet states of the DNA bases frequently leads to nonplanar geometries.[117,118,122,124,133] The nonplanar distortions include ring puckering, folding of the purine bases along the C4−C5 bond that joins the five- and six-membered rings, and amino group pyramidalization. Besides loss of planarity, single- and double-bond inversion is commonly observed in $^1\pi\pi^*$ excited states; examples include Ade,[124] Gua,[149] Cyt,[134,149] and Ura.[143] Pyramidalization of the amino group in Cyt,[117] Ade, and several Ade derivatives in the electronic ground state[124] is often predicted by methods that include electron correlation. Further pyramidalization and amino group twisting are observed in the lowest $^1\pi\pi^*$ excited state, especially for 7H-Ade[124] and the N6-alkylated adenines.[150] This has led to the suggestion that some Ade derivatives undergo ultrafast internal conversion via a twisted intramolecular-charge-transfer (TICT) state.[150,151]

Geometry optimization can have more drastic implications for excited-state decay, in that it often leads to reordering of the excited states compared to the order calculated at the Franck−Condon geometry. Shukla and Mishra[133] found that optimizing the geometry of Cyt and Thy switches the order of the $^1\pi\pi^*$ and $^1n\pi^*$ states of the isolated molecule. For Cyt, other calculations predicted that the $^1n\pi^*$ state becomes lowest in energy during excited-state relaxation.[117,134] Mennucci et al.[126] found in their TD-DFT study of 9H-Ade that a $^1n\pi^*$ state lies above the $^1\pi\pi^*$ state at the ground-state geometry, but becomes lower in energy upon nuclear relaxation in the excited state, in agreement with an earlier finding by Broo.[124] Such state crossings can indicate the presence of significant nonadiabatic couplings, a topic that will be discussed later in section 2.4.3.

2.3. Photophysics of Isolated Bases: Supersonic Jet Experiments

Experiments in supersonic jets reveal the intrinsic excited-state dynamics of the bases.[20] By comparing experimental results for isolated bases with ones obtained in solution, the role of the solvent in radiationless decay can be understood. It is also interesting to compare results from molecular beam experiments with quantum chemical calculations,[20] which most often model isolated molecules. Several excellent reviews of supersonic jet experiments on DNA bases have appeared recently,[130,152,153] and our chief aim in presenting this material is to compare the results, especially time-resolved ones, with those of the femtosecond solution-phase experiments described in section 2.1.

This section is organized as follows: After describing the vibronic spectra that have been measured for jet-cooled bases, we will compare the observed transition energies with the quantum chemical calculations described in the previous section. Next, we will review the growing number of time-resolved experiments performed under isolated molecule conditions, and compare these findings with ones from high-temperature solution-phase and low-temperature matrix experiments.

Thy and Ura were the first nucleobases studied in supersonic jet expansions.[154,155] The spectra recorded in these pioneering experiments showed only broad and diffuse bands, and the lack of sharp vibronic features discouraged further efforts for many years. Then, Nir, de Vries, and their co-workers[156] showed in 1999 that sharp transitions could be observed in jet-cooled Gua. Since that time, sharp vibronic transitions have been found in supersonic expansions of

Ade and Cyt, and study of the electronic spectroscopy of isolated bases has grown rapidly.[20]

Vibronic resonances of isolated molecules are detected most often by resonance-enhanced multiphoton ionization (REMPI) or laser-induced fluorescence (LIF). Dynamics may be inferred indirectly from spectral line widths measured by either method. Missing or very weak transitions may indicate rapid excited-state relaxation. For example, if the laser pulse durations are long compared to the time scale of excited-state decay, REMPI ion signals can decrease dramatically in intensity or vanish altogether as the rate of nonradiative decay becomes competitive with the rate of optical pumping to the ionizing level.[157−159] Thus, Nir et al. have commented that the apparent failure to detect 9-substituted guanines, including Guo, in molecular beam experiments, may reflect the very short excited-state lifetimes of these species.[130] On the other hand, the observation of a strong ion signal when nanosecond excitation and ionization pulses are used may indicate a long-lived excited state. In this case, fluorescence lifetimes can be directly measured by time-resolved LIF.[131] Pump−probe REMPI detection with picosecond[147] and femtosecond[93,94] laser pulses has been used to characterize even shorter lived excited states, as will be discussed below.

A notable success of workers in this field has been the assignment of individual vibronic transitions to specific tautomers.[130,153] This is accomplished by comparing IR absorption frequencies measured in spectral hole-burning or double-resonance experiments with ones calculated by quantum chemical methods. Tautomer identification is critical because individual tautomers can have dramatically different excited-state properties, as discussed in section 2.1.3 for Ade in aqueous solution. In addition, the DNA bases are generally detected in a number of tautomeric forms in the supersonic jet experiments. One reason for the apparently greater tautomeric complexity in the jet experiments may be that true thermodynamic equilibrium is not attained in the supersonic expansion.[131]

Figure 10 shows the one-color REMPI spectrum recorded by Kim and co-workers for jet-cooled Ade.[138] This spectrum has features typical of REMPI and LIF spectra of the other bases. Sharp vibronic transitions are seen at low energy, which gradually give way to unstructured and continuous absorption at higher energy. Kim et al.[138] assigned the strong transition labeled D in Figure 10 at 36 108 cm^{-1} to the origin of a $^1\pi \rightarrow \pi^*$ transition. Other workers have agreed with this assignment.[130,147,160] Lührs et al.[147] observed similar REMPI spectra for Ade and m^9Ade. Plützer et al.[161] showed by IR−UV double-resonance spectroscopy that the more intense bands at >36 050 cm^{-1} have IR spectra that agree best with ab initio predictions for the 9H tautomer. Thus, the $^1\pi \rightarrow \pi^*$ origin (peak D in Figure 10) is due to 9H-Ade.

Kim et al.[138] observed several weaker peaks (labeled A and B in Figure 10) below the $^1\pi \rightarrow \pi^*$ origin. They assigned the redmost feature labeled A at 35 503 cm^{-1} to the origin of a $^1n \rightarrow \pi^*$ transition. The appreciable intensity of this peak is explained by

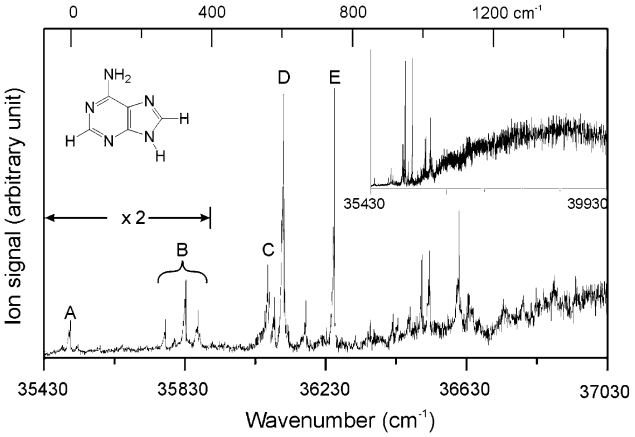

Figure 10. One-color R2PI spectrum of isolated Ade. The relative ion intensity scaling was determined by the use of spectra that contain both segments of the spectrum. Band A is the origin of the $^1n \rightarrow \pi^*$ transition, and band D is the origin of the $^1\pi \rightarrow \pi^*$ transition. The top scale is in wavenumbers relative to the $^1n \rightarrow \pi^*$ origin. The inset shows the larger spectrum, which includes most of the broad absorption band. Reprinted with permission from ref 138. Copyright 2000 American Institute of Physics.

extensive mixing with the highly allowed $^1\pi \rightarrow \pi^*$ transition.[138] The identification of a $^1n\pi^*$ electronic state has been controversial. Thus, Lührs et al.,[147] who detected the weak A and B bands only at high laser intensity, suggested that these peaks arise from a minor tautomer produced by the higher nozzle temperature of Kim and co-workers. However, recent experiments have shown that the weak bands observed by Kim et al.[138] are reproducible. Nir et al.[130] showed that the A band of Figure 10 has the same IR spectrum as the much stronger band at 36 105 cm^{-1}. Both bands must therefore originate from the same 9H-amino tautomer of Ade. Nir et al.[130] and Plützer and Kleinermanns[160] concluded that the weak A band is associated with a $^1n \rightarrow \pi^*$ transition, as suggested previously by Kim and co-workers.[138] Nir et al.[130] assigned a band in their spectrum at 35 824 cm^{-1}, corresponding to peak B in Figure 10, to 7H-Ade, which is present as a minor species.

In light of the considerable experimental and theoretical evidence for two closely spaced $^1\pi\pi^*$ states for Ade (section 2.2.1), it is striking that none of the vibronic features observed so far in the jet experiments have been assigned to a second $^1\pi\pi^*$ state. Nir et al.[130] considered this possibility for the band in their spectrum at 35 497 cm^{-1}, but rejected this possibility because of this line's low intensity compared to the band at 36 105 cm^{-1}. As discussed above, the 35 497 cm^{-1} band was instead assigned to the origin of a $^1n \rightarrow \pi^*$ transition.

Origin transition energies for all bases are summarized in Table 7. There has been some debate about whether the 0−0 transitions have really been located in these experiments. The REMPI resonances are often more closely spaced than expected from the vibrational structure of the ground states.[147,162,163] Nir et al.[163] noted that the redmost line in their REMPI spectrum of Cyt is not the most intense, but they discounted a large geometry change in the excited state, which would explain this observation, on the basis that such a change is unlikely for an aromatic

Table 7. Origin Transition Frequencies (cm^{-1}) of Jet-Cooled Nucleobases[a]

Ade	Gua	Cyt	ref
35 503 (4.402), $^1n \rightarrow \pi^*$			138
36 108 (4.477)			
	34 443 (4.270), Guo		176
36 101 (4.476)	32 878 (4.076)		162
35 550 (4.408), Ado	34 492 (4.276), Guo		
36 105 (4.476), 9H tautomer			147
36 136 (4.480), m^9Ade			
	32 864 (4.075), 7H-enol		131
	33 269 (4.125), 7H-keto		
	33 910 (4.204), 9H-keto		
	34 755 (4.309), 9H-enol		
		~32 000[b] (4.0), keto	163
		~36 000[c] (4.5), enol	

[a] Transition energies are for $^1\pi \rightarrow \pi^*$ transitions, unless otherwise indicated. Energies (eV) are shown in parentheses to facilitate comparison with results in other tables. [b] The origin is not identified in this study. Several vibronic peaks can be observed at frequencies below 32 000 cm^{-1}. [c] Vibronic peaks are superimposed on a diffuse band.

ring molecule. This is frequently true for aromatic hydrocarbons, but aromatic nitrogen heterocycles can become significantly nonplanar because of vibronic coupling between nearby $^1n\pi^*$ and $^1\pi\pi^*$ states, as indicated by the results in section 2.2.3. Strong interactions between nearby $^1n\pi^*$ and $^1\pi\pi^*$ states as a result of curve crossings could significantly broaden the adiabatic potential energy surfaces, leading to more closely spaced vibrational features.[163] The fact that vibronic peaks are seen only in a narrow energy range is consistent with curve-crossing behavior. Vibronic coupling between nearby $^1\pi\pi^*$ and $^1n\pi^*$ states offers an appealing explanation of many of the experimentally observed features, even though evidence for $^1n \rightarrow \pi^*$ transitions in the gas phase has been rather modest.

By measuring transition frequencies with millielectronvolt accuracy, the jet experiments provide a stringent test for quantum chemical calculations. At the current time, comparison is hardly fair since the best excited-state calculations have accuracies no better than ~0.1 eV. It is also important to note that the vertical transition energies from the calculations (Tables 4−6) are not the same as origin frequencies. The latter are adiabatic quantities, and the difference between the two reflects the energetic stabilization of the excited state upon nuclear relaxation. Because geometry optimization of excited states is presently so difficult, there have been few calculations of adiabatic excitation energies.[118,164]

From Table 7, the origin frequencies of the lowest energy $^1\pi \rightarrow \pi^*$ transitions of the canonical base tautomers increase in the order C < G < A, where C stands for the keto tautomer of Cyt, G stands for the 9H-keto tautomer of Gua, and A stands for the 9H-amino tautomer of Ade. The TD-DFT calculations summarized in Tables 4−6 predict the same order for the vertical transition energies. Roos and coworkers studied all five bases by the CASPT2 method.[101,123,132] This method, which is believed to be particularly accurate for the $^1\pi \rightarrow \pi^*$ transitions that are readily seen in absorption, yields the order Cyt < Gua < Thy < Ura < Ade, which again agrees with the order of the adiabatic transition energies from the molecular beam experiments. Daniels and Hauswirth[5] estimated 0−0 transition frequencies from the intersection point of the fluorescence and absorption spectra in aqueous solution, and found the order Gua < Thy < Cyt < Ade. The same order is seen for the nucleosides.[8] In this case, Cyt is not lowest in energy, but the difference may not be significant since all of the 0−0 frequencies are reported to be within ~1400 cm^{-1} of each other.[8]

A further test is whether the quantum chemical predictions about state order agree with results from molecular beam experiments. Unfortunately, evidence for a second excited electronic state has only been obtained for Ade. Kim et al.[138] first suggested that a vibronic feature seen 600 cm^{-1} below the $^1\pi \rightarrow \pi^*$ origin is the $^1n \rightarrow \pi^*$ origin. This is in better agreement with the TD-DFT predictions, provided that the adiabatic transition energies follow the same trends as the calculated vertical ones.

We now turn to time-resolved measurements of electronically excited, jet-cooled bases, obtained by pump−probe ionization techniques using nano-, pico-, and femtosecond laser pulses. Gua has a complex REMPI spectrum, arising from four distinct tautomers. Upon excitation of their respective origins, fluorescence lifetimes of 12, 22, 25, and 17 ns (all values ±2 ns) were observed by Chin et al.[129] for the 7H-enol, 7H-keto, 9H-keto, and 9H-enol tautomers, respectively. A broad absorption background was observed about 1000 cm^{-1} above the origin of each Gua tautomer in the jet experiments. Chin et al.[129] reported that fluorescence lifetimes could not be measured upon excitation into this broad background, indicating lifetimes of <10 ns.

Recently, He et al.[165] studied Thy and Ura and their methylated derivatives in molecular beam experiments. Using two-color REMPI detection, they determined that a significant fraction of the molecules excited in the UV relax to a lower lying "dark state", which has a lifetime of tens to hundreds of nanoseconds. Because a triplet state is expected to have a longer lifetime, He et al.[165] concluded that the long-lived state is most likely a $^1n\pi^*$ state. Although they were unable to measure a fluorescence lifetime, they did observe weak, red-shifted (relative to the solution phase) emission from this state. He et al. suggested that this state is strongly quenched by solvation with just one or two water molecules. On

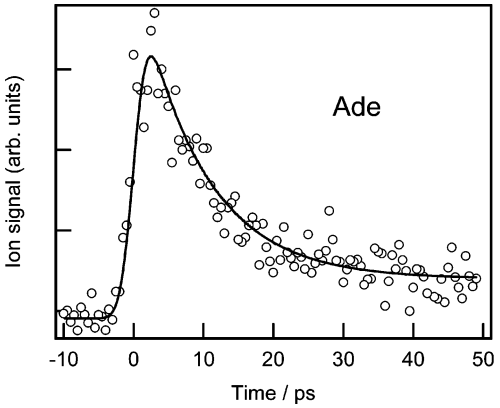

Figure 11. Time-resolved photoionization trace of the 36 105 cm^{-1} band of isolated Ade (circles). The line represents a convolution of a 9 ps exponential decay with the 3.5 ps instrument response function. Reprinted with permission from ref 147. Copyright 2001 The Owner Societies.

the basis of this finding, they concluded that ultrafast decay seen for Thy in the condensed phase is due to solvent interactions, and is not intrinsic to the gas-phase dynamics.[165] They argued that the offset is the same as one seen for thymine in femtosecond experiments by Kang et al.,[94] which will be discussed below.

In contrast, Lührs et al.[147] found evidence for much faster relaxation in two-color picosecond time-resolved photoionization experiments on Ade. In their experiment, excitation was at the $^1\pi \rightarrow \pi^*$ origin (276.9 nm, 36 105 cm^{-1}). Ionization was performed with a second variably delayed picosecond laser pulse at 290 nm. Their transient ion signal is reproduced in Figure 11. The 9 ps decay seen in their data corresponds to a homogeneous line width of 0.6 cm^{-1}. This value is probably too close to the spectral resolution to provide an independent check on the lifetime. Kim et al.[138] previously reported that the lifetime of Ade's origin band is <6 ns, the limit of their time resolution.

Lührs et al.[147] assigned the 9 ps lifetime to the S_1 lifetime of 9H-Ade, the majority tautomer in their molecular beam. Significantly, the signal in Figure 11 does not decay to the pump-only background signal level, but instead gives an offset. The long-lived offset, i.e., the persistence of an ionizable state, is presumably the reason that this band is detectable at all in the many experiments performed with nanosecond pulses. Lührs et al.[147] ruled out vibrationally highly excited molecules in S_0 as the source of the offset since Franck−Condon factors with the accessible ion states should be poor. They ruled out assignment to a $^1n\pi^*$ state for the same reason, arguing instead that a triplet state is responsible for the long-lived offset. It is unclear why a triplet state, which should also have significant vibrational energy, would have better Franck−Condon factors than a $^1n\pi^*$ state, which is believed to lie at higher energy.

Kang et al.[93,94] performed the first pump−probe transient ionization experiments on jet-cooled bases with femtosecond pulses. In their experiments, excitation was at 267 nm, high above the reported origin frequencies, and ionization was performed using three photons from the laser fundamental at 800 nm. Results from their work are shown in

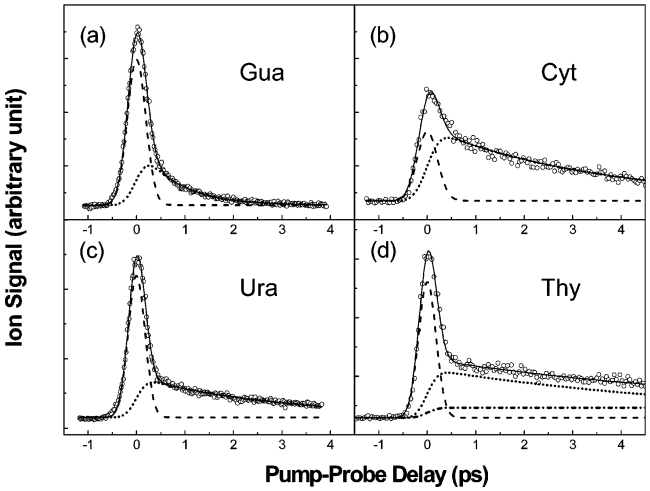

Figure 12. Time-resolved transient ionization signals of (a) Gua, (b) Cyt, (c) Ura, and (d) Thy at a pump wavelength of 267 nm. Circles: experimental data. Solid line: theoretical fit to the data. Dashed line: Gaussian component due to coherent absorption of pump and probe photons. Dotted line: fit of exponential decay convoluted with an instrument response function. Dashed−dotted line: fit of the triplet Thy signal. Lifetimes are 0.8, 3.2, and 2.4 ps for Gua, Cyt, and Thy, respectively. Thy was fit to a 6.4 ps short decay and a triplet decay with a lifetime >100 ps. Reprinted with permission from ref 94. Copyright 2002 American Chemical Society.

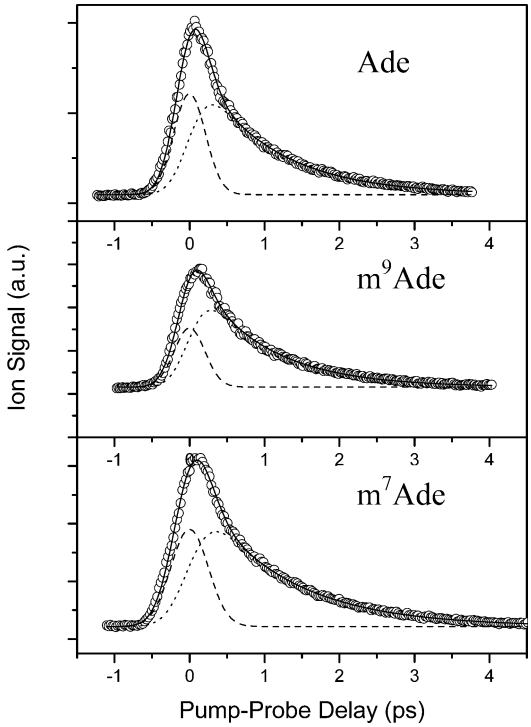

Figure 13. Transient ionization traces of Ade, m^9Ade, and m^7Ade pumped at 267 nm. The notation is the same as in Figure 12. The instrument response was 400 fs. Reprinted with permission from ref 93. Copyright American Institute of Physics.

Figures 12 and 13. At short times, a Gaussian component with significant amplitude was observed, which Kang et al.[94] attributed to ionization of a higher lying singlet state (at ~200 nm) that can only be accessed by coherent absorption of one pump and one probe photon, when pump and probe pulses

overlap. This signal contribution is shown by the dashed curves in Figures 12 and 13.

The remaining signal shown by the dotted curves decayed on an ultrafast time scale, and was assigned to decay of the S_1 states of the isolated nucleobases. From least-squares fitting, they determined lifetimes of 1.0, 0.8, 3.2, 6.4, and 2.4 ps for Ade, Gua, Cyt, Thy, and Ura, respectively.[94] Uncertainties were not stated. A longer decay component was additionally seen for Thy and assigned to a triplet state, which was proposed to have energy levels coincident with the experimental ionization scheme. Using the same technique, Kang et al.[93] reported lifetimes of 1.00 ± 0.05, 0.94 ± 0.03, and 1.06 ± 0.08 ps for Ade, m^9-Ade, and m^7Ade (see Figure 13).

The ultrashort decay times reported by Kim and co-workers[93,94] appear reasonable in light of the broad and diffuse bands observed ≥1000 cm^{-1} above the origin transition frequencies in the molecular beam experiments. In addition, the longer lifetimes reported by Kang et al.[94] for Cyt and Thy than for Ade and Gua match the pattern seen in solution-phase experiments on the corresponding nucleosides.[21] However, the order seen by Kang et al.[94] (Gua ≤ Ade < Ura < Cyt < Thy) differs from the one seen for the nucleosides in aqueous solution (Urd < Ado < Guo ≤ Thd < Cyd; see section 2.1.2). Moreover, the finding of Kang et al.[93] that m^7Ade and m^9Ade have identical lifetimes of ∼1 ps is surprising in light of the 40-fold difference for these two species in room temperature aqueous solution.[53] Since the solution phase generally leads to higher quenching rates compared to the gas phase, it is difficult to understand the longer lifetime seen for m^7Ade in solution.[53] It is difficult to conceive of a solvent effect that could account for this behavior.

Recently, the first femtosecond time-resolved photoelectron spectroscopy study of a base in a supersonic expansion was reported.[139] This powerful technique provides detailed information about electronically nonadiabatic dynamics.[166,167] Ullrich et al.[139] found two important bands in their time-resolved photoelectron spectra of Ade, which they assigned to $^1\pi\pi^*$ and $^1n\pi^*$ states. The bands were separated by ∼1 eV in energy since the $^1\pi\pi^*$ and $^1n\pi^*$ states correlate to different ion states. According to their analysis, excitation above the origin at 267 and 250 nm populated the optically bright $^1\pi\pi^*$ state, which decayed in <50 fs to a $^1n\pi^*$ state. This latter state then decayed to S_0 in 750 fs. Excitation closer to the origin resulted in a longer lifetime of >2 ps, but it was not possible to assign the electronic character of this state due to a decreased signal-to-noise ratio. The energy-integrated decays upon excitation at 267 and 250 nm were biexponential, in agreement with previous results of Lührs et al.[147] Following the latter authors, Ullrich et al.[139] assigned this long-lived offset to a triplet state. However, there is little definitive evidence for the latter assignment, and a second possibility is a persistent $^1n\pi^*$ state. A particularly intriguing aspect of this study is the finding that a $^1n\pi^*$ state acts as an intermediate during internal conversion from the initial, bright $^1\pi\pi^*$ state to S_0. The same paradigm was described in an ab initio study of cytosine by Ismail et al.,[134] as will be discussed later in section 2.4.3.

It is interesting to compare the experiments on very cold base monomers in supersonic jets with experiments in low-temperature solid hosts. DNA base fluorescence was studied extensively in low-temperature glasses in the 1960s, as described in reviews by Eisinger and Lamola[168] and by Daniels.[24] The fluorescence lifetimes of various mononucleotides are reported to be several nanoseconds in ethylene glycol/water glasses at 77 K.[169] This is in striking contrast to the femtosecond time scale deactivation seen in room temperature polar solvents. The fluorescence quantum yields are somewhat higher than at room temperature, but the quantum yields for fluorescence and phosphorescence are still considerably less than one, and internal conversion is the dominant decay pathway at low temperatures.[168] However, the radiative lifetime estimated from eq 1 is considerably longer than the value predicted from the Strickler−Berg equation, suggesting that emission may be from a state with forbidden character.[37]

More recent measurements have confirmed that various DNA bases have nanosecond singlet lifetimes at low temperature.[91,170,171] Hart and Daniels[170] reported biexponential decay by Ado in 1:1 ethylene glycol/water glass at 77 K. The observed lifetime components were 1.2 (59%) and 7.0 (41%) ns. As in the earlier matrix experiments, the radiative lifetime predicted from the measured lifetimes and ϕ_f was much longer than the Strickler−Berg estimate. Holmén et al.[91] measured a fluorescence lifetime of 2.0 ns and a quantum yield of 0.26 for m^7Ade in 9:1 ethanol/methanol glass at 100 K. In this case, however, the Strickler−Berg prediction was in reasonable agreement with experiment.

Polewski et al.[171] studied fluorescence from Gua in N_2 matrixes at 15 K. They observed single-exponential fluorescence decays with lifetimes of 9−10 ns. The emission spectrum, which did not obey the mirror-image rule, was independent of excitation wavelength between 180 and 280 nm. The emission spectrum had about the same width at 15 K in a N_2 matrix as in ethylene glycol/water glass at 77 K, but was shifted by 30 nm to longer wavelengths. Interestingly, no vibrational structure was observed despite the ultracold, nonpolar environment. The fact that even longer lifetimes were observed in the experiments of Chin et al.[129] on jet-cooled Gua suggests that some degree of quenching by the N_2 matrix occurs, even at 15 K. Polewski et al.[171] pointed out that the red-shifted emission of Gua in the less polar matrix at 15 K compared to the more polar ethylene glycol/water glass is consistent with emission from a lowest excited state with $^1n\pi^*$ character. The emission spectrum at 15 K in the N_2 matrix has many similarities with the dispersed fluorescence spectra of various jet-cooled Gua tautomers observed by Chin et al.[129]

The one exception to the rule that excitation near the origin produces long-lived states is the 9 ps lifetime measured for Ade by Lührs et al.[147] However, their suggestion that intersystem crossing is the dominant decay channel for isolated Ade is surprising for several reasons. First, the 5′-ribonucleotide of

adenine (AMP) has a low intersystem crossing quantum yield of 0.02 at 77 K in 1:1 ethylene glycol/water glass.[172] It is unlikely that a matrix at this temperature could suppress intersystem crossing so effectively. Furthermore, AMP has a nanosecond fluorescence lifetime at 77 K, as do the other bases.[169] It is difficult to imagine how the lifetime could decrease so dramatically from several nanoseconds at 77 K in the condensed phase to just 9 ps at the much lower temperature conditions in the jet expansion.

In our view, an alternative explanation for the 9 ps decay seen by Lührs et al.[147] is intramolecular relaxation from an initially excited $^1\pi\pi^*$ state to a $^1n\pi^*$ state. The latter state still has favorable Franck−Condon factors to the accessible ion states, although they are less favorable than those of the initial $^1\pi\pi^*$ state because of the geometry change that takes place. This explains the lower ion signal seen at long times in the Lührs et al.[147] experiment.

The complex behavior described to this point likely results from mixing of nearby electronic states. Chin et al.[129] pointed out how the dispersed fluorescence spectra observed from Gua consist of a few discrete emission lines and a broad, featureless emission band, which they suggest indicates two distinct fluorescent species. They assign the broad emission band to a $^1n\pi^*$ state, which is strongly vibronically coupled to the $^1\pi\pi^*$ state.[129] The ability of the dark state to undergo internal conversion to S_0 depends sensitively on the time scale of intra- and intermolecular energy relaxation pathways.

Collectively, the results of this section point out the remarkably complex singlet-excited-state dynamics of isolated base monomers. The singlet-state dynamics appear to be extremely wavelength dependent. Optical preparation of excited states with significant vibrational excess energy leads to deactivation on a time scale of ~1 ps, while excitation closer to the origin produces states that live for tens of nanoseconds. No such wavelength dependence has been observed for emission from bases in condensed-phase environments, whether at low or high temperature, although there is a need for further experimental confirmation. Nonradiative decay rates generally increase with the amount of excess vibrational energy above the electronic origin, especially when that energy is deposited in low-frequency out-of-plane modes.[173−175] This pronounced sensitivity to excess vibrational energy is one of the hallmarks of vibronically coupled electronic states,[174] a theme that is continued in the next section.

2.4. Nonradiative Decay Mechanism

An excited singlet state can decay nonradiatively to a triplet state by intersystem crossing or to the electronic ground state by internal conversion. Nonradiative decay can also transform the initial excited state into a distinct chemical species. Intersystem crossing will not be discussed further because internal conversion is the dominant decay pathway for the DNA bases.[8] We review proposals for photochemical quenching of S_1 in section 2.4.1, and finish this section with discussion of photophysical decay in the weak and strong vibronic coupling limits in sections 2.4.2 and 2.4.3, respectively.

2.4.1. Photochemical Decay

There have been proposals from time to time that an excited-state photoreaction quenches the fluorescent singlet states of the DNA bases,[168,177] but photoproducts have never been detected in the high yields necessary to explain the ultralow fluorescence quantum yields. The detection of strong transient absorption signals at near-UV wavelengths (discussed in section 2.1.2) provides strong evidence that the overwhelming majority of excited molecules return in <1 ps to the electronic ground state. Of course, it is still possible that a transient photochemical intermediate formed initially rapidly repopulates the electronic ground state of the initially excited base in a second nonadiabatic step. An example of internal conversion via a photochemical intermediate is the aborted H atom dissociation mechanism invoked to explain quenching of $^1n\pi^*$ excited states in protic solvents.[178] A second example is the formation of a TICT state that subsequently reverts, perhaps radiatively, to the electronic ground state. In fact, dual emission bands consistent with the TICT hypothesis have been detected for N6-dialkylated adenines.[150,151,179] Because this mechanism is specific to only a few Ade derivatives, it will not be considered further.

The ultrashort S_1 lifetimes indicate that any photochemical reaction in the excited state must take place on a time scale of hundreds of femtoseconds in a nearly barrierless process. Reactions that occur on this time scale include proton- and hydrogen-atom-transfer reactions. Intermolecular proton transfer in which a solvent molecule acts as proton donor or acceptor is conceivable, but the observation of ultrafast decay by Ade in protic and aprotic solvents suggests that this is not the case.[53] A further possibility is excited-state proton transfer between the partners in a base pair. This decay mechanism is irrelevant to single bases, but could be important in nucleic acid duplexes (see section 3.3.2). Finally, conversion of one tautomeric form to another via an intramolecular hydrogen atom transfer is a further possibility for ultrafast photochemical decay. There are now many examples of excited-state intramolecular-proton-transfer (ESIPT) reactions that take place on the femtosecond time scale.[180−183] Nonetheless, the absence of a deuterium isotope effect on the S_1 lifetime of Ade[53] and the similar kinetics observed in protic and aprotic solvents argues against excited-state deactivation by tautomer interconversion.

The possibility of excited-state tautomerism has been investigated for all of the bases computationally.[117,122,133,143,164,184] The new tautomer produced in the excited state could decay by reverse proton transfer to the ground state of the original tautomer, or it could persist in solution. The former possibility is frequently encountered in enol → keto ESIPT reactions, while Salter and Chaban[164] suggest that the latter is the reason UV-irradiated solutions of Ade develop a new absorption band at 300 nm. They calculated the barrier to hydrogen atom transfer from N9 to N3 using the intrinsic reaction coordinate method to be 63.0 kcal mol^{-1} in S_0 and 43 kcal mol^{-1} in the $^1\pi\pi^*$ excited state along a minimum-energy

path.[164] This high barrier suggests, however, that phototautomerism should be insignificant for isolated Ade, and cannot explain the picosecond and subpicosecond dynamics observed in the molecular beam experiments.[93,94,139,147]

N9 to N7 phototautomerism in Gua was investigated by Mennucci et al.[140] They suggested that protonation of the 9H form occurs in the excited state at N7. This cation is subsequently claimed to deprotonate, forming an electronically excited 7H tautomer, which subsequently decays by emission. The authors did not attempt to explain the very low fluorescence quantum yield of Gua. They also did not calculate barriers to proton transfer, and their proposal must be considered speculative at present.

ESIPT was suggested as a decay path for Cyt by Shukla and Leszczynksi.[117] This conclusion rests on their finding that the geometry-optimized $^1n\pi^*$ state of the 3H tautomer is lower in energy than all geometry-optimized excited singlet states of the 1H tautomer, both in vacuo and in solution.[117] It is important to point out, however, that these authors did not calculate the barrier to 1H → 3H conversion. Furthermore, the ribonucleoside Cyd has a lifetime, ~1 ps, identical to that of the free base,[72] despite the fact that the 1H → 3H shift is impossible in this case.

There is no experimental evidence to support excited-state tautomerism. High barriers for proton transfer have been seen in quantum chemical studies.[164] These barriers could be reduced through proton-transfer catalysis by solvent molecules, as seen for 7-azaindole,[186] but then isotope effects should be observed. As discussed earlier, Ade has identical dynamics in H_2O and D_2O.[53]

Some evidence in favor of excited-state proton transfer may come from supersonic jet experiments, where ions have been detected in mass channels corresponding to protonated products. For example, Nir et al.[163] observed proton-transfer products in photoexcited Cyt clusters. However, these products were also observed in the absence of photoexcitation, suggesting that reaction may occur during the laser desorption step or in the high-collision region of the supersonic expansion.[163] This and other evidence suggests that radiationless decay occurs by internal conversion, which will be discussed next.

2.4.2. Weak Vibronic Coupling: Energy Gap Law and Proximity Effect

The theory of radiationless transitions was developed intensely during the 1960s and 1970s, and has been reviewed frequently.[174,187−192] In this section, we describe qualitative aspects of this theory to comment critically on various proposals in the literature to explain rapid radiationless decay by the nucleobases. In the presence of nonadiabatic coupling between two or more electronic states, the eigenstates of the adiabatic Born−Oppenheimer (BO) Hamiltonian cease to be stationary states of the full Hamiltonian, and nonradiative transitions are possible.

Some authors use *vibronic coupling* as a synonym for nonadiabatic coupling since coupled electronic and nuclear motions are the cause of the couplings. We will use vibronic coupling throughout this section to mean nonadiabatic couplings that lead to nonradiative transitions between different electronic states. The closer the two states are in energy, the stronger the coupling between them. The nuclear kinetic energy operator, which is responsible for this nonadiabatic coupling in the case of internal conversion, can be viewed as inducing transitions between the two adiabatic BO states. Thus, to understand nonradiative decay, it is necessary to go beyond the BO approximation of quantum mechanics.[193]

A description of nonradiative decay in the weak coupling limit begins with the BO approximation and first-order perturbation theory for the coupling between the two electronic states. For large molecules in the statistical limit, nonradiative decay occurs irreversibly with rate constant k_{NR}, which can be calculated by time-dependent perturbation theory:

$$k_{NR} = \frac{2\pi}{\hbar}|\langle\psi_i|H_1|\psi_f\rangle|^2\rho(E_f) \qquad (2)$$

In eq 2, the initial and final vibronic states connected by the nonradiative transition have wave functions ψ_i and ψ_f, respectively, $\rho(E_f)$ is the density of states at the final state energy, E_f, and H_1 is the part of the molecular Hamiltonian that induces the nonradiative transition. For internal conversion, H_1 is the nuclear kinetic energy operator.

This Golden Rule formula is developed further by using the BO approximation to separate electronic and nuclear coordinates. In the Condon approximation, the electronic matrix elements are independent of nuclear coordinates and eq 2 can be reduced to products of electronic matrix elements and vibrational overlap integrals, or Franck−Condon factors. In this case, k_{NR} can be written as

$$k_{NR} = \frac{2\pi}{\hbar}J^2F(E_f)\,\rho(E_f) \qquad (3)$$

where J is an electronic matrix element that describes the coupling between the initial and final electronic states and $F(E_f)$ is a Franck−Condon factor.

The Franck−Condon factors in eq 3 are much more difficult to calculate than the "spectroscopic" Franck−Condon factors encountered in the description of radiative vibronic transitions because the former quantities must be evaluated at considerably higher vibrational excess energies.[187] The Franck−Condon factors decrease rapidly as the energy gap between the two electronic states increases, and this is the basis for the classic energy gap law—the prediction that nonradiative decay rates decrease rapidly as the energy separation between the initial and the final electronic states increases. Below we show that the nonradiative decay rates observed for the nucleobases cannot be explained well by the energy gap law. Non-Condon effects are more important for large energy gaps, but they do not alter the qualitative predictions of the energy gap law.[194]

High-frequency accepting modes generally have the largest Franck−Condon factors because they require fewer quanta of excitation to equal the initial vibronic energy. This is the reason C−H stretches are usually

the best accepting modes for aromatic hydrocarbons. The significantly reduced frequency of C−D stretches requires that they have higher vibrational quantum numbers for a given vibrational energy. The resulting decrease in the Franck−Condon factors explains the large reduction in nonradiative decay typically observed for aromatic hydrocarbons upon deuteration.[192] No isotope effect has been observed on decay rates of adenines in molecular beam experiments.[93] However, it is important to keep in mind that other accepting modes may be important in other classes of molecules.[195]

The energy gap law cannot explain subpicosecond nonradiative decay from the initial excited state to S_0, as there is little correlation between the vertical energy gaps of the bases and the fluorescence lifetimes. Experimentally, the adiabatic transition energies of the standard nucleosides are ordered as follows: Ado ≥ Urd > Thd ≥ Cyd > Guo.[8] Thus, Urd and Ado, the two nucleosides with the shortest S_1 lifetimes, have the largest singlet−singlet energy gaps. In fact, for both the purine and pyrimidine bases, the energy gaps are ordered oppositely to the lifetimes measured in solution.

A frequently cited explanation for ultrafast internal conversion in the bases is the *proximity effect*. The proximity effect invokes three coupled electronic states to explain radiationless transitions in aromatic nitrogen heterocycles. Coupling between nearby $^1\pi\pi^*$ and $^1n\pi^*$ excited electronic states controls the nonradiative decay rate between the lowest excited state and the electronic ground state. Lim eloquently described the qualitative predictions of the proximity model in a 1986 review paper.[196] The significance of vibronic coupling between nearby $^1n\pi^*$ and $^1\pi\pi^*$ excited states was first recognized in low-temperature experiments.[197,198] According to Lim's proximity effect, internal conversion from S_1 to S_0 should occur at a higher rate as the vertical energy gap between S_1 and S_2 is reduced. The lower gap between the latter two states results in lower frequency out-of-plane modes in S_1 than in S_0 as a result of vibronic coupling. These modes therefore become excellent accepting modes on account of their increased Franck−Condon factors.[196]

A variety of computational studies claim to support a proximity effect explanation of nonradiative decay by the bases. In some cases, the evidence consists of calculated energies that demonstrate a small vertical energy difference between nearby $^1\pi\pi^*$ and $^1n\pi^*$ states.[124,126,140,144,146] In other cases, the optimized geometries of the lowest excited $^1\pi\pi^*$ and $^1n\pi^*$ states suggest that out-of-plane vibrations can act as coupling modes.[124] Rachofsky et al.[146] investigated the applicability of the proximity effect model to 2AP photophysics. In their CASSCF study of 2AP, the $^1n\pi^*$ state was found to lie above the $^1\pi\pi^*$ state. The $^1n \rightarrow \pi^*$ transition consists predominantly of a single configuration in which an electron is promoted from a nonbonding orbital localized on N1 to an antibonding orbital localized on C6. The uncoupling of a π bond in the pyrimidine ring causes C6 to buckle out of the molecular plane. The electron density of the singly occupied π^* orbital is very similar in both the $^1n\pi^*$ and $^1\pi\pi^*$ states, suggesting that an out-of-plane vibrational mode can effectively couple both states. This vibronic coupling is suggested to be responsible for quenching the fluorescence of the $^1\pi\pi^*$ state.[146]

Marian et al.[144] suggested that mixing of the $^1\pi\pi^*$ and $^1n\pi^*$ states in Ura occurs because of coupling by a carbonyl out-of-plane mode. Mennucci et al.[126] suggested coupling of $^1\pi\pi^*$ and $^1n\pi^*$ states of Ade occurs with the ground state through vibrational coupling. For Gua they suggested that 9H-Gua may decay because puckering in the excited state causes the out-of-plane modes to effectively couple the excited state to the ground state.[140]

A study by Broo[124] found an avoided crossing between the lowest $^1n\pi^*$ and $^1\pi\pi^*$ states of 9H-Ade, with a coupling between the states of 4200 cm^{-1}. Ring puckering in the six-membered ring of Ade (particularly at N1−C2−N3) was identified as the coordinate that transforms the initially planar $^1\pi\pi^*$ state into the nonplanar $^1n\pi^*$ state. The quasi-stationary points corresponding to these two states are close in energy and separated by a small barrier of only 0.6 kJ mol^{-1}. Broo argues that coupling of these two states by an out-of-plane mode is responsible for ultrafast excited-state decay.[124] Broo's model can explain a rapid state switch from an initial $^1\pi\pi^*$ state to a $^1n\pi^*$ state, but it does not explain how S_0 is subsequently reached.

Although the proximity effect is widely cited as the reason for the short S_1 lifetimes of the DNA bases, experimentally measured lifetimes correlate poorly with the magnitude of the energy gap between the lowest $^1\pi\pi^*$ and $^1n\pi^*$ states. Let this gap be written as $|\Delta E|$. The CASPT2 calculations of Roos and coworkers listed in Tables 4−6 predict that Ade and Gua have larger $|\Delta E|$ values than Cyt and Thy in vacuo.[101,123,132] Yet, Ade and Gua have shorter lifetimes than Cyt and Thy in the gas phase, according to the results of Kang et al.[94] Of course, comparison with gas-phase lifetimes is difficult since they depend sensitively on the vibrational energy content of the isolated base (section 2.3). Even comparing $|\Delta E|$ values only among closely related bases yields no consistent correlations. Furthermore, the experimental findings do not obey two classic, proximity effect predictions, made in the limit of weak vibronic coupling.

The first prediction involves the effect of methylation on nonradiative decay rates.[196] Because $^1n\pi^*$ states generally shift to higher energies upon methylation, replacement of hydrogen by an electron-donating group such as a methyl group will increase $|\Delta E|$, increasing the lifetime, whenever the lowest energy state is $^1\pi\pi^*$ with a $^1n\pi^*$ state located above it. For most theoretical methods, all bases except Thy and Ura are predicted to have a lowest energy $^1\pi\pi^*$ state. The longer lifetime found for m^5Cyt vs Cyt[72] follows the rule, but the lifetime of m^7Ade is shorter than that of 7H-Ade.[53] For Ura, calculations predict a lowest energy $^1n\pi^*$ state. Thus, methylation should reduce $|\Delta E|$, leading to a decreased lifetime, yet Thd (2′-deoxy-5-methyluridine) has a substantially longer lifetime than Urd (section 2.1.2).

The second proximity effect prediction concerns the effect of the solvent on nonradiative decay.[196] Moving

from an aprotic to a protic solvent is expected to increase the gap between the $^1n\pi^*$ and $^1\pi\pi^*$ states, when the $^1\pi\pi^*$ state is lowest in energy, leading to an increase in fluorescence. As Tables 4−6 show, nearly all calculations predict a larger gap between the $^1\pi\pi^*$ and $^1n\pi^*$ states in aqueous solution than in vacuo. The proximity effect would therefore predict slower rates of nonradiative decay in solution, but this is not observed. Lifetimes are subpicosecond in aqueous solution, while lifetimes of a few picoseconds[93,94] or even less[139] are observed in supersonic jet experiments when excitation is significantly above the origin. For excitation near the origin, lifetimes of several nanoseconds were observed. Furthermore, the femtosecond experiments found only modest changes in S_1 lifetimes when the solvent was varied.[53]

2.4.3. Strong Vibronic Coupling: Conical Intersections

Vibronic interactions increase as the energy gap between nonadiabatically coupled electronic states is reduced. When the interacting states are degenerate, or nearly so, electronic and nuclear motions are very strongly coupled. When this occurs, eq 3 no longer holds. To reach this strong coupling limit, the degeneracies between the adiabatic Born−Oppenheimer states must occur in regions of coordinate space that are accessible to the nuclei. Under the appropriate conditions, the degeneracy between two electronic states can give rise to a conical intersection (CI). Once thought to be highly exotic, CIs are now recognized to play a central role in the photophysics and photochemistry of many polyatomic molecules.[199−202] The importance of CIs for nonadiabatic dynamics has been a subject of great interest.[203−213]

Pecourt et al.[21] proposed in 2000 that conical intersections are responsible for ultrafast internal conversion in the DNA bases. Previously, Sobolewski and Domcke[214] stressed the importance of CIs in the photochemical dynamics of heteroaromatic molecules. Kim and co-workers[94] suggested that a CI between the lowest $^1n\pi^*$ state and S_0 is responsible for ultrafast internal conversion of Ade. It is apparent from the literature that the proximity effect is not understood to encompass dynamics resulting from conical intersections. Lim discusses in his 1986 paper the possibility that strong vibronic coupling could lead to real surface crossings, but this is not explored further.[196] Furthermore, the CI responsible for ultrafast nonradiative decay need not involve nearby $^1n\pi^*$ and $^1\pi\pi^*$ states at all,[135,215] and could thus fall outside the purview of the proximity effect.

In 2002, two theoretical studies were published independently which identified CIs responsible for ultrafast internal conversion in Ade[215] and Cyt.[134] In the case of Ade, Sobolewski, Domcke, and co-workers described how the $^1\pi\pi^*$ state created by excitation crosses over to a predissociative $^1\pi\sigma^*$ state, which has a CI with the electronic ground state at large values of the N−H bond distance.[135,215] The relevant potential energy surfaces are shown in Figure 14. A similar decay process was studied earlier for indole by Sobolewski and Domcke,[216] and later generalized by them to a wider group of compounds.[214] In indole, low-lying Rydberg states, first located by Serrano-Andrés and Roos,[217] are dissociative along the N−H

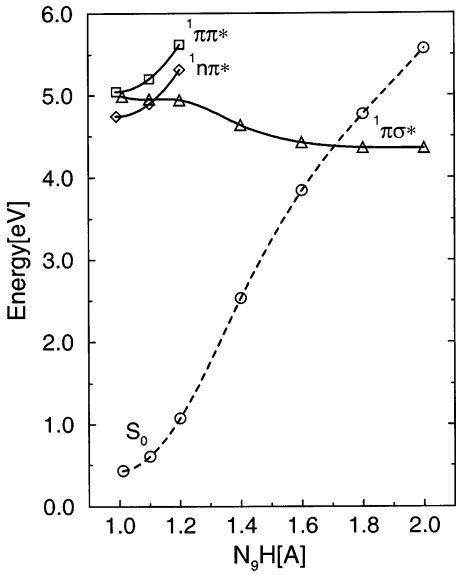

Figure 14. TD-DFT(B3LYP) potential energy profiles for 9H-adenine at CASSCF geometries. The reaction coordinate is the N9−H stretch coordinate. Circles: S_0. Tilted squares: lowest $^1n\pi^*$ state. Triangles: lowest $^1\pi\sigma^*$ state. Squares: lowest $^1\pi\pi^*$ state. Reprinted with permission from ref 215. Copyright 2002 The Owner Societies.

stretching coordinate. Earlier, Tatischeff et al.[218] had proposed that hydrogen dissociation is responsible for radiationless decay by indole in non-hydrogen-bonding solvents.

Sobolewski et al.[135,215] carried out calculations in support of this mechanism for 9H-Ade and suggested that this could be a general excited-state decay mechanism for all the bases. The large dipole moment of the $^1\pi\sigma^*$ state leads to a large stabilization of this state with the result that fluorescence from the $^1\pi\pi^*$ state is essentially completely quenched. This is qualitatively consistent with fluorescence from bases at low temperature and sharp vibronic resonances in the multiphoton photoionization spectra in the supersonic jet experiments. The high polarity of the $^1\pi\sigma^*$ state would appear to predict a greater sensitivity of nonradiative decay to the solvent than has been observed to date, but Sobolewski et al. wrote that the basic mechanism should be unchanged in the condensed phase.

The Sobolewski and Domcke mechanism is difficult to reconcile with recent experimental lifetime measurements on substituted adenines.[53] Subpicosecond lifetimes were observed for Ado,[21,38,39,41] and for m^1-Ade, m^3Ade, and m^9Ade.[53] None of these compounds has a hydrogen atom bonded to a ring nitrogen. Instead, the only N−H coordinates in these systems are those of adenine's exocyclic amino group. The calculations of Sobolewski and Domcke[135] considered only the N9−H bond of Ade, and did not provide evidence that their model extends to the amino group N−H stretches. Moreover, it is difficult to envision how a $^1\pi\sigma^*$ state associated with the amino group could interact strongly with $^1\pi\pi^*$ and $^1n\pi^*$ states localized in the rings. Kang et al.,[93] who found an ultrashort lifetime for m^9Ade in a supersonic jet, also questioned the applicability of the Sobolewski and Domcke model. An aborted hydrogen dissociation might be expected to show a kinetic isotope effect,

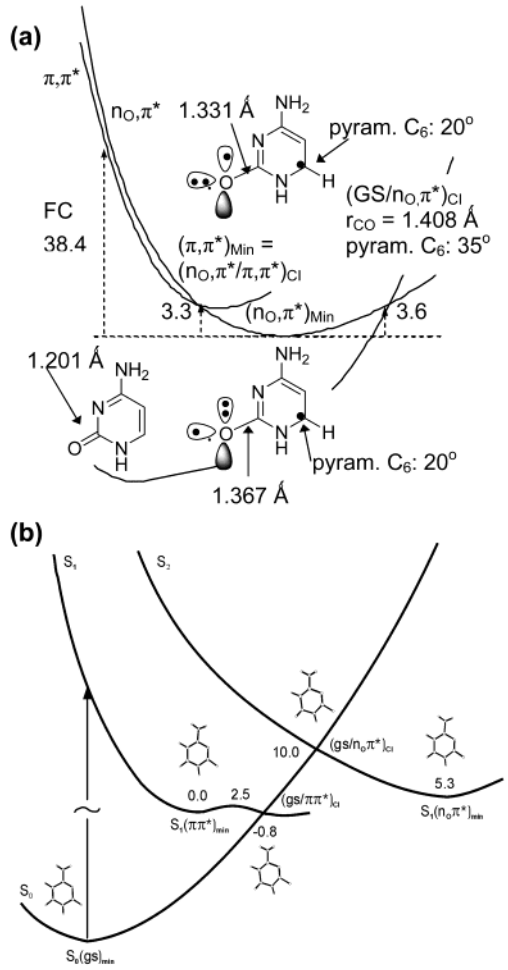

Figure 15. (a) Proposed decay path for cytosine from an optically prepared $^1\pi\pi^*$ state to the ground state, through a state switch to a $^1n\pi^*$ state associated with the carbonyl oxygen. Energies are given in kilocalories per mole. Reprinted with permission from ref 134. Copyright 2002 American Chemical Society. (b) Proposed decay path for cytosine through a $(gs/\pi\pi^*)_{CI}$. Energies are in kilocalories per mol. Reprinted with permission from ref 141. Copyright 2003 American Chemical Society.

but neither deuterated Ade under isolated molecule conditions[93] nor Ade in D_2O[53] showed any observable isotope effect.

In the second study, Robb, Olivucci, and co-workers[134] located a $^1n\pi^*$ state associated with the carbonyl oxygen just above the lowest singlet state of Cyt, which is of $^1\pi\pi^*$ type. These states are very close in energy at both the TD-DFT and CASSCF levels of theory. The authors further studied reaction paths by the CASSCF method. They proposed a decay mechanism in which a state switch occurs from the optically prepared $^1\pi\pi^*$ state to the $^1n\pi^*$ state associated with the carbonyl oxygen. A sloped conical intersection connects the $^1n\pi^*$ state with the electronic ground state. A small barrier of 3.6 kcal mol^{-1} separates the minimum of the $^1n\pi^*$ state and the CI as shown in Figure 15a.

Malone et al.[72] discussed how the results of the Ismail et al.[134] study can rationalize the pH-dependent photophysics of Cyt. The cation of Cyt has a somewhat shorter lifetime ($\tau \approx 600$ fs) than neutral Cyt, while the Cyt anion is significantly more fluorescent with a lifetime of ~13 ps.[72] Similar trends were found for m^{5}Cyt. Protonation, which occurs at N3 for Cyt, eliminates the $^1n\pi^*$ transition associated with the N3 lone pair. On the other hand, Malone et al.[72] argued that deprotonation of Cyt would significantly perturb the $^1n\pi^*$ state on oxygen. Thus, the greater fluorescence of the Cyt anion appeared to signal a key intermediate role for the carbonyl $^1n\pi^*$ state, and not for the $^1n\pi^*$ state associated with the N3 nitrogen.[134] The agreement is encouraging, but protonation/deprotonation could significantly alter the energetics of more than one electronic state, and further theoretical work is warranted. It is also important to point out that some theoretical studies did not find the lowest energy $^1n\pi^*$ state of Cyt to be associated with the carbonyl oxygen lone pair.[117,132,219]

A later computational study of Cyt by Merchán and Serrano-Andrés[141] questioned the intermediacy of the $^1n\pi^*$ state. When the CASPT2 method was used to calculate energies at the CASSCF geometries found by Ismail et al.,[134] the $^1\pi\pi^*$ state was found to be 15−20 kcal mol^{-1} lower in energy than the $^1n\pi^*$ state, making a state switch no longer necessary.[141] Instead, Merchán and Serrano-Andrés located a $^1\pi\pi^*/S_0$ CI at the CASPT2 level of theory, which they believe is the funnel responsible for ultrafast internal conversion. A schematic of the relevant potential energy surfaces is shown in Figure 15b. The reaction coordinate responsible for internal conversion (initial π bond inversion, followed by pyramidalization at C6) is the same as in the earlier study of Ismail et al.[134]

In summary, the base monomers display remarkably rapid nonradiative decay both in aqueous solution at room temperature and in vacuo with sufficient internal energy. The combined experimental and theoretical results make a compelling case that nonradiative decay occurs as a result of significant nonadiabatic coupling between the lower excited singlet states. It appears that state degeneracies (i.e., conical intersections) arise in regions of nuclear coordinate space that can be accessed after small barriers are overcome. Considerably more work is needed to bring these complex nonadiabatic dynamics into sharper focus.

3. Singlet-Excited-State Dynamics in Assemblies of Two or More Bases

The results of the previous section form the backdrop for our discussion here of the singlet excitations produced by UV light in complex molecules containing two or more DNA or RNA bases. In the assemblies of interest, pairs of bases are close enough to have nonnegligible electronic coupling with one another. These interactions lead to new photophysical effects not observed in monomeric bases. The bases may be brought into close spatial proximity through covalent linkages, as in the di-, oligo-, and polynucleotides, which are joined by the phosphodiester linkages found in natural DNAs and RNAs. Unnatural covalent linkages are also possible.[220−230] The latter compounds offer intriguing possibilities for studying conformational effects on excited-state dynamics, but they have been rarely studied from a photophysical viewpoint.[227] Noncovalent interactions are responsible for other base assemblies such as aggregates of two or more π-stacked bases or hydrogen-bonded base

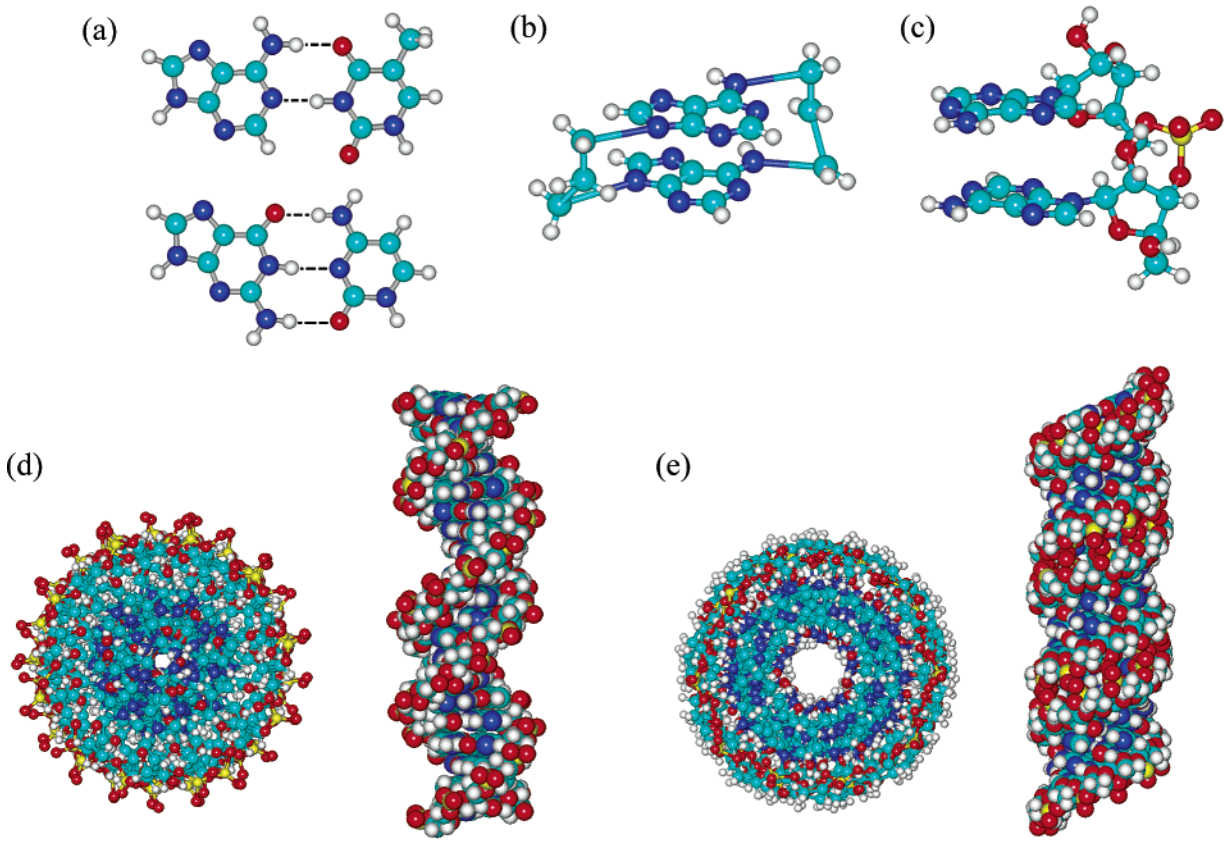

Figure 16. Representative structures of base multimers: (a) Watson and Crick base pair, A-T (top) and G-C (bottom); (b) a purinophane from ref 223; (c) base-stacked form of the dinucleoside monophosphate ApA; (d) B-form double-stranded DNA, views down the helical axis (left) and from the side (right); (e) A-form double-stranded DNA, views down the helical axis (left) and from the side (right). All structures were drawn using HyperChem 7 (Hypercube, Inc.).

pairs. Hydrogen bonding is of course one of the stabilizing forces in duplex DNAs and RNAs, and the effect of base pairing on photophysics will be considered later in section 3.3.2. In what follows, we shall use the term *base multimers* to refer collectively to the diverse molecular systems illustrated by the previous examples. Some representative structures are shown in Figure 16.

Base multimers are complex multichromophoric systems that pose great experimental and theoretical challenges. In comparison to the monomers, there has been much less experimental work on room temperature luminescence of base multimers, particularly using time-resolved techniques. The first time-resolved emission experiment with a base multimer was reported in 1982 for poly(A),[44] although picosecond laser techniques were applied as early as 1975 to study dye-labeled DNA.[231] The femtosecond techniques that have had such impact on monomer photophysics have been applied only recently to di-, oligo-, and polynucleotides.[61,232,233] The results, which are still primarily phenomenological, have already shown that electronic energy relaxation in the polymers occurs over a wider range of time scales than previously thought.

The most striking photophysical attribute of base multimers is the appearance of long-lived emissive states not found in base monomers.[8,9] Figure 17, which shows time- and wavelength-resolved data from a study by Plessow et al.[234] using 80 ps excitation pulses, dramatically makes this point. In Figure 17a, time-resolved fluorescence from the mononucleotide CMP results in a short, instrument-limited decay. Longer decay components and red-shifted emission are faintly visible for the dimer $d(C)_2$ (Figure 17b), but readily apparent for the 15-mer $d(C)_{15}$ (Figure 17c). Figure 17c shows that decay components of several nanoseconds are observed in the Cyt oligonucleotide. Base multimers can retain electronic energy in some cases for over 4 orders of magnitude longer in time than the monomers.[233] Despite their longer fluorescence decay times, base multimers, such as synthetic polynucleotides, are not significantly more fluorescent than the monomeric bases. For example, the fluorescence quantum yield of poly(A) is only 6 times greater than that of Ado.[8,22] This has important implications for the nature of the states, as will be discussed later in more detail.

It has been suggested that the slow rate of energy relaxation by these long-lived states could make them the precursors of DNA photolesions, including the photodimers.[233,235−238] Any long-lived excitation could potentially migrate to low-energy trapping sites such as the ones created by minor bases (e.g., m^5Cyt) that have lower singlet energies than the natural bases. This migration could depend on base sequence and polynucleotide conformation, offering a possible explanation for the experimental finding that the photolesions in UV-irradiated DNA are distributed in a spatially nonrandom way.[239−241] However, as discussed by Ruzsicska and Lemaire,[9] there is presently no definitive evidence actually linking the long-

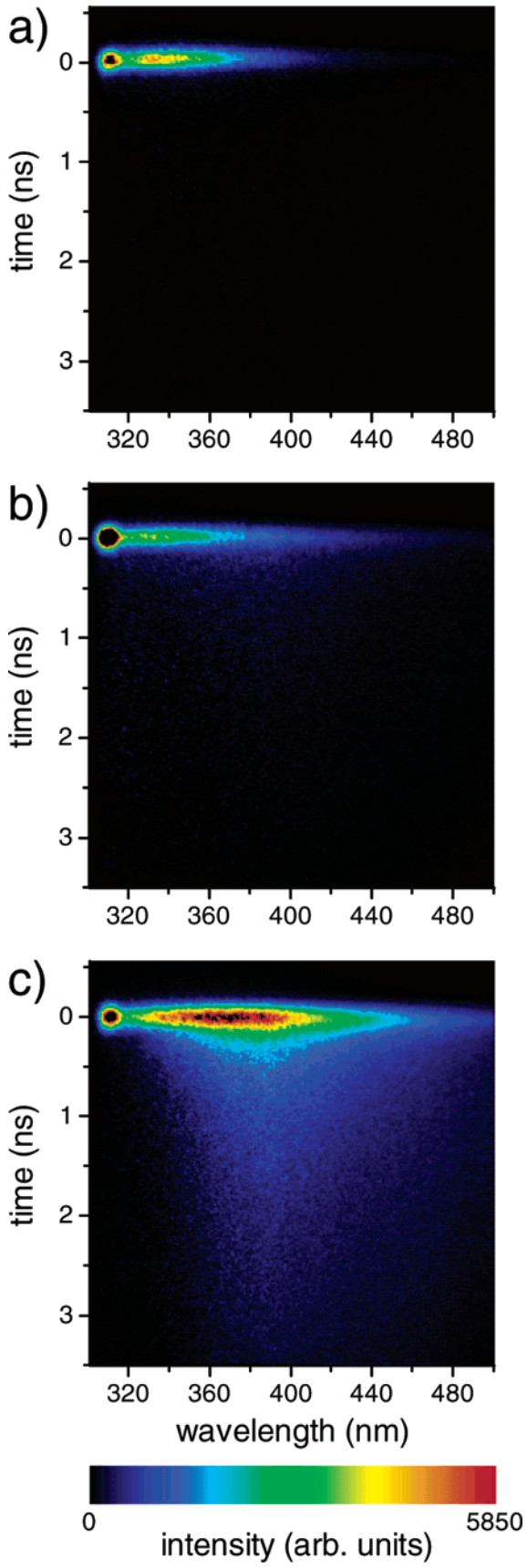

Figure 17. Simultaneous wavelength- and time-resolved fluorescence intensity measurements for (a) CMP, (b) $d(C_2)$, and (c) $d(C)_{15}$. Data were recorded with 80 ps, 283 nm excitation pulses. Reprinted with permission from ref 234. Copyright 2000 American Chemical Society.

lived states in the multimers to any photolesion.

At this point it is useful to make a few remarks about the nature of the excited states in base multimers. The new excitations in base multimers depend on conformation and base sequence.[242] In double-stranded B-form DNA, neighboring bases are arranged in roughly coplanar fashion, separated by 3.4 Å (Figure 16d). The precise distances and mutual orientations are controlled by the conformation of the sugar−phosphate backbone. Two manifestations of the electronic coupling between nearby bases are the well-known hypochromism of the long-wavelength absorption band[239,243,244] and the ionization potential lowering seen, for example, in guanine runs.[245] The coupling between bases is not large enough, however, to be readily apparent in absorption, and the absorption spectrum of any given base multimer differs only modestly from the sum of the spectra of its constituent monomers.[37] For this reason, it has been assumed by many workers that UV absorption produces excited states initially localized on a single base, although there is little evidence that this is the case (see section 3.3.3).

The red-shifted emission seen in some base multimers was first termed excimer emission by Eisinger et al. in 1966.[246] Excimer and the related term exciplex have been used frequently in the literature since that time to describe excited states in base multimers.[247−250] Strictly speaking, an excimer is an emissive excited state formed when an electronically excited molecule diffusively encounters a second identical one, which is in its electronic ground state.[251,252] An exciplex is a similar complex between two different molecules. These terms were originally introduced to describe states produced by diffusive encounter of two molecules, one excited and one unexcited, which were initially separated by a considerable distance at the moment of optical excitation. Because of their initial separation, excitation is completely localized on just one of the molecules, and the initial excited state is the same as in the isolated molecule.

Unfortunately, there is much that is misleading about the term excimer when applied to nucleic acid photophysics.[253,254] The goal of excited-state dynamics is to fully characterize the temporal evolution of an excited molecule from the instant of light absorption through its eventual photochemical or photophysical deactivation. It is important to keep in mind that the initial excited state may be utterly different from the one detected at some later point in time, as is the case, for example, when triplet−triplet absorption is detected following excitation of an initial singlet state. In base multimers, it is clear that the initial excited state has an electronic character very different from that of the long-lived emissive one, a property shared with conventional aromatic excimers. However, an inadequacy of the term excimer for describing excitations in nucleic acids is the dynamical picture that is immediately suggested of an excitation initially localized on one base evolving to an emissive excited state (excimer or exciplex) that spans two neighboring bases. In fact, the evidence that the initial and final excited states are as

described in the previous sentence is far from definite. Support for the emissive states being localized on two bases comes from the similar emission spectra observed for di- and polynucleotides in low-temperature glasses.[246,255] Even if the emissive states involve just two bases, it is not clear that the initial excited states are localized on just one base.

It is uncertain whether the dynamical evolution that connects the initial Franck−Condon excited state with the one responsible for the long-lived emission has much in common with the dynamical processes behind classical excimer formation. The language of excimers suggests that significant nuclear motions are required to bring two interacting bases into the proper geometry, as is the case when classical excimers are formed from two freely diffusing molecules. Diffusive encounter is clearly unnecessary in base multimers, in which the most strongly interacting bases may be in van der Waals contact at the time of excitation, as in base-stacked polynucleotides (Figure 16d,e). It is difficult to imagine that large-scale nuclear motions, which might be required to bring two neighboring bases into a more idealized sandwich dimer geometry, can compete with the ultrafast nonradiative decay pathways available to single bases (section 2.1.2). This suggests that the formation of the long-lived emissive states is primarily an electronic process mediated by more subtle nuclear motions. At first glance, a more appropriate term would appear to be *static excimer*. This term was coined to describe pairs of aromatic molecules that exhibit excimer-like emission, but which are in contact at the time of absorption.[256] The close proximity of the two chromophores in a system that forms static excimers can lead to changes in absorption (i.e., hypochromism) and differences in fluorescence excitation spectra, two effects that are observed in base multimers.

In a nutshell, there is great uncertainty about the nature of both the initial Franck−Condon excited state and the long-lived state responsible for emission in base multimers, so labels for these states must be used cautiously. Molecular exciton theory is a natural way to describe the interactions between nearby chromophores, and several investigators have suggested that the excimer states observed in base multimers are excitons in which excitation is initially delocalized to some degree over a pair of bases.[257,258] Excitons are a well-established concept in nucleic acid photophysics, and exciton theory was used over 40 years ago to explain DNA hypochromism.[239,243] In what follows, we shall use the term *exciton* (without specifying the extent of delocalization) when referring to the bright state responsible for absorption. Until the electronic structure of the emissive states in base multimers is definitively understood, the well-entrenched term excimer will continue to be used, despite the limitations outlined above. We shall therefore write of *excimer-like* states when referring to the long-lived singlet states detected in many emission experiments.[259]

Finally, it must be kept in mind that larger base multimers such as the polynucleotides can be microscopically heterogeneous, as in the case of more conventional multichromophoric polymers. This heterogeneity can give rise to complex photophysical kinetics, a fact underscored by recent femtosecond results.[61,233] A variety of experiments discussed below indicate that the long-lived excited states in base multimers depend sensitively on multimer conformation. Whenever a distribution of conformational substates exists, complex kinetics can be expected. In the remainder of this section, we review experimental and theoretical progress at understanding excited-state dynamics in these challenging systems.

3.1. Steady-State Emission Experiments

3.1.1. Di- and Oligonucleotides

The dinucleoside monophosphates can adopt base-stacked geometries in room temperature aqueous solution.[260−262] Stacking forces result in a distribution of stacked and partially stacked conformers.[263] Different conformers generally differ in electronic structure because of the variable electronic coupling between the bases. Because of their ability to base stack and their small size, base dimers were once objects of intense study,[247−250] but there have been almost no steady-state photophysical investigations in the past 15 years. Emission properties of oligonucleotides containing only naturally occurring bases have not been reported, although there have been many steady-state investigations of 2AP-labeled oligonucleotides.[75−80]

Many dinucleoside monophosphates show emission at longer wavelengths than their constituent mononucleotides. This red-shifted emission has been assigned to excimer states created as a result of electronic coupling between the π electrons of stacked bases.[25,37] Browne et al.[220] showed that excimer-like emission was only observed in base dimers in which the bases were joined by variable-length polymethylene chains that allowed the bases to adopt a stacked configuration. Kononov et al.[255] found significant differences between fluorescence excitation spectra and absorption spectra for ApA and CpC at 77 K, but not for TpT and GpG. They attributed the differences to exciton formation, which they said is highly favored in the former systems.[255] Daniels and co-workers[247,248,257,258,264,265] presented evidence that the red-shifted emission band seen in various dinucleotides arises from at least two different stacked conformations.

3.1.2. Single- and Double-Stranded Polynucleotides

As mentioned already, the absorption spectra of nucleic acid polymers hardly differ at all from the sum of the spectra of their constituent monomers. Despite the similarities in absorption, the emission spectra of many polymers show red-shifted, excimer-like emission that is absent in the emission spectra of the monomeric bases. Steady-state emission by the single-stranded Ade homopolymer, poly(A), was studied at room temperature and pH 8 by Kononov and Bukina.[266] They assigned red-shifted emission to two distinct luminescent excited states. One of these states has absorption identical to that of poly(A), while the second state is characterized by a weak

transition at 320 nm, which can only be detected in the fluorescence excitation spectrum.

The steady-state photophysical properties of the duplexes poly(dA-dT)·poly(dA-dT) and poly(dG-dC)·poly(dG-dC) were studied at room temperature in aqueous solution.[236,267,268] Two emission bands were observed with maxima at 330 and 410 nm for poly(dA-dT)·poly(dA-dT), [236,267] whereas poly(dG-dC)·poly(dG-dC) exhibited only one emission band at 325 nm.[268] The intensity of the long-wavelength emission band of poly(dA-dT)·poly(dA-dT) decreased strongly with increasing temperature, and was assigned by Vigny and Ballini to emission from an excimer state.[236]

Ge et al.[267] showed that the emission anisotropy and the emission spectrum depend on the excitation wavelength. In analogy with low-temperature experiments,[168] the results were interpreted as indicating that the short-wavelength emission originates from Thy, whereas the long-wavelength emission originates from an exciplex state, formed when either Ade or Thy was excited.[267] On the basis of the weak fluorescence and low anisotropy values observed for poly(dA-dT)·poly(dA-dT),[267] structural flexibility of the polymer during the excited-state lifetime was proposed to allow the bases to achieve a more favorable configuration for excimer formation.

Interestingly, although poly(dA-dT)·poly(dA-dT) forms excimer-like states, only a single emission band with a maximum at 325 nm was observed for poly(dA)·poly(dT) with no evidence of excimer-like emission.[269] On the other hand, Plessow et al.[234] reported excimer-like emission from an equimolar mixture of $d(A)_{15}$ and $d(T)_{15}$ under conditions in which double helices form. The emission in this case was essentially identical to that observed from single-stranded $d(A)_{15}$ oligonucleotides, and Plessow et al.[234] concluded that double-strand formation does not diminish the ability of stacked dAdo residues to form excimer-like states.

Huang and Georghiou[268] observed no changes in the shape of the single 325 nm emission band of poly(dG-dC)·poly(dG-dC) upon excitation at 265, 280, and 297 nm. However, the fluorescence anisotropy measured near the emission maximum decreased from 0.18 to 0.05 when the excitation wavelength was decreased from 297 to 265 nm. Earlier, Wilson and Callis[253] showed that the fluorescence anisotropy of CMP is independent of wavelength over this range, while that of GMP decreases sharply at short wavelengths. On this basis, Huang and Georghiou[268] claimed that emission from poly(dG-dC)·poly(dG-dC) originates from Gua. Efficient nonradiative transitions due to base-stacking interactions were proposed to account for the apparent lack of fluorescence from Cyt in poly(dG-dC)·poly(dG-dC).[268] Huang and Georghiou[268] observed enhanced excimer-like emission from poly(dG-dC) in unbuffered conditions which they claimed resulted in denaturation of the duplexes observed in buffered solution. The enhanced mobility of the bases in this denatured state was claimed by the authors to enhance excimer formation.

3.1.3. DNA

The fluorescence quantum yield of natural DNA was determined to be approximately 4×10^{-5} in room temperature aqueous solution by independent laboratories in the 1970s and early 1980s.[236,270] There was less agreement, however, about the nature of the emission spectrum, and about whether excimer-like emission can be observed. Natural DNAs are difficult to study since they can be contaminated by minute quantities of considerably more fluorescent protein, even after extensive purification.[270] A fundamental problem not restricted to natural DNAs is the inability to control the site of initial excitation due to overlapping absorption bands of the different bases. This is one reason for the large number of studies of synthetic homopolymers.

3.2. Time-Resolved Absorption and Fluorescence Experiments

3.2.1. Dinucleoside Monophosphates

A few time-resolved experiments have been performed on dinucleoside monophosphates. Ballini et al.[257] used synchrotron radiation to obtain time-resolved emission spectra from the sequence isomers d(TpA) and d(ApT) with ~80 ps time resolution. They presented evidence for three components in the emission decays, a rapid one below 100 ps and two longer decays of ~2 and ~7 ns. The emission spectrum corresponding to the picosecond component was similar for d(TpA) and d(ApT), and resembled emission by the free nucleotides. Emission spectra corresponding to the nanosecond components were red-shifted and strongly broadened relative to the picosecond emission spectrum, consistent with excimer-like emission. Excitation spectra for the picosecond emission matched the absorption spectra reasonably well. On the other hand, the excitation spectra for the longer lived emission did not agree with the absorption spectra, but instead resembled anisotropic absorption seen in crystals of 1:1 hydrogen-bonded complexes between m^1Thy and m^9Ade.[271] On this basis, Ballini et al.[257] assigned the short-lived emission to excitations localized on unstacked bases, while the nanosecond emission was assigned to out-of-plane transitions that arise in vertically stacked bases. In other words, excimers were ruled out, and the red-shifted emission was instead assigned to excited stacked complexes. Calculations to be discussed in section 3.3.1 support the viewpoint that base stacking creates new excitations that are not monomer-like.

Ballini et al.[257] suggested that the two different nanosecond decay components are due to right-handed (B-like) and left-handed (Z-like) stacked conformations, but they acknowledged the great difficulties in assigning known conformations to the various emitting states. In particular, they conceded that their experiments could not differentiate between a model in which two kinds of emissive states are produced by excitation of two different stacked forms and a second model in which the two emitting states are generated dynamically from a common precursor state.

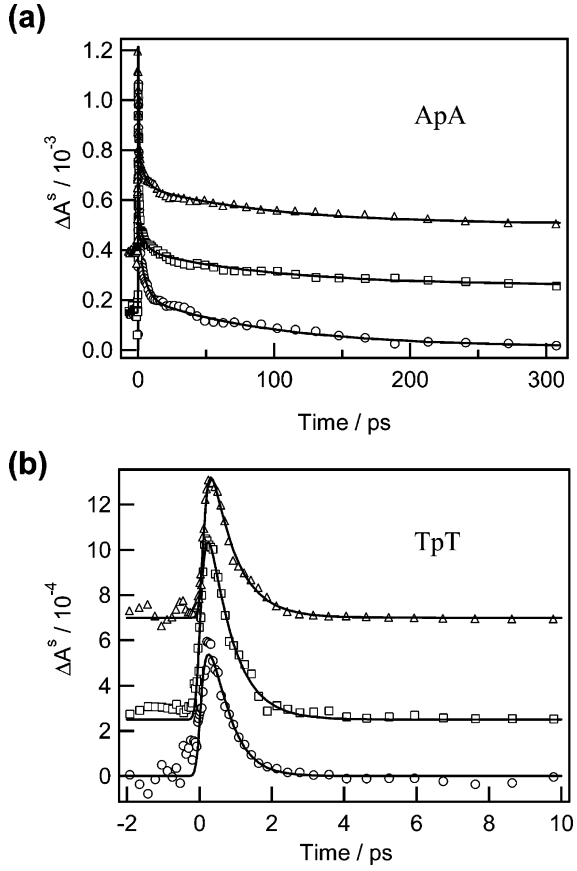

Figure 18. Transient absorption decays of (a) ApA and (b) TpT in aqueous solution at neutral pH induced by a 263 nm pump pulse. The probe wavelengths are 570 (○), 600 (□), and 630 (△) nm. Global fits are shown by the solid curves. All signals were water subtracted using the procedure in ref 233. The signals were offset vertically for clarity.

Recent femtosecond pump−probe experiments on TpT and ApA at room temperature and neutral pH have shown that electronic energy relaxation occurs on different time scales in these two dinucleosides (Figure 18).[272] For ApA, global fits to transients measured at 570, 600, and 630 nm give two time constants of 530 ± 100 fs and 60 ± 16 ps. The former time constant is in excellent agreement with the value τ = 520 ± 160 fs measured by Peon and Zewail[39] for Ado using fluorescence upconversion. For TpT, the global fit yielded a single time constant of 680 ± 40 fs, close to values measured previously for Thd.[21,39] On the basis of previous findings[255] that ApA has strong excitonic interactions at low temperature, while TpT does not, these experiments suggest that the long-lifetime component is the dynamical signature of an excitonic state in ApA, while the subpicosecond component is associated with a monomer-like excited state in both dinucleotides.

3.2.2. Oligonucleotides

Three time-resolved studies have been published on oligonucleotides.[232,234,273] Plessow et al.[234] used 80 ps excitation pulses and a streak camera positioned after a spectrograph to study emission from room temperature aqueous solutions of a variety of single- and double-stranded oligomers. Time- and wavelength-resolved data for $d(AT)_8$ and $d(GC)_8$ are shown in Figure 19. From the figure, it is easy to see the greater amount of red-shifted and slowly decaying fluorescence from the former oligomer. Emission by $d(AT)_8$ was red-shifted compared to that by the Ade and Thy oligomers. In contrast, the emission from $d(GC)_8$ was weaker than from the corresponding Gua and Cyt oligomers. The authors therefore concluded that any long-lived emission in DNA would result predominantly from excitations localized on AA and AT steps.[234]

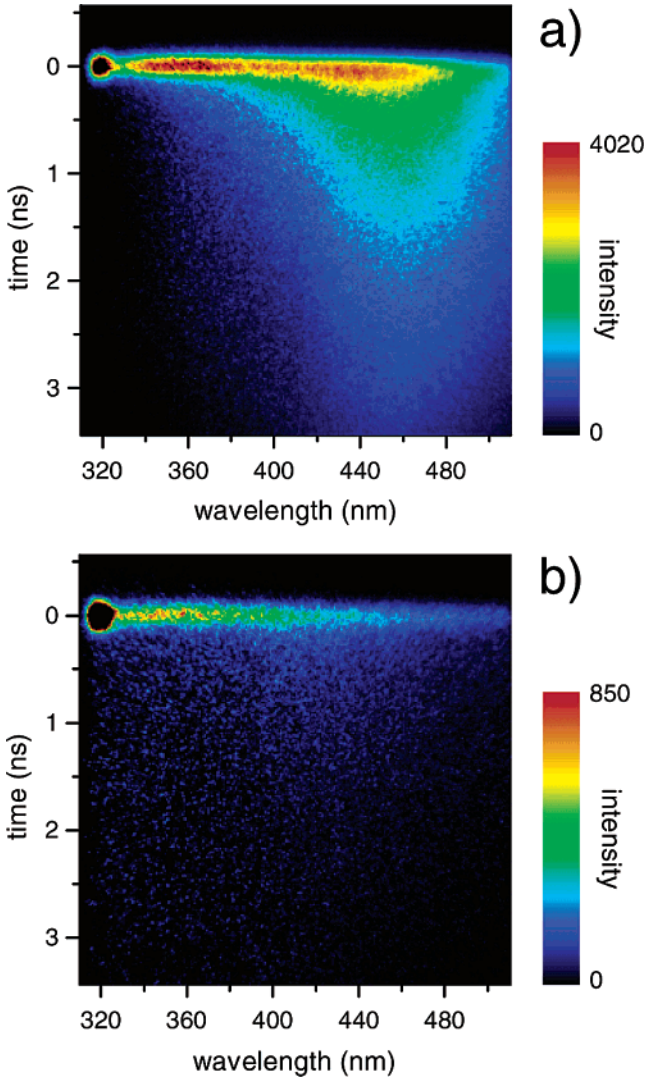

Figure 19. Simultaneous time- and wavelength-resolved measurements of the fluorescence intensity for self-complementary oligonucleotides: (a) $d(AT)_8$ and (b) $d(GC)_8$. Data were recorded with 80 ps, 283 nm excitation pulses. Reprinted with permission from ref 234. Copyright 2000 American Chemical Society.

The time- and wavelength-resolved data of Plessow et al.[234] were fitted to biexponential functions at fixed emission wavelengths. For the oligomers studied, the short-time component varied between 40 ps, the limit of the experimental time resolution, and 260 ps, while the long-time component ranged from 0.4 to 2.0 ns, as shown by a summary of the best fit lifetimes in Table 8. The fast decay was assigned to monomer emission, while the slower decay component, which had the greatest amplitude at longer emission wave-

Table 8. Emission Lifetimes of Various Oligonucleotides

system	τ_1/ps	τ_2/ns	time resolution	ref
$d(A)_{15}$	150, 240, 260[a]	1.05, 1.64, 1.80[a]	40 ps	234
$d(C)_{15}$	50, 110, 110[a]	0.70, 1.43, 2.05[a]	40 ps	234
$d(G)_{15}$	80, 120, 150[a]	0.42, 0.78, 1.01[a]	40 ps	234
$d(T)_{15}$	40, 110, 270[a]	−, 1.20, 1.34[a]	40 ps	234
$d(AT)_8$	90, 170, 230[a]	1.40, 1.41, 1.87[a]	40 ps	234
$d(GC)_8$	60, 140, 160[a]	1.64, 0.97, 1.09[a]	40 ps	234
$d(A)_{20}$	0.3[b]	1.6 ps[b]	450 fs	232
$d(T)_{20}$	0.3[b]	1.5 ps[b]	450 fs	232
$d(A)_{20}$·$d(T)_{20}$	0.4[b]	2.4 ps[b]	450 fs	232

[a] At emission wavelengths of 340, 400, and 460 nm, respectively. [b] Emission observed at 330 nm.

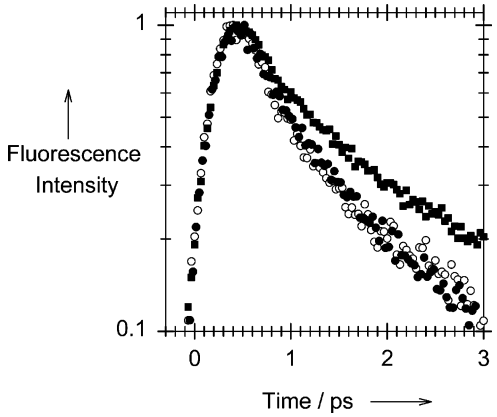

Figure 20. Normalized fluorescence decays recorded at 330 nm for the double-stranded oligomer $(dA)_{20}$·$(dT)_{20}$ (■) and the corresponding single-stranded oligomers $(dA)_{20}$ (○) and $(dT)_{20}$ (●) in aqueous buffer solutions at room temperature, λ_{ex} = 267 nm. Reprinted with permission from ref 232. Copyright 2003 John Wiley & Sons, Inc.

lengths, was assigned to excimer fluorescence.[234] As illustrated by the data in Figure 19, the slower components had the most intensity in the Ade-containing oligomers. Oligomers of Cyt showed a somewhat reduced tendency to form excimers, while emission by Gua and Thy oligomers was dominated by monomer fluorescence.[234] The assignment of decay components of between 40 and 260 ps to monomer fluorescence is doubtful since the mononucleotides have subpicosecond lifetimes (section 2.1.2). Femtosecond experiments to be described in the next section suggest that these components are in fact associated with excitations in base stacks. Plessow et al.[234] also studied long-wavelength excimer-like emission from double-stranded oligonucleotides. In one experiment, an equimolar mixture of $(dA)_{15}$ and $(dT)_{15}$ produced strong excimer fluorescence that was indistinguishable from that of $(dA)_{15}$. They concluded that single- vs double-stranded character of the oligonucleotides has very little effect on the excimer emission.

Markovitsi et al.[232] reported the first femtosecond fluorescence upconversion study of base oligomers. Their results obtained at the single wavelength of 330 nm for single-stranded $d(A)_{20}$ and $d(T)_{20}$ and for double-stranded $d(A)_{20}$·$d(T)_{20}$ are shown in Figure 20. Their main finding was that the single-stranded homo-oligonucleotides have somewhat slower fluorescence decays than the corresponding mononucleotides. The double-stranded oligonucleotide $d(A)_{20}$·$d(T)_{20}$ had slower relaxation than either of its constituent single strands. The majority of the fluorescence observed decayed on an ultrafast time scale with lifetimes on the order of 1−2 ps (see Table 8). Absent in their signals are the long-time components of between 150 ps and several nanoseconds seen in time-resolved studies of closely related base multimers.[44,45,61,234]

Markovitsi et al.[232] did observe a weak, persistent tail with an amplitude of ≤2% in the fluorescence decays of all of the oligonucleotides studied, which they were unable to characterize further due to experimental limitations. While it is possible that this tail is the long-lived emission seen in the other studies, it is unclear why it is so much weaker. One reason may be the short detection wavelength in their study since much of the longer lived emission is likely to be red-shifted. However, Plessow et al.[234] reported decay times of 150 ps and 1.05 ns for $d(A)_{15}$ at the nearby emission wavelength of 340 nm. The amplitude of the 1.05 ns component was ∼30% of the 150 ps component in this study.[234]

A further discrepancy is that Markovitsi et al.[232] reported maximum emission from $d(A)_{20}$·$d(T)_{20}$ at 330 nm upon photoexcitation at 267 nm. In contrast, the emission maximum of $d(A)_{15}$·$d(T)_{15}$ was red-shifted by several tens of nanometers under photoexcitation at 283 nm in the study by Plessow et al.[234] Clearly, fluorescence experiments that span the time range from femtoseconds to nanoseconds are highly desirable. In the next section, transient absorption experiments on homopolynucleotides are described which provide evidence that electronic energy relaxation occurs on time scales from femtoseconds to nanoseconds.[61,233]

3.2.3. Synthetic Homopolymers and Natural Nucleic Acids

Various groups reported multiexponential emission decays from Ade homopolymers at room temperature and neutral pH.[44,45,233,254] The results, which are summarized in Table 9, depend strongly on the experimental time resolution. Ballini et al.[44,254] studied poly(A) emission using synchrotron radiation with 1.8 ns excitation pulses. The emission decays were multiexponential and varied with the emission wavelength.[44] Kobayashi et al.[45] recorded time- and wavelength-resolved spectra for poly(A) at room temperature with ∼24 ps time resolution. They found an 8 ps component with maximum emission at 340 nm in addition to two longer components of 510 ps and 1.3 ns with maximum emission at 380 nm.

Rigler et al.[274−276] studied the alternating polynucleotides poly(dA-dT)·poly(dA-dT) and poly(dG-dC)·poly(dG-dC) by time-correlated single-photon counting with 40 ps pulses. They measured lifetimes for these double-stranded heteropolymers ranging from picoseconds to nanoseconds. Multiexponential decays were observed by Ballini and co-workers[254] for poly(dA-dT)·poly(dA-dT). Georghiou, Beechem, and their co-workers[273] studied poly(dA)·poly(dT) and $(dA)_{20}$·$(dT)_{20}$ in neutral buffer solution, as well as the corresponding single-stranded poly(dT) and $(dT)_{20}$

Table 9. Emission Lifetimes of DNA and RNA Polymers

system	τ_1/ps	τ_2/ps	τ_3/ns	time resolution	ref
poly(dA-dT)·poly(dA-dT)	<100	3000 ± 300		1.76 ns	254
	94 ± 1	872 ± 15		43 ps	274
	90	870	8.64	40 ps	274
poly(dA)·poly(dT)	5−20	200	1, 4	60 ps	273
poly(dG-dC)·poly(dG-dC)	255 ± 27	2926 ± 30		43 ps	274
	250	2930	7.81		275
	10	65		25 ps	71
	<0.4[a]			1.5 ps	46
poly(A)	100,[b] 310	850	4.7, 4.6, 4.0	1.76 ns	44
	8[c]	510[d]	1.3[d]	24 ps	45
	1.33 ± 0.13[e]	154 ± 14	∞	200 fs	233
poly(dA)	1.33 ± 0.13[e]	154 ± 14	∞	200 fs	233
poly(C), pH 7	1.7 ± 0.2	8.0 ± 1.0			61
poly(C), pH 5	8.7 ± 2.0	310 ± 30			61
methylated DNA	20	80		25 ps	71
DNA	<100	2900 ± 400			254

[a] From transient absorption measurements, excitation at 280 nm. [b] At emission wavelengths of 330, 406, and 460 nm, respectively. [c] Emission at 340 nm. [d] Emission at 380 nm. [e] From simultaneous fit to poly(A) and poly(dA) transients at 570 nm.

systems by time-correlated picosecond fluorescence anisotropy measurements. They observed a biexponential decrease in the anisotropy with a large-amplitude component on the picosecond time scale and a slower smaller amplitude component on the nanosecond time scale for both the single- and double-stranded systems. The anisotropy profile for poly(dT) and $(dT)_{20}$ decayed more slowly than that of poly(dA)·poly(dT) and $(dA)_{20}$·$(dT)_{20}$, respectively. Through study of the viscosity dependence of the emission, it was argued that the bases in the single-stranded forms are coupled more strongly to the solvent through greater solvent exposure than in the double-stranded ones.[273]

Few time-resolved studies have been carried out on native DNAs. Long-wavelength emission with a lifetime of 2.9 ns was detected in calf thymus DNA by Ballini et al.[254] Georghiou et al.[71] measured the emission decay times of double-stranded DNA in aqueous solution at room temperature using 25 ps laser pulses (Table 9). They studied emission from DNA taken from calf thymus and *E. coli* in the native state and after methylation by treatment with dimethyl sulfate. It was assumed that methylation occurs predominantly at N7 on the Gua residues. They found a dominant decay component with time constants of 10 and 20 ps for DNA and methylated DNA, respectively. These components accounted for 90% (DNA) and 40−60% (methylated DNA) of the total decay, depending on the transmission filter used. A second decay component of 65 ps (DNA) and 80 ps (methylated DNA) was also observed. At the time of this study, the lifetimes of the monomer bases had not been established, and Georghiou et al.[71] assumed these decays were due to monomers and ruled out excimer-like states, which they expected to have nanosecond lifetimes.[71]

Recently, Crespo-Hernández and Kohler used the transient absorption technique with 200 fs time resolution to study singlet excitations in poly(A) and poly(dA).[61,233] These two homopolymers have identical chromophores, but differ in secondary structure because of their different sugar−phosphate backbones.[277] Poly(A) adopts an A-like structure, while

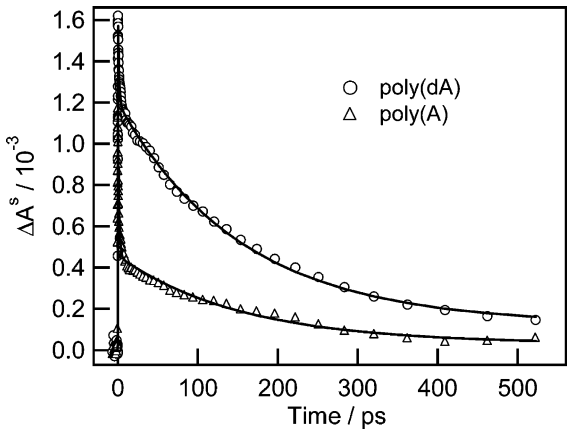

Figure 21. Transient absorption of pH 6.8 solutions of poly(dA) (○) and poly(A) (△) for 263 nm pump and 570 nm probe wavelengths. Global, nonlinear fits are shown by the solid curves. All signals have been water subtracted using the procedure in ref 233.

poly(dA) is B-like.[185,278−284] Poly(A) and poly(dA) also differ dramatically in photoreactivity. Poly(dA) forms dimeric photoproducts[285] nearly as efficiently as poly(dT) and poly(dC), whereas poly(A) is nearly photochemically inert.[286−289] The excited singlet state is believed to be the precursor to the Ade photodimers.[288]

Back-to-back scans of poly(A) and poly(dA) recorded on equal absorbance solutions in buffered (pH 7), room temperature solutions are shown in Figure 21. The water ionization signal was subtracted from these scans as described elsewhere.[61,233] An ultrafast decay component is visible at early times, while the signals still have not reached the baseline at the longest delay time, demonstrating that electronic energy relaxation occurs in these homopolymers over a very wide range of time scales. Both curves were satisfactorily fit to a sum of three exponentials with a common set of time constants: $\tau_1 = 1.33 \pm 0.13$ ps and $\tau_2 = 154 \pm 14$ ps, while τ_3 was fixed at infinity on account of the limited experimental time interval. The associated amplitudes are $A_1 = 0.46$, $A_2 = 0.25$, and $A_3 = 0.018$ for poly(A), and $A_1 = 0.29$, $A_2 = 0.64$, and $A_3 = 0.075$ for poly(dA). Since the transients were

recorded in back-to-back scans, the relative amplitudes are meaningful. Significantly, the poly(dA) transient absorption signal agrees well at times greater than a few picoseconds with the transient emission decay recorded by Plessow et al.[234] for the oligomer $d(A)_{15}$ at 340 nm.[233] This good agreement holds for both time constants and amplitudes, suggesting that the decays seen in the transient absorption experiment are assignable to the same emissive states seen in the time-resolved emission experiment. Further evidence for this comes from the ratio of the areas under the curves shown in Figure 21 after the decay due to τ_1 is complete. This ratio agrees well with the ratio of the fluorescence quantum yields observed for the two polymers.[233]

As described earlier, it is probable that the singlet states initially created by light absorption are not the same ones responsible for the long-time signals. If the former states are precursors for the latter ones, then the quantum yield of the long-lived states could be significantly less than unity, if other decay channels exist for the initial excited states. It is impossible to know the transition cross sections of the long-lived states (either in absorption or in emission) without knowing what percentage of the initial excited states decay to the long-lived ones. For example, it could be the case that ESA by the long-lived excited states is much stronger than by monomeric bases with the result that a low yield of such states can account for the observed signals. On the other hand, if the yield were high, then the radiative transition probability would have to be low (i.e., forbidden character) to account for the low emission quantum yields observed for both poly(A) and poly(dA).

It is challenging at the moment to tell whether the different decay components correspond to distinct excited states, which are created at the time of excitation, or whether the longer decay components represent states formed from faster decaying precursor ones. The subpicosecond-lifetime component resembles dynamics seen for single bases in solution, suggesting that this signal arises in regions where bases are unstacked, as in random-coil segments. On the other hand, increasing the temperature, modifying the pH, or adding a denaturing cosolvent such as dioxane decreased the amplitudes of the long-time signal components, indicating that they arise from excitations formed in base-stacked regions of the polymers.[61,233]

Transient absorption experiments with 200 fs time resolution were performed on the Cyt homopolymer poly(C) as a function of pH.[61] Poly(C) adopts a double-stranded form in the pH range between 3.8 and 5.5[290,291] which is more highly fluorescent.[292] In this form, two poly(C) strands are joined in a parallel fashion by hemiprotonated base pairs in which paired Cyt residues share a single proton. At higher pH values, poly(C) is present solely in a single-stranded form. The transition from the single-stranded to the double-stranded form can be conveniently monitored by CD spectroscopy.[293]

Figure 22 compares transient absorption at a probe wavelength of 570 nm upon UV excitation of poly(C) and CMP at neutral pH. The transients of poly(C) at

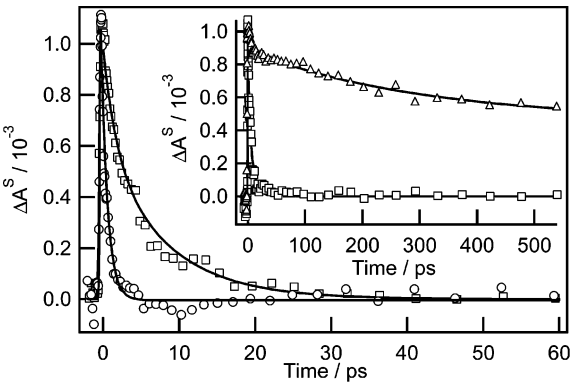

Figure 22. Transient absorption signals of poly(C) (□) and CMP (○) in aqueous solution at pH 7, pump at 259 nm and probe at 570 nm. Full lines are from global fits using a monoexponential (CMP) and a biexponential (poly(C)) function. Inset: Transient absorption at 570 nm from poly(C) in aqueous solution at pH 7 (□) and pH 5 (△) together with the global fit to a biexponential function (solid curve). The signals were water subtracted using the procedure in ref 61.

neutral pH were globally fitted by a biexponential function to give a monomer-like lifetime of 1.7 ± 0.2 ps and a longer lifetime of 8.0 ± 1.0 ps. No evidence was found for longer decay components, even though Plessow et al.[234] observed emission from the $d(C)_{15}$ oligonucleotide that decayed on time scales from tens of picoseconds to a few nanoseconds. A possible explanation for this discrepancy could be that $d(C)_{15}$ was partially protonated and double stranded in the experiments of Plessow et al.[234] as a result of the higher transition pH of poly(dC) compared to poly(C).[294]

The inset of Figure 22 shows a comparison of the transient absorption signal of poly(C) at pH 7 and 5. The signal at pH 5 decayed biexponentially with lifetimes of 8.7 ± 2.0 and 310 ± 30 ps. The slow decay component is consistent with past reports that poly(C) is more fluorescent at reduced pH.[292] The fast component matches the longer of the two lifetimes observed at neutral pH. This could imply that some unprotonated poly(C) chains are still present. The reason for the increased fluorescence by the hemiprotonated form of poly(C) is not evident. Protonation does not appear to be the cause since the Cyt cation monomer has a lifetime of 630 fs, even shorter than the lifetime of neutral Cyt.[72]

3.2.4. Solvent Effects

Time-resolved experiments on probe molecules incorporated into duplex DNAs reveal that the polymer creates a "solvent" environment substantially different from bulk water.[295−298] Hydrophobic interactions exclude water from the interior of duplex DNA, reducing the exposure of individual bases to solvent molecules. Furthermore, the water molecules that the bases do encounter are motionally constrained and show a unique dynamical response.[299] Using ultrafast fluorescence Stokes shift measurements on a dye molecule incorporated into DNA duplexes, Berg, Coleman, Murphy, and co-workers[295−297] showed that the solvation response of DNA spans many time scales. While the solvent environment clearly differs

in DNA, it is not clear how this affects electronic energy relaxation. As shown in section 2.1.4, solvent effects on emission dynamics of the canonical bases are minor. The subpicosecond decay component observed in femtosecond transient absorption[61,233] and fluorescence upconversion experiments[232] on base multimers made up of just one kind of base is consistently somewhat longer than the lifetime of the same base in monomeric form. One explanation could be a subtle solvent effect. Plessow et al.[234] explained the different lifetimes observed for the fast, momomer-like emission in their oligonucleotide experiments to varying degrees of solvent exposure. It is conceivable that the longer lived excited states seen in polymers could be even more sensitive to solvent effects, but this has not yet been studied. Finally, the solvent can profoundly modify the nuclear motions that might be necessary to form certain kinds of excited states. Using the formation of an excimer state in poly(dA-dT)·poly(dA-dT) as a probe of molecular motions, Georghiou et al. concluded that deformability of the helix in DNA is greatly reduced at high viscosities.[300]

3.3. Electronic Structure Calculations: Base Dimers, Trimers, and Polymers

There are many more quantum chemical studies of excited states in monomeric bases (see section 2.2) than in covalent and noncovalent assemblies of two or more bases. An obvious reason for this is the large size of these systems, which limits calculations to the lowest levels of theory. Nonetheless, the number of studies is growing. Two bases can be stacked or paired, and the effects of these noncovalent interactions on excited-state properties are considered in sections 3.3.1 and 3.3.2, respectively. Section 3.3.3 discusses theoretical studies of larger systems.

3.3.1. Base Stacks

Danilov et al.[238] investigated the lowest excited singlet state of the stacked Cyt dimer with cis-syn geometry using a semiempirical configuration interaction method. A stable singlet excimer was found with a binding energy of 3 kcal mol^{-1} and a sandwich-type geometry in which the planes of the two bases are nonparallel. The closest approach was found between the two C5−C6 double bonds, which are separated by just 2.4 Å in the optimized geometry of the excimer.[238] Emission from the excimer state was predicted to be red-shifted by approximately 150 nm relative to that from a single excited Cyt molecule, in rough agreement with experimental observations. Interestingly, a stable excimer was not observed when the base planes were constrained to be parallel to one another.

Because of the close approach of the C5−C6 bonds, Danilov et al.[238] suggested that their calculated excimer is the precursor of the cis-syn Cyt photodimer. Similar geometries were located for dimers of other pyrimidine derivatives by Pechenaya et al.[237] The dominant configuration in the excimer state was found to be highest occupied molecular orbital (HOMO) → lowest unoccupied molecular orbital (LUMO) excitation (93%). Both HOMO and LUMO orbitals are delocalized nearly equally over both Cyt bases, suggesting that the Cyt excimer state has nearly equal contributions from excitation-resonance and charge-resonance interactions. However, the difference of the net atomic charges in the ground and the excited singlet states was found to be only 0.006 electron, suggesting little net charge transfer. The noncoplanar geometry of the excimer state could explain the out-of-plane components seen in polarized emission experiments without the need to invoke charge-resonance interactions.[238]

More recently, Jean and Hall[301] used time-dependent density functional theory with the B3LYP functional to study 2AP fluorescence quenching in nucleotide dimers and trimers.[302] Particularly noteworthy is the authors' exploration of how stacking conformation affects electronic structure. For the B-form of the 5′-2AP-T-3′ dimer they found a bright state (S_2) that consists mostly of the configuration HOMO → LUMO + 1 (Figure 23a). S_1 is a dark state with low oscillator strength that arises primarily from transfer of an electron from the HOMO, which is localized primarily on 2AP, to the LUMO, which is localized primarily on Thy. Jean and Hall suggested that this charge-transfer state could act as a nonradiative trap for an initial excitation to the optically bright state. Indeed, femtosecond experiments by Fiebig et al.[100] on 2AP complexed with one of the natural nucleotides provided evidence of charge-transfer quenching. Similar results were found for the 5′-T-2AP-3′ dimer, in which the order of the nucleobases was reversed (Figure 23b).

Upon changing the conformation of 5′-2AP-T-3′ from B to A, Jean and Hall[301] found dramatic differences in the predicted electronic structure. In particular, the S_1 and S_2 states now had approximately equal oscillator strengths, which decreased significantly compared to that of the bright state found in the B-form dimer. This suggests that the longer radiative lifetimes of these delocalized states are responsible for fluorescence quenching, and similar conclusions were reached for dimers containing 2AP and either Ade or Gua.

Jean and Hall extended these calculations to base trimers containing 2AP.[302] The electronic structure of the 5′-T-2AP-T-3′ trimer was found to be a superposition of excitations of each of the dimers (Figure 23c), indicating that the flanking bases act independently of one another. On the other hand, when both flanking bases were guanines, trimer electronic transitions were found that could not be reduced to a superposition of dimer transitions. This was explained by the stronger stacking (and hence greater electronic coupling) between purine bases.

The calculations suggest two different fluorescence-quenching mechanisms for 2AP in base trimers. On one hand, charge-transfer states that are lower in energy than the dipole-allowed 2AP-like state create additional nonradiative decay pathways, leading to dynamic quenching. However, a second mechanism involves reduction in the oscillator strength and a corresponding decrease in the radiative rate. The calculations show the importance of the various stacked geometries in determining the electronic

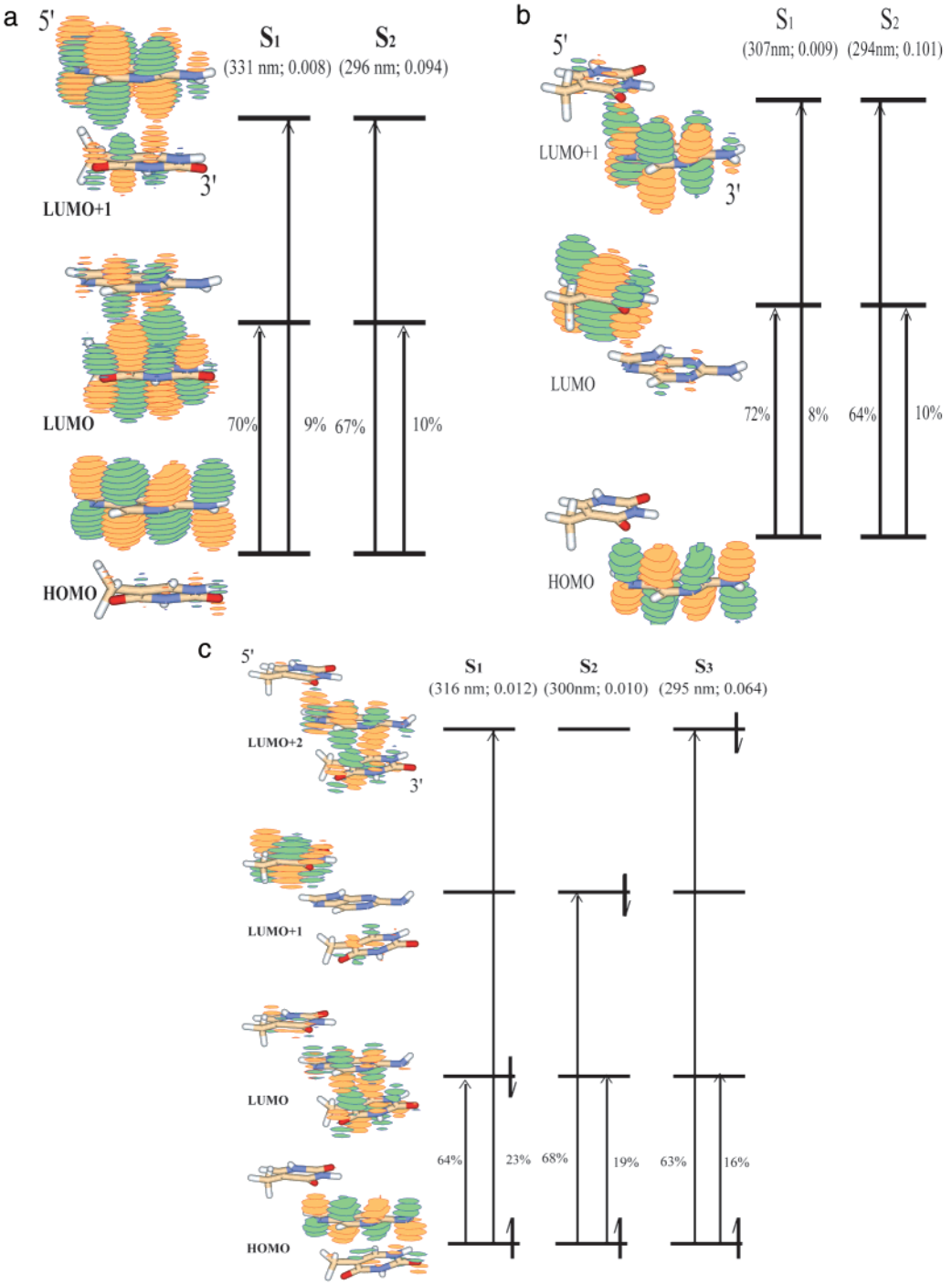

Figure 23. TD-DFT(B3LYP) transition wavelengths, oscillator strengths, and one-electron contributions (>10%) for the low-lying excited singlet transitions for 2AP-containing dimers and trimers with canonical B-form geometries: (a) 5′-2AP-T-3′, (b) 5′-T-2AP-3′, and (c) 5′-T-2AP-T-3′. In panel c, the electron configuration for the dominant one-electron contribution to each excited-state transition is shown. Reprinted with permission from ref 302. Copyright 2002 American Chemical Society.

structure and nature of the excited-state transitions. However, caution is required when TD-DFT predictions are interpreted for excited states with charge-transfer character. It is well-known that density functional theory significantly underestimates the transition energies of long-distance charge-transfer (CT) excitations.[303] The close proximity of stacked bases may ensure that the CT states actually have more local character, and the TD-DFT predictions could be reasonable. At present, both favorable[304] and unfavorable[116,305] reports can be found on the usefulness of TD-DFT for modeling CT states. It also remains to be seen whether the results for the 2AP-containing dimers and trimers are applicable to ones containing just the natural bases. Jean and Hall's supermolecule approach is easily adaptable to these systems, and work in this direction is under way.[306]

3.3.2. Base Pairs

In double-stranded nucleic acids, base pairing occurs alongside base stacking. While the latter interactions are assumed by most investigators to

have the greatest effect on photophysical properties, dramatic effects have sometimes been attributed to base pairing. One example is the lower fluorescence reported for double-stranded poly(dG-dC)·poly(dG-dC) than for single-stranded poly(dG-dC).[268] Another is the quenching of poly(A) fluorescence at 77 K upon complexation with poly(U).[307] In addition, large exciton splitting has been reported for H-bonded Gua dimers in the gas phase.[308] These results suggest that base pairing may influence singlet excited-state dynamics, and this has been the impetus for a number of computational studies.

The intermolecular analogue of excited-state tautomerism (see section 2.4.1) is excited-state proton transfer between paired bases in a DNA duplex, and several authors have studied this potential decay channel computationally.[149,309−312] Guallar et al.[311] studied the possibility of excited-state proton transfer in A-T and G-C base pairs using the CIS technique. They found that the lowest excited singlet states have excitation localized on just one of the bases in the base pair. Proton transfer is endothermic on the excited-state surface, and significant barriers exist to double-proton transfer. They observed a CT state with a low energy minimum corresponding to a single-proton transfer. They suggested that this state could be populated by internal conversion, but there is no barrier to forming this state, and it could have a long lifetime. Domcke and Sobolewski[305] observed a similar state in the 2-aminopyridine dimer, but found a near crossing with the electronic ground state and argued that it would have a very short lifetime. There is a sizable barrier to double-proton transfer in the electronic ground state. This barrier is reduced in magnitude on the excited-state surface of the A-T base pair, but is not changed significantly on the excited state of the C-G base pair. Even from the Franck−Condon point, proton transfer is endothermic for all excited states considered except for A*-T, where it is weakly exothermic, but still has an intervening barrier.

Shukla and Leszczynski studied the excited singlet states formed in A-U,[312] A-T,[149] and G-C[149] base pairs at the CIS level of theory. Nearly all of the lowest energy transitions were found to be localized on just one of the bases in each pair, suggesting that hydrogen bonding between complementary bases does not significantly alter the excited singlet states. The $^1\pi\pi^*$ states had virtually the same energies as those of the separate bases. On the other hand, the $^1n \rightarrow \pi^*$ transition energies were somewhat higher in energy in the base pair than in the individual bases, consistent with the frequently observed blue shifting of $^1n \rightarrow \pi^*$ transition energies due to hydrogen bonding. As a result, state reversal was sometimes observed when the excited states localized on a given base in a base pair were compared with the states calculated for that base in isolation.

On the experimental side, base pairing has been studied in molecular beams.[313−316] Interestingly, Watson−Crick base pairing has not yet been observed for isolated base pairs. Nir et al.[316] found that G adopts the canonical form in the G-C base pair, while C is present exclusively in an enol tautomer. Apparently, pairing with the complementary base may not be sufficient to produce the tautomeric preferences observed in aqueous solution. So far, gas-phase studies have not found evidence for excited-state proton transfer in canonical base pairs.[315,317] Catalan studied Ade in acetic acid and concluded that double-proton transfer is unlikely for $^1\pi\pi^*$ states of canonical base pairs, but is not ruled out for Hoogsteen pairs.[317]

In summary, there is no evidence from experimental or theoretical studies for excited-state proton transfer in neutral DNA base pairs. The enduring interest in this question is associated with the observation of double-proton transfer in the 7-azaindole dimer,[318−320] which has been described as a model base pair. Others have designed new models of phototautomerizable base pairs.[321,322] Recently, Sobolewski and Domcke[305] listed several reasons why the 7-azaindole dimer is in their opinion an unsatisfactory model for excited-state dynamics in a DNA base pair. They presented computational evidence for ultrafast internal conversion triggered by hydrogen atom transfer, in the 2-aminopyridine dimer, which they suggested is a better model system.[305] Their methods have recently been extended to the natural G-C base pair.[323]

3.3.3. Larger Systems

Calculations of excited singlet states of larger assemblies of bases become rapidly intractable without drastic approximations. Bouvier et al.[324,325] modeled excited singlet states in DNA duplexes using a Frenkel exciton Hamiltonian. Several other studies have computed molecular orbital energies for larger systems in the electronic ground state.[326−329] Although these studies have been motivated by a desire to understand charge transport in nucleic acids, the resulting energies are basic ingredients in a configuration interaction description of the polymer excited states. They can thus provide qualitative insights.

Lewis et al.[328] found extended, Bloch-like molecular orbitals for a $(dA)_{10}$·$(dT)_{10}$ duplex with enforced periodicity (Figure 24a). The authors studied the effect of disorder by computing electronic states for geometries obtained from snapshots from a molecular dynamics simulation that included explicit solvent molecules and counterions. (See refs 330 and 331 for reviews of molecular dynamics simulation methods applied to nucleic acids.) This disorder caused the extended states in the perfectly periodic duplex to localize in a manner reminiscent of Anderson localization (Figure 24b). Localization occurred even though the atomic coordinates of the disordered duplex differed only slightly from those of the perfectly periodic one. As the simulation proceeded, the localized HOMO hopped randomly and at times by large jumps throughout the simulated 10-mer.[328]

Recently, π-orbital coupling in guanine assemblies was studied by ab initio methods.[332] In stacked columns, $\pi-\pi$ coupling induced dispersive energy bands, while no dispersion was observed in the hydrogen-bonded planar ribbons. In assemblies with both π-stacking and hydrogen bonding, it was found that hydrogen-bonding interactions of the individual ribbons do not affect the electronic properties of the stacked bases.[332]

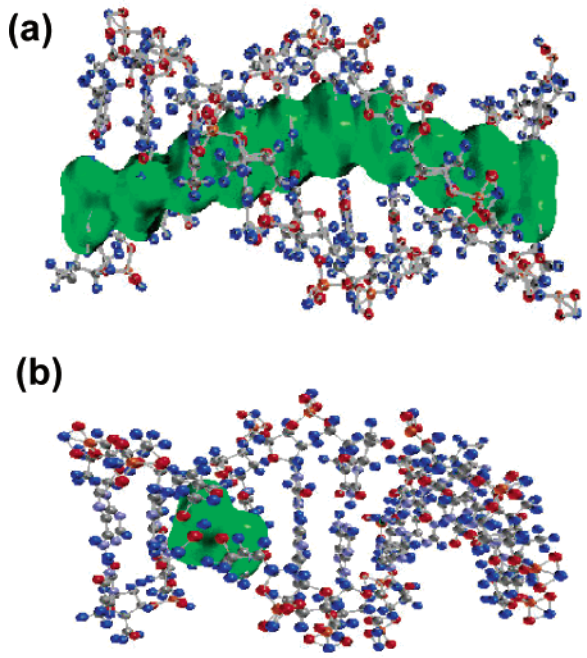

Figure 24. Population densities for the HOMOs for poly(dA)·poly(dT) in the case of (a) the idealized, periodic duplex geometry, and (b) the same system in an aperiodic, thermally disordered state. Similar results were found for the lowest unoccupied molecular orbitals. Reprinted with permission from ref 328. Copyright 2003 American Chemical Society.

Bouvier et al.[324] used semiempirical methods to study Frenkel exciton states created in DNA fragments. Their procedure, which used the method of atomic transition charges to model dipolar couplings between zero-order excitations localized on individual bases, is equivalent to supermolecule CIS in the limit that the perturbation is small and all orbital overlap interactions may be neglected. Their calculations, which were performed on the oligomers $(dA)_{20}\cdot(dT)_{20}$ and $(dA\text{-}dT)_{10}\cdot(dA\text{-}dT)_{10}$ in idealized geometries, indicate that excitons are delocalized all along the duplex. In fact, the proposal that exciton states extend over a significant number of base pairs is an old one; Rhodes[239] discussed this in 1961 in his theoretical study of polynucleotide hypochromism.

Lewis et al.[328] have presented computational evidence that structural disorder leads to spatial localization of the excitons. However, Bouvier et al.[325] published a study recently which suggests that disorder does not significantly decrease delocalization. The latter authors point out that many bases contribute to the exciton states due to the long-range character of the dipolar couplings. Thus, they argue that structural disorder is of less importance than it might be for more local properties.

Bouvier et al.[325] found further that their extended states, which are delocalized over 4−8 bases, do not result in spectral shifts vis-à-vis the sum-of-monomers spectrum. They thus conclude that the absence of shifts does not indicate the absence of delocalized exciton states. It is worth keeping in mind that excitons in polymers made of conventional aromatic chromophores rarely exhibit a delocalization length greater than 7−13 repeat units,[333] so claims of longer delocalization lengths in nucleic acid polymers should be viewed cautiously. There is currently no credible experimental evidence of emission from extended excitons, even at low temperature.[255] Nonetheless, theoretical studies such as the ones above are an important first step toward understanding exciton delocalization. Advances in theoretical methods for treating electronic excitations in polymers[334] will undoubtedly be of assistance.

3.4. Excited-State Decay Mechanisms

There are still such large gaps in the experimental picture that it may seem premature to discuss mechanisms for singlet-state deactivation in the base multimers. Nevertheless, we briefly consider here possibilities not found in the monomers—charge and energy transfer. Femtosecond experiments by Zewail and co-workers have shown that 2AP fluorescence is quenched by charge transfer in oligonucleotides.[99,100] Fiebig et al.[100] looked for long-wavelength emission in steady-state fluorescence experiments on 2AP−nucleotide complexes. Not finding any, they concluded that exciplex emission does not result from radiative recombination by states with charge-transfer character.[100] It is uncertain whether charge-transfer quenching is significant for pairs of the natural bases on account of their more similar redox properties.

The possibility of electronic energy transfer within base multimers has been discussed for many years by a number of authors.[172,239,335,336] The question of the distance scale over which singlet energy transfer can take place in DNA is at least formally analogous to the question of long-distance charge transport.[337−346] Both phenomena depend on the strength of interbase electronic couplings. Just as there have been reports of unusually facile, long-distance electron or hole transfer over distances of many base pairs, there have been analogous claims of singlet−singlet energy transfer over great distances.[347,348]

Nikogosyan and co-workers proposed that singlet−singlet energy transfer could occur to sites as many as 170 base pairs away from the initial excitation site in double-stranded DNA.[55] A later study questioned this conclusion.[241] More convincing evidence for singlet energy transfer came from experiments by the Sutherlands, who observed sensitization of ethidium bromide fluorescence when excited states were formed in nucleobases 3−4 base pairs away.[349,350] Other reports provide evidence of very limited migration of singlet energy in DNA. Rayner et al.[335] found no evidence for singlet energy transfer from an excited base to an intercalated dye molecule more than two base pairs away. Xu and Nordlund[75] found no evidence for significant singlet energy migration in DNA. However, these authors found evidence for facile transfer from native bases to 2AP, particularly when transfer could take place along a run of consecutive Ade residues. On this basis, they proposed that Ade is 10 times more efficient as an energy donor than Gua, Cyt, or Thy.

The "antenna effect" of Ade runs seen by Xu and Nordlund may provide evidence that the excimer-like state formed in $(A)_n$ sequences is trapped by the lower singlet state of 2AP. There is otherwise little to no

evidence to support energy transfer in base multimers. All theoretical treatments of energy transfer in nucleic acids have so far only considered Coulombic coupling at the level of the point dipole approximation. The use of this formalism is questionable, however, for stacked bases, which are in van der Waals contact with one another. It would be interesting to apply to nucleic acids the more rigorous approaches developed recently for treating energy transfer among pigments in bacterial light-harvesting complexes.[351−353]

4. Conclusions and Outlook

The works covered by this review demonstrate the impressive array of experimental and theoretical techniques that have been used to study excited singlet states in nucleic acids and their constituents. Femtosecond pump−probe experiments have been particularly helpful for elucidating the dynamics of these states. They have shown convincingly that the fluorescence lifetimes of single DNA bases are subpicosecond in room temperature solution, ending decades of uncertainty.

Significant advances in understanding the singlet-state photophysics have occurred in just the past several years. For base monomers, the relative lack of solvent effects in the condensed phase and reports of ultrashort lifetimes in supersonic jet experiments suggest that internal conversion is not the result of strong solute−solvent interactions, but is instead the inevitable outcome of nonadiabatic dynamics on the complex potential energy landscape of the bases. Still, there are many remaining puzzles. For example, the character of the excited states responsible for the nanosecond emission from base monomers in low-temperature glasses and in supersonic expansions, and by the base multimers in solution, is poorly understood. Also, while there are a number of indications that $^1n\pi^*$ states are important intermediates during electronic relaxation, it is unclear why the solvent effects observed to date have been so modest, given how sensitive these states are to polarity changes.

Quantum chemical calculations are increasingly up to the task of providing quantitative information about excited states in monomeric bases. Predictions of $^1\pi \rightarrow \pi^*$ vertical transition energies now agree well with experiment. Further work is needed to establish the accuracy of the theoretical methods for the $^1n\pi^*$ and $^1\pi\sigma^*$ states, which may play a crucial role in nonradiative decay. Improved methods are urgently needed for computing electronic structure as a function of molecular geometry to obtain adiabatic transition energies and to identify state crossings important in ultrafast nonradiative decay. Such calculations can locate conical intersections that may be responsible for ultrafast internal conversion by the nucleobases.

The greatest future challenges concern excited-state dynamics in base multimers, including natural DNAs and RNAs. Promising results have been obtained by recent femtosecond experiments which demonstrate that noncovalent base-stacking interactions dramatically affect electronic energy relaxation. These interactions give rise to long-lived excited states that decay on time scales from femtoseconds to nanoseconds. An important future issue is whether these complex signals reflect static or dynamic heterogeneity. A great deal of work remains to be done to understand how conformation controls electronic energy relaxation. More experiments are urgently needed to identify the factors that control the formation and evolution of excitations in di-, oligo-, and polynucleotides. Long-lived excited states in some base multimers can potentially report on dynamics for up to several nanoseconds. If the mapping between structure and excited-state dynamics can be understood, then the ultrafast fluorescence and absorption techniques that harness the intrinsic chromophores may become powerful tools for studying nucleic acid conformational change over the full range of time scales currently accessible through molecular dynamics simulation. Understanding the excitations in these multichromophoric systems offers great challenges to experimentalists and theorists alike.

5. Acknowledgment

We gratefully acknowledge financial support from the National Institutes of Health through the National Institute of General Medical Sciences (Grant R01-GM064563). We thank the many colleagues who kindly shared insights from their published and unpublished work. We extend special thanks to those who allowed us to reprint figures from their papers. We also thank current and former members of the Kohler group who have contributed to our work on DNA photophysics.

6. Abbreviations

Ade	adenine
Ado, A	adenosine
dAdo	2′-deoxyadenosine
AMP	adenosine 5′-monophosphate
dAMP	2′-deoxyadenosine 5′-monophosphate
m^1Ade	1-methyladenine
m^3Ade	3-methyladenine
m^7Ade	7-methyladenine
m^9Ade	9-methyladenine
2AP	2-aminopurine
Cyt	cytosine
Cyd, C	cytidine
CMP	cytidine 5′-monophosphate
m^5Cyt	5-methylcytosine
m^5Cyd	5-methylcytidine
m^5dCyd	2′-deoxy-5-methylcytidine
fl^5Cyt	5-fluorocytosine
ac^4Cyt	N^4-acetylcytosine
ac^4CMP	N^4-acetylcytidine 5′-monophosphate
Gua	guanine
Guo, G	guanosine
m^7Guo	7-methylguanosine
m^7GMP	7-methylguanosine 5′-monophosphate
GMP	guanosine 5′-monophosphate
Thy	thymine
Thd, T	thymidine
TMP	thymidine 5′-monophosphate
Ura	uracil, same as 5-methylthymine
Urd, U	uridine
ApA	adenylyl(3′→5′)adenine

CpC	cytidylyl(3′→5′)cytidine
TpT	thymidylyl(3′→5′)thymidine
GpG	guanylyl(3′→5′)guanine
d(TpA)	thymidylyl(3′→5′)-2′-deoxyadenosine
d(ApT)	2′-deoxyadenylyl(3′→5′)thymidine
poly(A)	poly(adenylic acid)
poly(dA)	poly(deoxyadenylic acid)
poly(C)	poly(cytidylic acid)
poly(dC)	poly(deoxycytidylic acid)
poly(dT)	poly(thymidylic acid)
poly(U)	poly(uridylic acid)
poly(dA-dT)·poly(dA-dT)	poly(deoxyadenylic-thymidylic acid)
poly(dA)·poly(dT)	poly(deoxyadenylic acid)·poly(thymidylic acid)
poly(dG-dC)·poly(dG-dC)	poly(deoxyguanylic-deoxycytidylic acid)

7. References

(1) Miller, D. L.; Weinstock, M. A. *J. Am. Acad. Dermatol.* **1994**, *30*, 774.
(2) Kraemer, K. H. *Proc. Natl. Acad. Sci. U.S.A.* **1997**, *94*, 11.
(3) Young, A. R. *Br. J. Clin. Pract.* **1997**, *89*, 10.
(4) Callis, P. R. In *Methods in Enzymology*; Academic Press: New York, 1997; Vol. 278, p 113.
(5) Daniels, M.; Hauswirth, W. *Science* **1971**, *171*, 675.
(6) Kool, E. T. *Acc. Chem. Res.* **2002**, *35*, 936.
(7) Murphy, C. J. *Adv. Photochem.* **2001**, *26*, 145.
(8) Cadet, J.; Vigny, P. In *Bioorganic Photochemistry*; Morrison, H., Ed.; Wiley: New York, 1990; Vol. 1, p 1.
(9) Ruzsicska, B. P.; Lemaire, D. G. E. In *CRC Handbook of Organic Photochemistry and Photobiology*; Horspool, W. M., Song, P.-S., Eds.; CRC Press: Boca Raton, FL, 1995; p 1289.
(10) Davies, R. J. H. *Biochem. Soc. Trans.* **1995**, *23*, 407.
(11) Davies, R. J. H. *Biochem. Soc. Trans.* **1997**, *25*, 323.
(12) Pfeifer, G. P. *Photochem. Photobiol.* **1997**, *65*, 270.
(13) Cadet, J.; Delatour, T.; Douki, T.; Gasparutto, D.; Pouget, J. P.; Ravanat, J. L.; Sauvaigo, S. *Mutat. Res.—Fundam. Mol. Mech. Mutagen.* **1999**, *424*, 9.
(14) Pfeifer, G. P.; Tang, M. S.; Denissenko, M. F. *Curr. Top. Microbiol. Immunol.* **2000**, *249*, 1.
(15) Ravanat, J.-L.; Douki, T.; Cadet, J. *J. Photochem. Photobiol., B* **2001**, *63*, 88.
(16) Gut, I. G.; Wood, P. D.; Redmond, R. W. *J. Am. Chem. Soc.* **1996**, *118*, 2366.
(17) Wood, P. D.; Redmond, R. W. *J. Am. Chem. Soc.* **1996**, *118*, 4256.
(18) Song, Q.; Lin, N.; Yao, S.; Zhang, J. *Prog. Nat. Sci.* **2000**, *10*, 81.
(19) Desfrancois, C.; Carles, S.; Schermann, J. P. *Chem. Rev.* **2000**, *100*, 3943.
(20) Weinkauf, R.; Schermann, J. P.; de Vries, M. S.; Kleinermanns, K. *Eur. Phys. J. D* **2002**, *20*, 309.
(21) Pecourt, J.-M. L.; Peon, J.; Kohler, B. *J. Am. Chem. Soc.* **2000**, *122*, 9348. Erratum: *J. Am. Chem. Soc.* **2001**, *123*, 5166.
(22) Vigny, P.; Duquesne, M. In *Excited States of Biological Molecules*; Birks, J. B., Ed.; Wiley: New York, 1976; Vol. 3; p 167.
(23) Vigny, P.; Ballini, J. P. *Jerusalem Symp. Quantum Chem. Biochem.* **1977**, *10*, 1.
(24) Daniels, M. In *Photochemistry and Photobiology of Nucleic Acids*; Wang, S. Y., Ed.; Academic Press: New York, 1976; Vol. 1, p 23.
(25) Hauswirth, W. W.; Daniels, M. In *Photochemistry and Photobiology of Nucleic Acids*; Wang, S. Y., Ed.; Academic Press: New York, 1976; Vol. 1, p 109.
(26) Daniels, M. *Photochem. Photobiol.* **1983**, *37*, 691.
(27) Callis, P. R. *Annu. Rev. Phys. Chem.* **1983**, *34*, 329.
(28) Lesk, A. M. *J. Chem. Educ.* **1969**, *46*, 821.
(29) *Compendium of Biochemical Nomenclature and Related Documents*; 2nd ed.; Liébecq, C., Ed.; Portland Press: London, 1992.
(30) Watson, J. D.; Crick, F. H. C. *Nature* **1953**, *171*, 737.
(31) Eastman, J. W. *Ber. Bunsen-Ges. Phys. Chem.* **1969**, *73*, 407.
(32) Wilson, R. W.; Callis, P. R. *Photochem. Photobiol.* **1980**, *31*, 323.
(33) Voet, D.; Gratzer, W. B.; Cox, R. A.; Doty, P. *Biopolymers* **1963**, *1*, 193.
(34) Strickler, S. J.; Berg, R. A. *J. Chem. Phys.* **1962**, *37*, 814.
(35) Kasha, M. *Faraday Discuss.* **1950**, *9*, 14.
(36) Callis, P. R. *Chem. Phys. Lett.* **1979**, *61*, 563.
(37) Eisinger, J.; Shulman, R. G. *Science* **1968**, *161*, 1311.
(38) Pecourt, J.-M. L.; Peon, J.; Kohler, B. *J. Am. Chem. Soc.* **2001**, *123*, 10370.
(39) Peon, J.; Zewail, A. H. *Chem. Phys. Lett.* **2001**, *348*, 255.
(40) Gustavsson, T.; Sharonov, A.; Markovitsi, D. *Chem. Phys. Lett.* **2002**, *351*, 195.
(41) Gustavsson, T.; Sharonov, A.; Onidas, D.; Markovitsi, D. *Chem. Phys. Lett.* **2002**, *356*, 49.
(42) Nikogosyan, D. N.; Letokhov, V. S. *Riv. Nuovo Cimento Soc. Ital. Fis.* **1983**, *6*, 1.
(43) Oraevsky, A. A.; Sharkov, A. V.; Nikogosyan, D. N. *Chem. Phys. Lett.* **1981**, *83*, 276.
(44) Ballini, J. P.; Daniels, M.; Vigny, P. *J. Lumin.* **1982**, *27*, 389.
(45) Kobayashi, S.; Yamashita, M.; Sato, T.; Muramatsu, S. *IEEE J. Quantum Electron.* **1984**, *QE-20*, 1383.
(46) Nikogosyan, D. N.; Angelov, D.; Soep, B.; Lindqvist, L. *Chem. Phys. Lett.* **1996**, *252*, 322.
(47) Reuther, A.; Nikogosyan, D. N.; Laubereau, A. *J. Phys. Chem.* **1996**, *100*, 5570.
(48) Reuther, A.; Iglev, H.; Laenen, R.; Laubereau, A. *Chem. Phys. Lett.* **2000**, *325*, 360.
(49) Häupl, T.; Windolph, C.; Jochum, T.; Brede, O.; Hermann, R. *Chem. Phys. Lett.* **1997**, *280*, 520.
(50) Fujiwara, T.; Kamoshida, Y.; Morita, R.; Yamashita, M. *J. Photochem. Photobiol., B* **1997**, *41*, 114.
(51) Udenfriend, S.; Zaltzman, P. *Anal. Biochem.* **1962**, *3*, 49.
(52) Børresen, H. C. *Acta Chem. Scand.* **1963**, *17*, 921.
(53) Cohen, B.; Hare, P. M.; Kohler, B. *J. Am. Chem. Soc.* **2003**, *125*, 13594.
(54) Nikogosyan, D. N.; Angelov, D. A.; Oraevsky, A. A. *Photochem. Photobiol.* **1982**, *35*, 627.
(55) Nikogosyan, D. N.; Oraevsky, A. A.; Letokhov, V. S.; Arbieva, Z. K.; Dobrov, E. N. *Chem. Phys.* **1985**, *97*, 31.
(56) Yamashita, M.; Kobayashi, S.; Torizuka, K.; Sato, T. *Chem. Phys. Lett.* **1987**, *137*, 578.
(57) Morsy, M. A.; Al-Somali, A. M.; Suwaiyan, A. *J. Phys. Chem. B* **1999**, *103*, 11205.
(58) Knutson, J. R.; Beechem, J. M.; Brand, L. *Chem. Phys. Lett.* **1983**, *102*, 501.
(59) Larsen, O. F. A.; van Stokkum, I. H. M.; Groot, M.-L.; Kennis, J. T. M.; van Grondelle, R.; van Amerongen, H. *Chem. Phys. Lett.* **2003**, *371*, 157.
(60) Jou, F.-Y.; Freeman, G. R. *J. Phys. Chem.* **1979**, *83*, 2383.
(61) Cohen, B.; Crespo-Hernández, C. E.; Hare, P. M.; Kohler, B. In *Ultrafast Molecular Events in Chemistry and Biology*; Martin, M., Hynes, J. T., Eds.; Elsevier: Amsterdam, 2004, in press.
(62) Cohen, B.; Crespo-Hernández, C. E.; Kohler, B. *Faraday Discuss.* **2004**, *127*, in press.
(63) Sharonov, A.; Gustavsson, T.; Carré, V.; Renault, E.; Markovitsi, D. *Chem. Phys. Lett.* **2003**, *380*, 173.
(64) Onidas, D.; Markovitsi, D.; Marguet, S.; Sharonov, A.; Gustavsson, T. *J. Phys. Chem. B* **2002**, *106*, 11367.
(65) Elsaesser, T.; Kaiser, W. *Annu. Rev. Phys. Chem.* **1991**, *42*, 83.
(66) Schwarzer, D.; Troe, J.; Votsmeier, M.; Zerezke, M. *J. Chem. Phys.* **1996**, *105*, 3121.
(67) Terazima, M. *Chem. Phys. Lett.* **1999**, *305*, 189.
(68) Nielsen, S. B.; Andersen, J. U.; Forster, J. S.; Hvelplund, P.; Liu, B.; Pedersen, U. V.; Tomita, S. *Phys. Rev. Lett.* **2003**, *91*, 048302/1.
(69) Andersen, J. U.; Andersen, L. H.; Hvelplund, P.; Lapierre, A.; Moeller, S. P.; Nielsen, S. B.; Pedersen, U. V.; Tomita, S. *Hyperfine Interact.* **2003**, *146*, 283.
(70) Nishimura, Y.; Takahashi, S.; Yamamoto, T.; Tsuboi, M.; Hattori, M.; Miura, K.; Yamaguchi, K.; Ohtani, S.; Hata, T. *Nucleic Acids Res.* **1980**, *8*, 1107.
(71) Georghiou, S.; Nordlund, T. M.; Saim, A. M. *Photochem. Photobiol.* **1985**, *41*, 209.
(72) Malone, R. J.; Miller, A. M.; Kohler, B. *Photochem. Photobiol.* **2003**, *77*, 158.
(73) Favre, A.; Thomas, G. *Annu. Rev. Biophys. Bioeng.* **1981**, *10*, 175.
(74) Rist, M. J.; Marino, J. P. *Curr. Org. Chem.* **2002**, *6*, 775.
(75) Xu, D.-G.; Nordlund, T. M. *Biophys. J.* **2000**, *78*, 1042.
(76) Pompizi, I.; Haberli, A.; Leumann, C. J. *Nucleic Acids Res.* **2000**, *28*, 2702.
(77) Kawai, M.; Lee, M. J.; Evans, K. O.; Nordlund, T. M. *J. Fluoresc.* **2001**, *11*, 23.
(78) Gargallo, R.; Vives, M.; Tauler, R.; Eritja, R. *Biophys. J.* **2001**, *81*, 2886.
(79) Rist, M.; Wagenknecht, H.-A.; Fiebig, T. *ChemPhysChem* **2002**, *3*, 704.
(80) Rai, P.; Cole, T. D.; Thompson, E.; Millar, D. P.; Linn, S. *Nucleic Acids Res.* **2003**, *31*, 2323.
(81) Sharonov, A.; Gustavsson, T.; Marguet, S.; Markovitsi, D. *Photochem. Photobiol. Sci.* **2003**, *2*, 362.
(82) Tommasi, S.; Denissenko, M. F.; Pfeifer, G. P. *Cancer Res.* **1997**, *57*, 4727.
(83) You, Y. H.; Li, C.; Pfeifer, G. P. *J. Mol. Biol.* **1999**, *293*, 493.
(84) Mitchell, D. L. *Photochem. Photobiol.* **2000**, *71*, 162.
(85) You, Y. H.; Pfeifer, G. P. *J. Mol. Biol.* **2001**, *305*, 389.
(86) Sagan, C. *J. Theor. Biol.* **1973**, *39*, 195.
(87) Cockell, C. S. *Origin Life Evol. Biosphere* **2000**, *30*, 467.
(88) Cockell, C. S.; Horneck, G. *Photochem. Photobiol.* **2001**, *73*, 447.
(89) Mulkidjanian, A. Y.; Cherepanov, D. A.; Galperin, M. Y. *BMC Evol. Biol.* **2003**, *3*.

(90) Dreyfus, M.; Dodin, G.; Bensaude, O.; Dubois, J. E. *J. Am. Chem. Soc.* **1975**, *97*, 2369.
(91) Holmén, A.; Broo, A.; Albinsson, B.; Nordén, B. *J. Am. Chem. Soc.* **1997**, *119*, 12240.
(92) Gonnella, N. C.; Nakanishi, H.; Holtwick, J. B.; Horowitz, D. S.; Kanamori, K.; Leonard, N. J.; Roberts, J. D. *J. Am. Chem. Soc.* **1983**, *105*, 2050.
(93) Kang, H.; Jung, B.; Kim, S. K. *J. Chem. Phys.* **2003**, *118*, 6717.
(94) Kang, H.; Lee, K. T.; Jung, B.; Ko, Y. J.; Kim, S. K. *J. Am. Chem. Soc.* **2002**, *124*, 12958.
(95) Georghiou, S.; Saim, A. M. *Photochem. Photobiol.* **1986**, *44*, 733.
(96) Szabo, A. G.; Berens, K. B. *Photochem. Photobiol.* **1975**, *21*, 141.
(97) Berens, K.; Smagowicz, W. J.; Wierzchowski, K. L. *Eur. Biophys. Congr., Proc., 1st* **1971**, *6*, 63.
(98) Ward, D. C.; Reich, E.; Stryer, L. *J. Biol. Chem.* **1969**, *244*, 1228.
(99) Wan, C.; Fiebig, T.; Schiemann, O.; Barton, J. K.; Zewail, A. H. *Proc. Natl. Acad. Sci. U.S.A.* **2000**, *97*, 14052.
(100) Fiebig, T.; Wan, C.; Zewail, A. H. *ChemPhysChem* **2002**, *3*, 781.
(101) Lorentzon, J.; Fülscher, M. P.; Roos, B. O. *J. Am. Chem. Soc.* **1995**, *117*, 9265.
(102) Stratt, R. M.; Maroncelli, M. *J. Phys. Chem.* **1996**, *100*, 12981.
(103) Jimenez, R.; Fleming, G. R.; Kumar, P. V.; Maroncelli, M. *Nature* **1994**, *369*, 471.
(104) Georghiou, S.; Gerke, L. S. *Photochem. Photobiol.* **1999**, *69*, 646.
(105) Hare, P. M.; Kohler, B. Unpublished results.
(106) Pal, S. K.; Peon, J.; Zewail, A. H. *Chem. Phys. Lett.* **2002**, *363*, 57.
(107) Hobza, P.; Sponer, J. *Chem. Rev.* **1999**, *99*, 3247.
(108) Sponer, J.; Leszczynski, J.; Hobza, P. *Biopolymers* **2001**, *61*, 3.
(109) Foresman, J. B.; Head-Gordon, M.; Pople, J. A.; Frisch, M. J. *J. Phys. Chem.* **1992**, *96*, 135.
(110) Andersson, K.; Malmqvist, P. A.; Roos, B. O. *J. Chem. Phys.* **1992**, *96*, 1218.
(111) Roos, B. O. *Acc. Chem. Res.* **1999**, *32*, 137.
(112) Huron, B.; Malrieu, J. P.; Rancurel, P. *J. Chem. Phys.* **1973**, *58*, 5745.
(113) Cimiraglia, R.; Persico, M. *J. Comput. Chem.* **1987**, *8*, 39.
(114) Mennucci, B.; Toniolo, A.; Cappelli, C. *J. Chem. Phys.* **1999**, *111*, 7197.
(115) Serrano-Andres, L.; Fülscher, M. P.; Karlstrom, G. *Int. J. Quantum Chem.* **1997**, *65*, 167.
(116) Grimme, S.; Parac, M. *ChemPhysChem* **2003**, *4*, 292.
(117) Shukla, M. K.; Leszczynski, J. *J. Phys. Chem. A* **2002**, *106*, 11338.
(118) Langer, H.; Doltsinis, N. L. *J. Chem. Phys.* **2003**, *118*, 5400.
(119) Cossi, M.; Barone, V. *J. Chem. Phys.* **2001**, *115*, 4708.
(120) Grimme, S.; Waletzke, M. *J. Chem. Phys.* **1999**, *111*, 5645.
(121) Neiss, C.; Saalfrank, P.; Parac, M.; Grimme, S. *J. Phys. Chem. A* **2003**, *107*, 140.
(122) Shukla, M. K.; Mishra, S. K.; Kumar, A.; Mishra, P. C. *J. Comput. Chem.* **2000**, *21*, 826.
(123) Fülscher, M. P.; Serrano-Andrés, L.; Roos, B. O. *J. Am. Chem. Soc.* **1997**, *119*, 6168.
(124) Broo, A. *J. Phys. Chem. A* **1998**, *102*, 526.
(125) Mishra, S. K.; Shukla, M. K.; Mishra, P. C. *Spectrochim. Acta, Part A* **2000**, *56*, 1355.
(126) Mennucci, B.; Toniolo, A.; Tomasi, J. *J. Phys. Chem. A* **2001**, *105*, 4749.
(127) Callis, P. R.; Rosa, E. J.; Simpson, W. T. *J. Am. Chem. Soc.* **1964**, *86*, 2292.
(128) Clark, L. B. *J. Phys. Chem.* **1995**, *99*, 4466.
(129) Chin, W.; Mons, M.; Dimicoli, I.; Piuzzi, F.; Tardivel, B.; Elhanine, M. *Eur. Phys. J. D* **2002**, *20*, 347.
(130) Nir, E.; Plutzer, C.; Kleinermanns, K.; de Vries, M. *Eur. Phys. J. D* **2002**, *20*, 317.
(131) Mons, M.; Dimicoli, I.; Piuzzi, F.; Tardivel, B.; Elhanine, M. *J. Phys. Chem. A* **2002**, *106*, 5088.
(132) Fülscher, M. P.; Roos, B. O. *J. Am. Chem. Soc.* **1995**, *117*, 2089.
(133) Shukla, M. K.; Mishra, P. C. *Chem. Phys.* **1999**, *240*, 319.
(134) Ismail, N.; Blancafort, L.; Olivucci, M.; Kohler, B.; Robb, M. A. *J. Am. Chem. Soc.* **2002**, *124*, 6818.
(135) Sobolewski, A. L.; Domcke, W. *Eur. Phys. J. D* **2002**, *20*, 369.
(136) Crespo-Hernández, C. E.; Marai, C.; Kohler, B. Unpublished results.
(137) Frisch, M. J.; Trucks, G. W.; Schlegel, H. B.; Scuseria, G. E.; Robb, M. A.; Cheeseman, J. R.; Montgomery, J. A., Jr.; Vreven, T.; Kudin, K. N.; Burant, J. C.; Millam, J. M.; Iyengar, S. S.; Tomasi, J.; Barone, V.; Mennucci, B.; Cossi, M.; Scalmani, G.; Rega, N.; Petersson, G. A.; Nakatsuji, H.; Hada, M.; Ehara, M.; Toyota, K.; Fukuda, R.; Hasegawa, J.; Ishida, M.; Nakajima, T.; Honda, Y.; Kitao, O.; Nakai, H.; Klene, M.; Li, X.; Knox, J. E.; Hratchian, H. P.; Cross, J. B.; Adamo, C.; Jaramillo, J.; Gomperts, R.; Stratmann, R. E.; Yazyev, O.; Austin, A. J.; Cammi, R.; Pomelli, C.; Ochterski, J. W.; Ayala, P. Y.; Morokuma, K.; Voth, G. A.; Salvador, P.; Dannenberg, J. J.; Zakrzewski, V. G.; Dapprich, S.; Daniels, A. D.; Strain, M. C.; Farkas, O.; Malick, D. K.; Rabuck, A. D.; Raghavachari, K.; Foresman, J. B.; Ortiz, J. V.; Cui, Q.; Baboul, A. G.; Clifford, S.; Cioslowski, J.; Stefanov, B. B.; Liu, G.; Liashenko, A.; Piskorz, P.; Komaromi, I.; Martin, R. L.; Fox, D. J.; Keith, T.; Al-Laham, M. A.; Peng, C. Y.; Nanayakkara, A.; Challacombe, M.; Gill, P. M. W.; Johnson, B.; Chen, W.; Wong, M. W.; Gonzalez, C.; Pople, J. A., Gaussian, Inc., Pittsburgh, PA, 2003.
(138) Kim, N. J.; Jeong, G.; Kim, Y. S.; Sung, J.; Kim, S. K.; Park, Y. D. *J. Chem. Phys.* **2000**, *113*, 10051.
(139) Ullrich, S.; Schultz, T.; Zgierski, M. Z.; Stolow, A. *J. Am. Chem. Soc.* **2004**, *126*, 2262.
(140) Mennucci, B.; Toniolo, A.; Tomasi, J. *J. Phys. Chem. A* **2001**, *105*, 7126.
(141) Merchán, M.; Serrano-Andrés, L. *J. Am. Chem. Soc.* **2003**, *125*, 8108.
(142) Broo, A.; Pearl, G.; Zerner, M. C. *J. Phys. Chem. A* **1997**, *101*, 2478.
(143) Shukla, M. K.; Leszczynski, J. *J. Phys. Chem. A* **2002**, *106*, 8642.
(144) Marian, C. M.; Schneider, F.; Kleinschmidt, M.; Tatchen, J. *Eur. Phys. J. D* **2002**, *20*, 357.
(145) Broo, A.; Holmén, A. *J. Phys. Chem. A* **1997**, *101*, 3589.
(146) Rachofsky, E. L.; Ross, J. B. A.; Krauss, M.; Osman, R. *J. Phys. Chem. A* **2001**, *105*, 190.
(147) Lührs, D. C.; Viallon, J.; Fischer, I. *Phys. Chem. Chem. Phys.* **2001**, *3*, 1827.
(148) Holmén, A.; Broo, A. *Int. J. Quantum Chem.* **1995**, *22*, 113.
(149) Shukla, M. K.; Leszczynski, J. *J. Phys. Chem. A* **2002**, *106*, 4709.
(150) Andreasson, J.; Holmén, A.; Albinsson, B. *J. Phys. Chem. B* **1999**, *103*, 9782.
(151) Albinsson, B. *J. Am. Chem. Soc.* **1997**, *119*, 6369.
(152) Desfrancois, C.; Schermann, J. P. In *Atomic and Molecular Beams: The State of the Art 2000*; Campargue, R., Ed.; Springer: Berlin, 2001; p 815.
(153) Fischer, I. *Chem. Soc. Rev.* **2003**, *32*, 59.
(154) Fujii, M.; Tamura, T.; Mikami, N.; Ito, M. *Chem. Phys. Lett.* **1986**, *126*, 583.
(155) Brady, B. B.; Peteanu, L. A.; Levy, D. H. *Chem. Phys. Lett.* **1988**, *147*, 538.
(156) Nir, E.; Grace, L.; Brauer, B.; de Vries, M. S. *J. Am. Chem. Soc.* **1999**, *121*, 4896.
(157) Weinkauf, R.; Aicher, P.; Wesley, G.; Grotemeyer, J.; Schlag, E. W. *J. Phys. Chem.* **1994**, *98*, 8381.
(158) Ledingham, K. W. D.; Singhal, R. P. *Int. J. Mass Spectrom. Ion Processes* **1997**, *163*, 149.
(159) Grun, C.; Heinicke, R.; Weickhardt, C.; Grotemeyer, J. *Int. J. Mass Spectrom. Ion Processes* **1999**, *187*, 307.
(160) Plützer, C.; Kleinermanns, K. *Phys. Chem. Chem. Phys.* **2002**, *4*, 4877.
(161) Plützer, C.; Nir, E.; de Vries, M. S.; Kleinermanns, K. *Phys. Chem. Chem. Phys.* **2001**, *3*, 5466.
(162) Nir, E.; Kleinermanns, K.; Grace, L.; de Vries, M. S. *J. Phys. Chem. A* **2001**, *105*, 5106.
(163) Nir, E.; Muller, M.; Grace, L. I.; de Vries, M. S. *Chem. Phys. Lett.* **2002**, *355*, 59.
(164) Salter, L. M.; Chaban, G. M. *J. Phys. Chem. A* **2002**, *106*, 4251.
(165) He, Y.; Wu, C.; Kong, W. *J. Phys. Chem. A* **2003**, *107*, 5145.
(166) Neumark, D. M. *Annu. Rev. Phys. Chem.* **2001**, *52*, 255.
(167) Stolow, A. *Annu. Rev. Phys. Chem.* **2003**, *54*, 89.
(168) Eisinger, J.; Lamola, A. A. In *Excited States of Proteins and Nucleic Acids*; Steiner, R. F., Weinryb, I., Eds.; Plenum Press: New York, 1971; p 107.
(169) Blumberg, W. E.; Eisinger, J.; Navon, G. *Biophys. J.* **1968**, *8*, A106.
(170) Hart, L. P.; Daniels, M. *Biochem. Biophys. Res. Commun.* **1989**, *162*, 781.
(171) Polewski, K.; Zinger, D.; Trunk, J.; Monteleone, D. C.; Sutherland, J. C. *J. Photochem. Photobiol., B* **1994**, *24*, 169.
(172) Guéron, M.; Eisinger, J.; Shulman, R. G. *J. Chem. Phys.* **1967**, *47*, 4077.
(173) Spears, K. G.; Rice, S. A. *J. Chem. Phys.* **1971**, *55*, 5561.
(174) Lim, E. C. *Adv. Photochem.* **1997**, *23*, 165.
(175) Sobolewski, A. L.; Lim, E. C.; Siebrand, W. *Int. J. Quantum Chem.* **1991**, *39*, 309.
(176) Nir, E.; Imhof, P.; Kleinermanns, K.; de Vries, M. S. *J. Am. Chem. Soc.* **2000**, *122*, 8091.
(177) Lee, Y. J.; Summers, W. A.; Burr, J. G. *J. Am. Chem. Soc.* **1977**, *99*, 7679.
(178) Sinicropi, A.; Nau, W. M.; Olivucci, M. *Photochem. Photobiol. Sci.* **2002**, *1*, 537.
(179) Parusel, A. B. J.; Rettig, W.; Rotkiewicz, K. *J. Phys. Chem. A* **2002**, *106*, 2293.
(180) Wang, H.; Zhang, H.; Abou-Zied, O. K.; Yu, C.; Romesberg, F. E.; Glasbeek, M. *Chem. Phys. Lett.* **2002**, *367*, 599.
(181) Lochbrunner, S.; Schultz, T.; Schmitt, M.; Shaffer, J. P.; Zgierski, M. Z.; Stolow, A. *J. Chem. Phys.* **2001**, *114*, 2519.
(182) Fournier, T.; Pommeret, S.; Mialocq, J. C.; Deflandre, A.; Rozot, R. *Chem. Phys. Lett.* **2000**, *325*, 171.
(183) Frey, W.; Elsaesser, T. *Chem. Phys. Lett.* **1992**, *189*, 565.
(184) Shukla, M. K.; Leszczynski, J. *Int. J. Quantum Chem.* **2000**, *77*, 240.
(185) Bush, C. A.; Scheraga, H. A. *Biopolymers* **1969**, *7*, 395.
(186) Chaban, G. M.; Gordon, M. S. *J. Phys. Chem. A* **1999**, *103*, 185.

(187) Siebrand, W. *J. Chem. Phys.* **1967**, *46*, 440.
(188) Bixon, M.; Jortner, J. *J. Chem. Phys.* **1968**, *48*, 715.
(189) Bixon, M.; Jortner, J. *J. Chem. Phys.* **1969**, *50*, 4061.
(190) Jortner, J.; Rice, S. A.; Hochstrasser, R. M. *Adv. Photochem.* **1969**, *7*, 149.
(191) Englman, R.; Jortner, J. *Mol. Phys.* **1970**, *18*, 145.
(192) Avouris, P.; Gelbart, W. M.; El-Sayed, M. A. *Chem. Rev.* **1977**, *77*, 793.
(193) Lin, S. H. *J. Chem. Phys.* **1966**, *44*, 3759.
(194) Nitzan, A.; Jortner, J. *J. Chem. Phys.* **1972**, *56*, 3360.
(195) Hochstrasser, R. M. In *Excited States of Proteins and Nucleic Acids*; Steiner, R. F., Weinryb, I., Eds.; Plenum Press: New York, 1971; p 1.
(196) Lim, E. C. *J. Phys. Chem.* **1986**, *90*, 6770.
(197) Hochstrasser, R. M. *Acc. Chem. Res.* **1968**, *1*, 266.
(198) Hochstrasser, R. M.; Marzzacco, C. *J. Chem. Phys.* **1968**, *49*, 971.
(199) Robb, M. A.; Bernardi, F.; Olivucci, M. *Pure Appl. Chem.* **1995**, *67*, 783.
(200) Domcke, W.; Stock, G. *Adv. Chem. Phys.* **1997**, *100*, 1.
(201) M.Garavelli, P. C., Bernardi, F.; Robb, M. A.; Olivucci, M. *J. Am. Chem. Soc.* **1997**, *119*, 11487.
(202) Garavelli, M.; Bernardi, F.; Olivucci, M.; Vreven, T.; Klein, S.; Celani, P.; Robb, M. A. *Faraday Discuss.* **1998**, *110*, 51.
(203) Teller, E. *Isr. J. Chem.* **1969**, *7*, 227.
(204) Woywod, C.; Domcke, W.; Sobolewski, A. L.; Werner, H. J. *J. Chem. Phys.* **1994**, *100*, 1400.
(205) Palmer, I. J.; Olivucci, M.; Bernardi, F.; Robb, M. A. *J. Org. Chem.* **1992**, *57*, 5081.
(206) Seidner, L.; Stock, G.; Sobolewski, A. L.; Domcke, W. *J. Chem. Phys.* **1992**, *96*, 5298.
(207) Stock, G.; Domcke, W. *J. Opt. Soc. Am. B* **1990**, *7*, 1970.
(208) Manthe, U.; Koeppel, H. *J. Chem. Phys.* **1990**, *93*, 1658.
(209) Schneider, R.; Domcke, W. *Chem. Phys. Lett.* **1988**, *150*, 235.
(210) Molnar, F.; Ben-Nun, M.; Martinez, T. J.; Schulten, K. *J. Mol. Struct.* **2000**, *506*, 169.
(211) Worth, G. A.; Robb, M. A. *Adv. Chem. Phys.* **2002**, *124*, 355.
(212) Applegate, B. E.; Barckholtz, T. A.; Miller, T. A. *Chem. Soc. Rev.* **2003**, *32*, 38.
(213) Yarkony, D. R. *J. Phys. Chem. A* **2001**, *105*, 6277.
(214) Sobolewski, A. L.; Domcke, W. *Chem. Phys.* **2000**, *259*, 181.
(215) Sobolewski, A. L.; Domcke, W.; Dedonder-Lardeux, C.; Jouvet, C. *Phys. Chem. Chem. Phys.* **2002**, *4*, 1093.
(216) Sobolewski, A. L.; Domcke, W. *Chem. Phys. Lett.* **1999**, *315*, 293.
(217) Serrano-Andrés, L.; Roos, B. O. *J. Am. Chem. Soc.* **1996**, *118*, 185.
(218) Tatischeff, I.; Klein, R.; Zemb, T.; Duquesne, M. *Chem. Phys. Lett.* **1978**, *54*, 394.
(219) Petke, J. D.; Maggiora, G. M.; Christoffersen, R. E. *J. Phys. Chem.* **1992**, *96*, 6992.
(220) Browne, D. T.; Eisinger, J.; Leonard, N. J. *J. Am. Chem. Soc.* **1968**, *90*, 7302.
(221) Leonard, N. J.; Ito, K. *J. Am. Chem. Soc.* **1973**, *95*, 4010.
(222) Doyama, K.; Higashii, T.; Seyama, F.; Sakata, Y.; Misumi, S. *Bull. Chem. Soc. Jpn.* **1988**, *61*, 3619.
(223) Seyama, F.; Akahori, K.; Sakata, Y.; Misumi, S.; Aida, M.; Nagata, C. *J. Am. Chem. Soc.* **1988**, *110*, 2192.
(224) Itahara, T. *Bull. Chem. Soc. Jpn.* **1996**, *69*, 3239.
(225) Bhat, B.; Leonard, N. J.; Robinson, H.; Wang, A. H. J. *J. Am. Chem. Soc.* **1996**, *118*, 10744.
(226) Itahara, T. *Chem. Lett.* **1993**, *2*, 233.
(227) Ito, T.; Shinohara, H.; Nishimoto, S. *Photochem. Photobiol.* **2000**, *72*, 719.
(228) Semenov, V. E.; Akamsin, V. D.; Reznik, V. S.; Chernova, A. V.; Dorozhkina, G. M.; Efremov, Y. Y.; Nafikova, A. A. *Tetrahedron Lett.* **2002**, *43*, 9683.
(229) Hocek, M.; Dvorak, D.; Havelkova, M. *Nucleosides, Nucleotides Nucleic Acids* **2003**, *22*, 775.
(230) Hocek, M.; Dvorakova, H.; Cisarova, I. *Collect. Czech. Chem. Commun.* **2002**, *67*, 1560.
(231) Shapiro, S. L.; Campillo, A. J.; Kollman, V. H.; Goad, W. B. *Opt. Commun.* **1975**, *15*, 308.
(232) Markovitsi, D.; Sharonov, A.; Onidas, D.; Gustavsson, T. *ChemPhysChem* **2003**, *4*, 303.
(233) Crespo-Hernández, C. E.; Kohler, B. *J. Phys. Chem. B.*, submitted for publication.
(234) Plessow, R.; Brockhinke, A.; Eimer, W.; Kohse-Hoeinghaus, K. *J. Phys. Chem. B* **2000**, *104*, 3695.
(235) Lamola, A. A.; Eisinger, J. *Proc. Natl. Acad. Sci. U.S.A.* **1968**, *59*, 46.
(236) Vigny, P.; Ballini, J. P. In *Excited States in Organic Chemistry and Biochemistry*; Pullman, B., Goldblum, N., Eds.; D. Reidel: Dordrecht, The Netherlands, 1977.
(237) Pechenaya, V. I.; Danilov, V. I.; Slyusarchuk, O. N.; Alderfer, J. L. *Photochem. Photobiol.* **1995**, *61*, 435.
(238) Danilov, V. I.; Slyusarchuk, O. N.; Alderfer, J. L.; Stewart, J. J. P.; Callis, P. R. *Photochem. Photobiol.* **1994**, *59*, 125.
(239) Rhodes, W. *J. Am. Chem. Soc.* **1961**, *83*, 3609.
(240) Texter, J. *Biopolymers* **1992**, *32*, 53.
(241) Angelov, D.; Spassky, A.; Berger, M.; Cadet, J. *J. Am. Chem. Soc.* **1997**, *119*, 11373.
(242) Kleinwachter, V.; Koudelka, J. *Collect. Czech. Chem. Commun.* **1972**, *37*, 3433.
(243) Tinoco, I., Jr. *J. Am. Chem. Soc.* **1960**, *82*, 4785.
(244) Bloomfield, V. A.; Crothers, D. M.; Tinoco, I., Jr. *Physical Chemistry of Nucleic Acids*; Harper & Row: New York, 1974.
(245) Saito, I.; Nakamura, T.; Nakatani, K.; Yoshioka, Y.; Yamaguchi, K.; Sugiyama, H. *J. Am. Chem. Soc.* **1998**, *120*, 12686.
(246) Eisinger, J.; Guéron, M.; Schulman, R. G.; Yamane, T. *Proc. Natl. Acad. Sci. U.S.A.* **1966**, *55*, 1015.
(247) Shaar, C. S.; Morgan, J. P.; Daniels, M. *Photochem. Photobiol.* **1984**, *39*, 747.
(248) Daniels, M.; Morgan, J. P. *Chem. Phys. Lett.* **1978**, *58*, 283.
(249) Daniels, M.; Morgan, J. P. *J. Lumin.* **1979**, *18*−*19*, 593.
(250) Callis, P. R. *Chem. Phys. Lett.* **1973**, *19*, 551.
(251) Stevens, B. *Nature* **1961**, *192*, 725.
(252) Birks, J. B. *Photophysics of Aromatic Molecules*; Wiley-Interscience: New York, 1970.
(253) Wilson, R. W.; Callis, P. R. *J. Phys. Chem.* **1976**, *80*, 2280.
(254) Ballini, J. P.; Vigny, P.; Daniels, M. *Biophys. Chem.* **1983**, *18*, 61.
(255) Kononov, A. I.; Bakulev, V. M.; Rapoport, V. L. *J. Photochem. Photobiol., B* **1993**, *19*, 139.
(256) Winnik, F. M. *Chem. Rev.* **1993**, *93*, 587.
(257) Ballini, J. P.; Daniels, M.; Vigny, P. *Biophys. Chem.* **1991**, *39*, 253.
(258) Daniels, M. S., C. S.; Morgan, J. P. *Biophys. Chem.* **1988**, *32*, 229.
(259) We shall use excimer even when writing of states formed between different bases. Some refer to these states as exciplexes, but we prefer to call them excimers since one writes of base dimers, even when the two bases differ. Birks[252] referred to *heteroexcimers* when the two molecules have similar chemical nature, as is arguably the case for all of the bases.
(260) Johnson, N. P.; Schleich, T. *Biochemistry* **1974**, *13*, 981.
(261) Cheng, D. M.; Sarma, R. H. *J. Am. Chem. Soc.* **1977**, *99*, 7333.
(262) Ezra, F. S.; Lee, C.-H.; Kondo, N. S.; Danyluk, S. S.; Sarma, R. H. *Biochemistry* **1977**, *16*, 1977.
(263) Gorenstein, D. G. *Chem. Rev.* **1994**, *94*, 1315.
(264) Morgan, J. P.; Daniels, M. *Photochem. Photobiol.* **1980**, *31*, 101.
(265) Morgan, J. P.; Daniels, M. *Photochem. Photobiol.* **1980**, *31*, 207.
(266) Kononov, A. I.; Bukina, M. N. *J. Biomol. Struct. Dyn.* **2002**, *20*, 465.
(267) Ge, G.; Georghiou, S. *Photochem. Photobiol.* **1991**, *54*, 301.
(268) Huang, C. R.; Georghiou, S. *Photochem. Photobiol.* **1992**, *56*, 95.
(269) Ge, G.; Georghiou, S. *Photochem. Photobiol.* **1991**, *54*, 477.
(270) Aoki, T. I.; Callis, P. R. *Chem. Phys. Lett.* **1982**, *92*, 327.
(271) Stewart, R. F.; Davidson, N. *J. Chem. Phys.* **1963**, *39*, 255.
(272) Crespo-Hernández, C. E.; Kohler, B. Unpublished results.
(273) Georghiou, S.; Bradrick, T. D.; Philippetis, A.; Beechem, J. M. *Biophys. J.* **1996**, *70*, 1909.
(274) Rigler, R.; Claesens, F.; Lomakka, G. In *Ultrafast Phenomena IV*; Auston, D. H., Eisenthal, K. B., Eds.; Springer-Verlag: Berlin, 1984; p 472.
(275) Rigler, R. *Spectrosc. Dyn. Mol. Biol. Syst.* **1985**, 35.
(276) Rigler, R.; Claesens, F.; Kristensen, O. *Anal. Instrum.* **1985**, *14*, 525.
(277) Alderfer, J. L.; Smith, S. L. *J. Am. Chem. Soc.* **1971**, *93*, 7305.
(278) Leng, M.; Felsenfeld, G. *J. Mol. Biol.* **1966**, *15*, 455.
(279) Brahms, J.; Michelson, A. M.; van Holde, K. E. *J. Mol. Biol.* **1966**, *15*, 467.
(280) Vournakis, J. N.; Poland, D.; Scheraga, H. A. *Biopolymers* **1967**, *5*, 403.
(281) Adler, A. J.; Grossman, L.; Fasman, G. D. *Biochemistry* **1969**, *8*, 3846.
(282) Mills, J. B.; Vacano, E.; Hagerman, P. J. *J. Mol. Biol.* **1999**, *285*, 245.
(283) Olsthoorn, C. S. M.; Bostelaar, L. J.; De Rooij, J. F. M.; Van Boom, J. H.; Altona, C. *Eur. J. Biochem.* **1981**, *115*, 309.
(284) Jolles, B.; Laigle, A.; Chinsky, L.; Turpin, P. Y. *Nucleic Acids Res.* **1985**, *13*, 2075.
(285) Wang, Y.; Taylor, J.-S.; Gross, M. L. *Chem. Res. Toxicol.* **2001**, *14*, 738.
(286) Poerschke, D. *J. Am. Chem. Soc.* **1973**, *95*, 8440.
(287) Poerschke, D. *Proc. Natl. Acad. Sci. U.S.A.* **1973**, *70*, 2683.
(288) Kumar, S.; Sharma, N. D.; Davies, R. J. H.; Phillipson, D. W.; McCloskey, J. A. *Nucleic Acids Res.* **1987**, *15*, 1199.
(289) Clingen, P. H.; Davies, R. J. H. *J. Photochem. Photobiol., B* **1997**, *38*, 81.
(290) Guschlbauer, W. *Nucleic Acids Res.* **1975**, *2*, 353.
(291) Michelson, A. M.; Massoulie, J.; Guschlbauer, W. *Prog. Nucleic Acid Res. Mol. Biol.* **1967**, *6*, 83.
(292) Favre, A. *FEBS Lett.* **1972**, *22*, 280.
(293) Antao, V. P.; Gray, D. M. *J. Biomol. Struct. Dyn.* **1993**, *10*, 819.
(294) Inman, R. B. *J. Mol. Biol.* **1964**, *9*, 624.
(295) Brauns, E. B.; Murphy, C. J.; Berg, M. A. *J. Am. Chem. Soc.* **1998**, *120*, 2449.

(296) Brauns, E. B.; Madaras, M. L.; Coleman, R. S.; Murphy, C. J.; Berg, M. A. *J. Am. Chem. Soc.* **1999**, *121*, 11644.
(297) Brauns, E. B.; Madaras, M. L.; Coleman, R. S.; Murphy, C. J.; Berg, M. A. *Phys. Rev. Lett.* **2002**, *88*.
(298) Hess, S.; Davis, W. B.; Voityuk, A. A.; Rosch, N.; Michel-Beyerle, M. E.; Ernsting, N. P.; Kovalenko, S. A.; Lustres, J. L. P. *ChemPhysChem* **2002**, *3*, 452.
(299) Pal, S. K.; Peon, J.; Bagchi, B.; Zewail, A. H. *J. Phys. Chem. B* **2002**, *106*, 12376.
(300) Georghiou, S.; Kubala, S. M.; Large, C. C. *Photochem. Photobiol.* **1998**, *67*, 526.
(301) Jean, J. M.; Hall, K. B. *Proc. Natl. Acad. Sci. U.S.A.* **2001**, *98*, 37.
(302) Jean, J. M.; Hall, K. B. *Biochemistry* **2002**, *41*, 13152.
(303) Dreuw, A.; Weisman, J. L.; Head-Gordon, M. *J. Chem. Phys.* **2003**, *119*, 2943.
(304) Vaswani, H. M.; Hsu, C.-P.; Head-Gordon, M.; Fleming, G. R. *J. Phys. Chem. B* **2003**, *107*, 7940.
(305) Sobolewski, A. L.; Domcke, W. *Chem. Phys.* **2003**, *294*, 73.
(306) Crespo-Hernández, C. E.; Marai, C.; Jean, J. M.; Kohler, B. Unpublished results.
(307) Kleinwaechter, V.; Drobnik, J.; Augenstein, L. *Photochem. Photobiol.* **1968**, *7*, 485.
(308) Nir, E.; Janzen, C.; Imhof, P.; Kleinermanns, K.; de Vries, M. S. *Phys. Chem. Chem. Phys.* **2002**, *4*, 740.
(309) Pechenaya, V. I.; Danilov, V. I. *Biofizika* **1973**, *18*, 560.
(310) Santamaria, R.; Vazquez, A. *J. Comput. Chem.* **1994**, *15*, 981.
(311) Guallar, V.; Douhal, A.; Moreno, M.; Lluch, J. M. *J. Phys. Chem. A* **1999**, *103*, 6251.
(312) Shukla, M. K.; Leszczynski, J. *J. Phys. Chem. A* **2002**, *106*, 1011.
(313) Sukhodub, L. F.; Yanson, I. K. *Nature* **1976**, *264*, 245.
(314) Dey, M.; Moritz, F.; Grotemeyer, J.; Schlag, E. W. *J. Am. Chem. Soc.* **1994**, *116*, 9211.
(315) Nir, E.; Kleinermanns, K.; de Vries, M. S. *Nature* **2000**, *408*, 949.
(316) Nir, E.; Janzen, C.; Imhof, P.; Kleinermanns, K.; de Vries, M. S. *Phys. Chem. Chem. Phys.* **2002**, *4*, 732.
(317) Catalan, J. *J. Phys. Chem. B* **2002**, *106*, 11384.
(318) Taylor, C. A.; El-Bayoumi, M. A.; Kasha, M. *Proc. Natl. Acad. Sci. U.S.A.* **1969**, *63*, 253.
(319) Abdoul-Carime, H.; Bouteiller, Y.; Desfrancois, C.; Philippe, L.; Schermann, J. P. *Acta Chem. Scand.* **1997**, *51*, 145.
(320) Folmer, D. E.; Wisniewski, E. S.; Hurley, S. M.; Castleman, A. W. *Proc. Natl. Acad. Sci. U.S.A.* **1999**, *96*, 12980.
(321) Ogawa, A. K.; Abou-Zied, O. K.; Tsui, V.; Jimenez, R.; Case, D. A.; Romesberg, F. E. *J. Am. Chem. Soc.* **2000**, *122*, 9917.
(322) Abou-Zied, O. K.; Jimenez, R.; Romesberg, F. E. *J. Am. Chem. Soc.* **2001**, *123*, 4613.
(323) Sobolewski, A. L.; Domcke, W. *Phys. Chem. Chem. Phys.* **2004**, *6*, in press.
(324) Bouvier, B.; Gustavsson, T.; Markovitsi, D.; Millie, P. *Chem. Phys.* **2002**, *275*, 75.
(325) Bouvier, B.; Dognon, J.-P.; Lavery, R.; Markovitsi, D.; Millie, P.; Onidas, D.; Zakrzewska, K. *J. Phys. Chem. B* **2003**, *107*, 13512.
(326) Otto, P.; Clementi, E.; Ladik, J. *J. Chem. Phys.* **1983**, *78*, 4547.
(327) Bogar, F.; Ladik, J. *Chem. Phys.* **1998**, *237*, 273.
(328) Lewis, J. P.; Cheatham, T. E., III; Starikov, E. B.; Wang, H.; Sankey, O. F. *J. Phys. Chem. B* **2003**, *107*, 2581.
(329) Gervasio, F. L.; Carloni, P.; Parrinello, M. *Phys. Rev. Lett.* **2002**, *89*, 108102.
(330) Cheatham, T. E., III; Kollman, P. A. *Annu. Rev. Phys. Chem.* **2000**, *51*, 435.
(331) Cheatham, T. E., III; Young, M. A. *Biopolymers* **2001**, *56*, 232.
(332) Di Felice, R. C., A.; Molinari, E.; Garbesi, A. *Phys. Rev. B: Condens. Matter* **2002**, *65*, 045104.
(333) McQuade, D. T.; Pullen, A. E.; Swager, T. M. *Chem. Rev.* **2000**, *100*, 2537.
(334) Tretiak, S.; Mukamel, S. *Chem. Rev.* **2002**, *102*, 3171.
(335) Rayner, D. M.; Szabo, A. G.; Loutfy, R. O.; Yip, R. W. *J. Phys. Chem.* **1980**, *84*, 289.
(336) Georghiou, S.; Zhu, S.; Widner, R.; Huang, C. R.; Ge, G. *J. Biomol. Struct. Dyn.* **1990**, *8*, 657.
(337) Holmlin, R. E.; Tong, R. T.; Barton, J. K. *J. Am. Chem. Soc.* **1998**, *120*, 9724.
(338) Lewis, F. D.; Liu, X.; Liu, J.; Miller, S. E.; Hayes, R. T.; Wasielewski, M. R. *Nature (London)* **2000**, *406*, 51.
(339) Wan, C.; Fiebig, T.; Kelley, S. O.; Treadway, C. R.; Barton, J. K.; Zewail, A. H. *Proc. Natl. Acad. Sci. U.S.A.* **1999**, *96*, 6014.
(340) Kelley, S. O.; Holmlin, R. E.; Stemp, E. D. A.; Barton, J. K. *J. Am. Chem. Soc.* **1997**, *119*, 9861.
(341) Kelley, S. O.; Barton, J. K. *Science* **1999**, *283*, 375.
(342) Arkin, M. R.; Stemp, E. D. A.; Holmlin, R. E.; Barton, J. K.; Hormann, A.; Olson, E. J. C.; Barbara, P. F. *Science* **1996**, *273*, 475.
(343) Jortner, J.; Bixon, M.; Langenbacher, T.; Michel-Beyerle, M. E. *Proc. Natl. Acad. Sci. U.S.A.* **1998**, *95*, 12759.
(344) Steenken, S. *Biol. Chem.* **1997**, *378*, 1293.
(345) Bixon, M.; Jortner, J. *J. Phys. Chem. B* **2000**, *104*, 3906.
(346) Schuster, G. B. *Acc. Chem. Res.* **2000**, *33*, 253.
(347) Baverstock, K. F.; Cundall, R. B. *Nature* **1988**, *332*, 312.
(348) Baverstock, K. F.; Cundall, R. B. *Int. J. Radiat. Biol.* **1989**, *55*, 151.
(349) Sutherland, B. M.; Sutherland, J. C. *Biophys. J.* **1969**, *9*, 1045.
(350) Sutherland, J. C.; Sutherland, B. M. *Biopolymers* **1970**, *9*, 639.
(351) Scholes, G. D. *J. Phys. Chem.* **1996**, *100*, 18731.
(352) Krueger, B. P.; Scholes, G. D.; Fleming, G. R. *J. Phys. Chem. B* **1998**, *102*, 5378.
(353) Scholes, G. D.; Gould, I. R.; Cogdell, R. J.; Fleming, G. R. *J. Phys. Chem. B* **1999**, *103*, 2543.

CR0206770